UNIVERSITY OF CALIFORNIA, SAN DIEGO

Investigating the link between mitotic defects and cell death in the *C. elegans* germline and in human tissue culture cells

A dissertation submitted in partial satisfaction of the requirements for the degree Doctor of Philosophy

in

Biomedical Sciences

by

Deanna Marie Stevens

Committee in charge:

Professor Arshad Desai, Chair
Professor Andrew Chisholm
Professor Richard Kolodner
Professor Leanne Jones
Professor Karen Oegema

2013

The Dissertation of Deanna Marie Stevens is approved, and it is acceptable in quality and form for publication on microfilm and electronically:

_____

_____

_____

_____

_____

Chair

University of California, San Diego

2013

Dedication

This thesis is dedicated to my high school AP biology teacher, Mr. William LoPotro, who ignited my passion for science and taught me to never, ever, ever give up.

Table of Contents

List of Figures

Acknowledgments

I am beyond appreciative for all of the advice, encouragement and support that I have received during my time here in graduate school. First and foremost, I must extend a huge thank you to my advisor, Arshad Desai. Arshad's genuine passion for research and willingness to go where the science takes you has been invaluable to my success as a graduate student. He allows you to carve your own path, but is always there to offer guidance whenever it is needed. He has help mold me into the scientist I am today and for that I will be forever grateful. I have also been fortunate enough to have a second mentor, Karen Oegema. Karen's ability to think through any problem and tackle it with determinism and ingenuity are remarkable. Her insight and advice has been a major contributor to my growth as a researcher.

I would also like to thank the members of my thesis committee: Richard Kolodner, Andrew Chisholm and Leanne Jones. This diverse, yet exceedingly knowledgeable group of individuals has kept me on course and always challenged me to work harder.

To the members of the Desai and Oegema labs, both past and present whose names are too many to mention, thank you for providing such a collaborative and stimulating environment in which to do science. I truly couldn't have asked for a better place to carry out my graduate work.

And last, but certainly not least, I must thank my family. Although my time in graduate school has forced us to be apart longer than I would have liked, I could not have gotten through my time here without your continued

support and encouragement. And to my fiancé, David, words will never be able to express how much you have done and continue to do for me. I can say for a fact that I would not be where I am today, or who I am today, without your unconditional love and support. Thank you for always believing in me and helping me see this thing through until the end.

Chapter 2, in full, has been submitted for publication. It may appear as Deanna Stevens, Karen Oegema and Arshad Desai. *Meiotic double-strand breaks act as a surveillance mechanism to uncover mitotic errors in the C. elegans germline*. The dissertation author was the primary researcher and author of this paper.

Chapter 3, in full, is a reprint of the material as it appears in the journal, Public Library of Science One. Deanna Stevens, Reto Gassmann, Karen Oegema and Arshad Desai. *Uncoordinated loss of chromatid cohesion is a common outcome of extended metaphase arrest* PLoS One 6(8): e22969 (2011). The dissertation author was the primary researcher and author of this paper.

Vita

EDUCATION

2004 Bachelor of Science, Biology, Brandeis University

2013 Doctor of Philosophy, Biomedical Sciences, University of California, San Diego

PUBLICATIONS

Stevens D, Oegema K, Desai A *Meiotic double-strand breaks act as a surveillance mechanism to uncover mitotic errors in the C. elegans germline* (submitted for publication)

Stevens D, Gassmann R, Oegema K, Desai A (2011) *Uncoordinated loss of chromatid cohesion is a common outcome of extended metaphase arrest* PLoS One 6(8): e22969

Lamming DW, Ye L, Katajisto P, Concalves MD, Saitoh M, **Stevens DM**, Davis JG, Salmon AB, Richardson A, Ahima RS, Guertin DA, Sabatini DM, Baur JA (2012) *Rapamycin-induced insulin resistance is mediated by mTORC2 loss and uncoupled from longevity* Science 335: 1638-1643

Guertin DA, **Stevens DM**, Saitoh M, Kinkel S, Crosby K, Sheen JH, Mullholland DJ, Magnuson MA, Wu H, and Sabatini DM (2009) *mTOR complex 2 is required for the development of prostate cancer induced by Pten loss in mice* Cancer Cell 15: 148-159

Guertin DA, **Stevens DM**, Thoreen CC, Burds AA, Kalaany NY, Moffat J, Brown M, Fitzgerald KJ, Sabatini DM (2006) *Ablation in mice of the mTORC components* raptor*,* rictor*, or* mLST8 *reveals that mTORC2 is required for signaling to Akt-FOXO and PKCalpha, but not S6K1* Developmental Cell 11:859-871

ABSTRACT OF THE DISSERTATION

Investigating the link between mitotic defects and cell death in the *C. elegans* germline and in human tissue culture cells

by

Deanna Marie Stevens

Doctor of Philosophy in Biomedical Sciences

University of California, San Diego, 2013

Professor Arshad Desai, Chair

Faithful segregation of genetic material during mitosis is a vital cellular function that ensures the accurate passage of critical information from one generation to the next. Errors in this process can be highly deleterious, often times leading to aneuploidy- a hallmark of cancer and the leading genetic cause of birth defects and miscarriages. Given the potentially harmful nature of cells resulting from defects in mitosis, a majority of these cells are eliminated via apoptosis to prevent further propagation of this damage. However, this is not always the case as sometimes these cells evade cell death and continue to proliferate. Although the link between mitotic defects and activation of the cell death machinery is relatively well established, the

underlying mechanism still remains unclear. The work presented here takes a closer look, in both the model system *Caenorhabditis elegans* and human tissue culture cells, at the direct effect of a variety of mitotic perturbations in an effort to better understand how mitotic defects can signal to cell death.

In the adult *C. elegans* germline, which is composed of both mitotic and meiotic cells, nuclei that result from a failed mitosis acquire an excess amount of double-strand breaks, activate the DNA damage checkpoint and are unable to successfully complete meiotic recombination. These nuclei are preferentially eliminated by apoptosis, a response that is dependent on the initiation of recombination, suggesting that the deliberate double strand breaks that are required for recombination survey and mark for elimination nuclei with the improper complement of chromosomes. In human tissue culture cells, perturbations that prevent proper exit from mitosis while allowing for perfect, or near perfect, alignment of chromosomes result in a distinct phenotype called chromosome scattering. Cells with scattered chromosomes show uncoordinated loss of chromatid cohesion and subsequent spindle defects, yet still maintain the hallmarks of an active mitosis. Most notably, cells with scattered chromosomes show an increased susceptibility to apoptosis. Overall the results of these studies reveal two distinct mechanisms by which mitotic defects signal to cell death helping to shed light on the driving force behind this phenomenon.

Chapter 1. Introduction

1.1 Mitosis and the cell cycle

Mitosis is defined as the specialized cellular program responsible for the proper segregation of genetic material from one mother cell into two daughter cells (Mitchison and Salmon, 2001). Prior to mitosis, the cell undergoes one round of DNA replication followed by a short growth phase to survey for and repair any damage that may have occurred during S phase (**Fig. 1A**; Bartek et al., 2004). The beginning of mitosis (**Fig. 1B**), or prophase, is marked by breakdown of the nuclear envelope, which is immediately followed by the condensation of chromosomes (Güttinger et al., 2009) – the distinct structures created by the packaging of DNA around proteins called histones (Woodcook and Ghosh, 2010) – during prometaphase. Concomitant with chromosome condensation is the formation of the bipolar spindle (Tanenbaum and Medema, 2010). The bipolar spindle consists of a network of dynamic microtubules emanating from the centrosome- the main microtubule organizing center of a cell and a vital component of the mitotic machinery (Bornens, 2012). The role of spindle microtubules is to search for, capture and align the chromosomes so that at metaphase they are properly bioriented along the bipolar spindle (Kapoor and Compton, 2002). Once all chromosomes have achieved proper biorientation, segregation occurs in anaphase such that each daughter cell receives an exact 1:1 complement of the genome and the cell exits mitosis (Sullivan and Morgan, 2007). The entire

process of mitosis is tightly regulated and requires the timely coordination of a multitude of cellular events and signaling cascades.

1.1.1 Function and formation of the kinetochore

Although there are many steps in place to ensure that accurate segregation of chromosomes occurs during mitosis, one of the most important is the proper alignment of chromosomes along the bipolar spindle. To aid in this process is the specialized protein complex known as the kinetochore, which serves as the direct interface between the spindle microtubules and the chromosomes (Cheeseman and Desai, 2008).

The kinetochore is built upon the portion of the chromosome known as the centromere (Cleveland et al., 2003). The centromere is the segment of chromatin defined by the presence of the histone variant CENP-A, a protein which is required for the localization and formation of the kinetochore (Black and Cleveland, 2011). In all species tested, from fungi to metazoans, CENP-A null mutants are completely inviable (Meluh et al., 1998; Howman et al., 2000; Takahashi et al., 2000; Blower and Karpen, 2001; Oegema et al., 2001; Goshima et al., 2003; Regnier et al., 2005). Once CENP-A has been incorporated into the chromatin one of the first kinetochore proteins to localize to the centromere is CENP-C, a highly conserved protein which plays an integral role in shaping structure of the inner kinetochore (Tomkiel et al., 1994). Other proteins involved in inner kinetochore assembly include KNL-1 (Cheeseman et al., 2008), KNL-2 (Maddox et al., 2007), the Mis12 complex

(Screpanti et al., 2011), the Mis18 complex (Hayashi et al., 2004) and members of the CCAN (constitutive centromere-associated network). The CCAN, originally discovered in human cells, is composed of CENP-C and 13 other proteins (CENP-H, CENP-I and CENP-K-U) and is well conserved in vertebrates (Obuse et al., 2004; Foltz et al., 2006; Okada et al., 2006; Izuta et al., 2006). A majority of the CCAN proteins have been discovered in fungi, however in both *C. elegans and Drosophila* no CCAN proteins except for CENP-C have been found (Cheeseman and Desai, 2008).

Built upon the inner kinetochore is the outer kinetochore, which serves as the major binding site for spindle microtubules (Kline-Smith et al., 2005). Outer kinetochore proteins include, but are not limited to, the Ndc80 complex (Tooley and Stukenberg, 2011), the RZZ (Rod-Zw10-Zwilch) complex (Karess, 2005), CENP-F (Feng et al., 2006), Spindly (Griffis et al., 2007), the Ska (Ska1-Ska2) complex (Guimaraes and DeLuca, 2009) and the spindle assembly checkpoint proteins (described in section 1.1.2). While a majority of the outer kinetochore components are conserved across species, the hierarchy of recruitment as well as the various feedback mechanisms in place during microtubule capture differ, to varying degrees, from fungi to vertebrates. Briefly, in all species tested, the Ndc80 complex is essential for kinetochore-microtubule interactions (Wigge and Kilmartin, 2001; DeLuca et al., 2002; Desai et al., 2003; McCleland et al., 2003) and together with KNL-1 and Mis12 forms the KMN network, which has been suggested to be the core microtubule attachment site on the kinetochore (Cheeseman et al., 2006;

Tanaka, 2013). Outside of the KMN network, the remaining outer kinetochore proteins all play various different roles in coupling dynamic microtubule chromosome capture to chromosome movement in order to get to an eventual state of biorientation along the metaphase plate. Instrumental in this process in metazoans is the kinesin CENP-E (Abrieu et al., 2000) and minus-end directed microtubule motor protein dynein and its cofactor dynactin (Bader and Vaughan, 2010), which require both Spindly and the RZZ complex for recruitment to kinetochores (Griffis et al., 2007; Gassmann et al., 2008; Yamamoto et al., 2008; Chan et al., 2009). In addition to being required for proper chromosome-microtubule attachments, the dynein/dynactin complex also plays a key role in allowing progression into anaphase once all chromosomes have bioriented by removing the spindle assembly checkpoint proteins from the kinetochore (Gassmann et al., 2010).

1.1.2 The spindle assembly checkpoint

The spindle assembly, or mitotic, checkpoint is an evolutionarily conserved pathway responsible for monitoring the state of the kinetochore-microtubule attachments (Lara-Gonzalez et al., 2012). The role of the SAC is to delay cell cycle progression until all chromosomes are properly oriented along the bipolar spindle. The proteins responsible for the SAC localize to the outer kinetochore during prometaphase and remain there until they are removed right before anaphase onset. It has previously been shown that a

single unattached kinetochore is enough to maintain the checkpoint-mediated cell cycle delay (Rieder et al., 1995).

The spindle assembly checkpoint was first discovered in budding yeast in two separate screens for genes involved in mitotic progression. The mitotic arrest deficient (Mad) (Li and Murray, 1991) and the budding uninhibited by benomyl (Bub) (Hoyt et al., 1991) genes both play key roles in mediating spindle assembly checkpoint function. These genes are conserved from yeast to metazoans but comprise only part of the spindle assembly checkpoint. Kinases such as Mps1 (Weiss and Winey, 1996) and Aurora B (Biggins and Murray, 2001) are also pivotal for proper checkpoint signaling and in higher eukaryotes the checkpoint has evolved to include the function of additional proteins for its regulation, such as the RZZ complex, CENP-E and dynein, to name a few (Musacchio and Salmon, 2007).

The spindle assembly checkpoint elicits its function by inhibiting the major protein complex responsible for exit from mitosis, the anaphase promoting complex/cyclosome (APC/C) (Peters, 2006; Pines, 2006). The SAC specifically targets Cdc20 (Hwang et al., 1998; Kim et al., 1998), which is required for the activation of the APC/C (Peters, 2006). By binding directly to Cdc20, the SAC prevents activation of the APC/C until all the chromosomes have successfully bioriented. Once activated the APC/C, an E3 ubiquitin ligase, targets two major mitotic proteins for destruction by the 26S proteasome: Cyclin B and securin (Thornton and Toczyski, 2003). Cyclin B activates the master mitotic kinase CDK1 (Cyclin-dependent kinase 1), and

securin inhibits the enzyme separase, the role of which is to cleave the cohesin complex that normally holds sister chromatids together. Both Cyclin B degradation and separase-mediated cleavage of cohesin are required for the metaphase to anaphase transition and subsequent mitotic exit.

1.1.3 The metaphase-to-anaphase transition

Arguably one of the most important steps in mitosis is the transition from one plate of fully aligned chromosomes at metaphase to two equally separated aggregates of sister chromatids at anaphase. The metaphase-to-anaphase transition is tightly regulated to ensure that chromosome segregation occurs faithfully with each new daughter cell receiving the correct 1:1 complement of genetic material (**Fig. 2**). Progression into anaphase requires two major signaling events- degradation of Cyclin B and separase-mediated cleavage of cohesin. Both events are controlled by the activation of the APC/C. Once the APC/C is activated by the silencing of the spindle assembly checkpoint, Cyclin B and securin are quickly degraded allowing the cell to enter anaphase.

Cyclin B is responsible for activation of the major mitotic kinase, CDK1, and was first discovered in frog egg extracts (Murray and Kirschner, 1989). Cyclin B levels are tightly transcriptionally regulated during the cell cycle, beginning in S phase and peaking just before the start of mitosis in G2 (Hwang et al., 1995). The number of proteins targets phosphorylated by active Cyclin B-CDK1 complex is expansive and include proteins involved in such

processes as chromosome condensation, chromosome cohesion and dissolution, assembly of the mitotic spindle, attachment of chromosomes to the spindle, spindle elongation and separation of chromosomes, mitotic exit and cytokinesis (Lindqvist et al., 2009). Cyclin B mutants unable to be targeted for degradation markedly prolong the cell cycle (Gallant et al., 1992; Holloway et al., 1993), highlighting just how important regulation of Cyclin B is for the proper timing of mitosis.

Prior to their separation at anaphase, sister chromatids are held together by the multi-protein complex cohesin (Peters et al., 2008; Onn et al., 2009). Cohesin is loaded along the length of each pair of sister chromatids in S phase (Uhlmann, 2009) and is removed via a two-step process during mitosis (**Fig. 2**). The cohesin along the arms of sister chromatids is removed by a non-proteolytic pathway in prophase that requires both the conserved protein Wapl and Polo-like kinase 1 (Hauf et al., 2005; Shintomi and Hirano, 2009). Centromeric cohesin is protected from this pathway and is catalytically cleaved at the onset of anaphase by the protease separase. Prior to the metaphase-to-anaphase transition, separase is held inactive due to binding of its inhibitor securin. Degradation of securin by activation of the APC/C assures that sister chromatids will remain together until all chromosomes are properly bioriented along the metaphase spindle (Hauf et al., 2001). Timing the coordinated loss of chromatid cohesion to full alignment in metaphase prevents the precocious separation of sister chromatids thus safeguarding the cell against a missegregation event.

1.2 Mitosis and cancer

Cancer, by its very definition, results from uncontrolled cell divisions. Most cancer cells acquire mutations that allow them to override the cell cycle machinery and proliferate unrestrained (Sherr, 2000; Malumbres and Barbacid, 2001; Jallepalli and Lengauer, 2001; Massague 2004). As cancer cells continue to divide without checkpoint control, errors in mitosis become more frequent and a majority of solid tumor cells exhibit genome instability (Bakhoum and Compton, 2012). The degree of chromosomal instability seen in most tumors ranges from a single translocated chromosome to more complex chromosome rearrangements, as well as the complete loss or gain of whole or parts of chromosomes (McGranahan et al., 2012). Although there is still debate over whether chromosomal instability drives tumor formation or is a consequence of such, abnormal chromosome content, or aneuploidy, remains one of the most common hallmarks of cancer (Holland and Cleveland, 2012).

1.2.1 The role of mitotic genes in tumorigenesis

Given the high prevalence of chromosomal instability in solid tumors, a substantial amount of research has been done trying to characterize the role of mitotic genes in the development and/or progression of cancer. This work has focused mainly on two aspects- determining the frequency of mitotic gene mutations in human tumor samples (Pérez de Castro et al., 2007) and utilizing

mice to determine the tumorigenic ability of a compromised mitotic gene function (Schvartzman et al., 2010).

A survey of a vast array of tumor samples revealed that while not as prevalent as mutations in classic cancer genes, such as Rb or p53, a variety of tumor types do possess mutations in key regulators of the mitotic cell cycle (Pérez de Castro et al., 2007). These genes include major regulatory kinases, such as Aurora A (Bischoff et al., 1998; Sen et al., 2002; Gritsko et al., 2003; Katayama et al., 1999; Li et al., 2003; Miyoshi et al., 2001; Sakakura et al., 2001), Aurora B (Bischoff et al., 1998; Chieffi et al., 2006; Araki et al., 2004; Smith et al., 2005; Chieffi et al., 2005; Sorrentino et al., 2005), CDK1 (Kallakury et al., 1997; Soria et al., 2000; Takeno et al., 2002) and PLK1 (Strebhardt and Ullrich, 2006), which are all over-expressed in a wide variety of tumors. Altered expression of kinetochore proteins CENP-F (Pimkhaokham et al., 2000; Zirn et al., 2006; Grützmann et al., 2004), ROD and HEC1 (NDC80) (Pérez de Castro et al., 2007) has also seen in a broad range of tumor types. Interestingly, the expression of many spindle assembly checkpoint proteins, BUB1 (Lin et al., 2002; Yuan et al., 2006; Moreno-Bueno et al., 2003; Grabsch et al., 2003), BUBR1 (Grabsch et al., 2003; Yuan et al., 2006), MAD1 (Nishigaki et al., 2005; Han et al., 2000) and MAD2 (Hernando et al., 2004; Yuan et al., 2006), is also modified, however in some cases the expression is reduced while in others it is increased. Although a majority of the mitotic genes displaying abnormal levels of expression have been shown to be regulated by the E2F family of transcription factors (Ren et al., 2002) and

therefore may be influenced by precedent mutations in the Rb pathway (Hernando et al., 2004), it does not discount the fact that the dysregulation of genes required for an accurate mitosis can aid in the progression of cancer.

To gain better insight into the direct role that aberrant mitotic gene function may have in tumor formation, myriad studies have been done in mice involving the under or over expression of a variety of key mitotic regulators (Schvartzman et al., 2010). Most of the genes involved in ensuring an accurate mitosis are required for viability, therefore a majority of the research investigating the tumor suppressive behavior of mitotic genes has been done on mice expressing a single copy of the gene of interest. Mice heterozygous for *Cenp-E* (Weaver et al., 2007), *Mad2* (Michel et al., 2001; Chi et al., 2009), *Mad1* (Iwanaga et al., 2007; Chi et al., 2009), *Cdh1* (Garcia-Higuera et al., 2008) or *Plk4* (Ko et al., 2005), as well as mice expressing a hypomorphic allele of *Bub1* (Schliekelman et al., 2009) show an increased incidence of spontaneous, late-onset tumor formation in the lymph nodes, as well as in the lung and liver. In addition mice expressing a single copy of a *Cdc20* mutant unable to bind to Mad2 are also prone to tumor formation (Li et al., 2009). However, these results do not represent a general relationship between mitotic gene haploinsufficiency and tumor formation as mice heterozygous for *BubR1* (Baker et al., 2004) or *Bub3* (Kalitsis et al., 2000) show no increased incidence in spontaneous tumor formation.

Since over expression rather than under expression of mitotic genes is more commonly seen in human tumors, research has also been aimed at

better understanding the oncogenic potential of a variety of genes involved in the mitotic program. Forced over expression of Mad2 (Sotillo et al., 2010) or Hec1 (Ndc80) (Diaz-Rodriguez et al., 2008) results in widespread tumor formation. Targeted over expression of Aurora A in mouse mammary epithelial cells causes increased proliferation and branching morphogenesis, leading to the development of mammary tumors (Wang et al., 2006). While the degree of tumor formation in the cases cited above is not as severe as that seen in mice over expressing more well-characterized oncogenes, such as Myc or Ras, these studies still indicate that tumors can form as a result of improper control of the mitotic cell cycle.

Overall the studies in both human tumor samples as well as in mice clearly point to an involvement of mitotic gene dysregulation in the progression of cancer. Although it is evident that chromosomal instability is a distinguishing feature of cancer cells, more work needs to be done to better understanding the mechanism responsible for its presence.

1.2.2 Chemotherapeutics aimed at targeting the mitotic machinery

The field of cancer chemotherapy has seen many advances since its implementation in the 1940s with the discovery of nitrogen mustard and folate analogs as antiproliferative agents (Chabner and Roberts, 2005). Although research is currently more focused on targeted chemotherapy, broad-spectrum inhibitors of basic cellular functions, such as DNA synthesis or mitosis, are still widely used as effective treatment for a variety of cancers.

The anti-mitotic drugs first gained notoriety in the early 1960s with the discovery of the *Vinca* alkaloids and the taxanes. This class of drugs elicits its antitumor activity by targeting tubulin, the building block of microtubules. Direct binding to tubulin interferes with microtubule dynamics, inhibits cell division and eventually leads to the death of the cell (Jordan and Wilson, 2004; Zhou and Giannakakou, 2005). While taxol (paclitaxel) is still one of the most widely prescribed anti-mitotic cancer drugs on the market, its efficacy spans a broad range depending on tumor type and since the biggest side effect is neurotoxicity (Boyette-Davis et al., 2013), many researchers are focused on finding new drug targets that inhibit mitosis. While the *Vinca* alkaloids and taxane are still the only drugs with FDA approval, the list of anti-mitotic drugs currently in clinical trials is expansive (Chan et al., 2012). The protein targets are diverse and include kinetochore proteins, mitotic kinases and the proteasome, as well as other spindle proteins such as microtubule-associated motor proteins (Schmidt and Bastians, 2007; Rao et al., 2012).

Given the predominance of the pursuit to find new, drugable mitotic protein targets in the field of cancer research, another aspect researchers are concentrating on is trying to better understand the cellular response to anti-mitotic drugs. Ideally, treatment with an anti-mitotic drug would result in an initial arrest of the cell cycle followed by death of the cell while still in mitosis. Unfortunately this is not the case, as different cell types, as well as different types of anti-mitotic drugs show a varied response. While the universal response to treatment with an anti-mitotic drug is a mitotic arrest, the

subsequent fate of the cell can be one of many outcomes. The cell can 1) remain chronically arrested in mitosis until the drug is removed, 2) die in mitosis or 3) reenter the cell cycle and either a) die in interphase, b) cease to proliferate and senesce or c) reproduce as an aneuploid cell (Rieder, 2004; Yamada and Gorbsky, 2005). A recent paper highlighted just how varied the cellular response to anti-mitotic drugs is by showing that different cell lines show both inter- and intra-line variation to the same drug (Gascoigne and Taylor, 2008). Many studies have been done to try to explain this difference at a molecular level, however no clear consensus has been achieved (Longley et al., 2005; Komlodi-Pasztor et al., 2012). Much like its role in tumor formation, the role of mitotic regulation in cancer chemotherapy is more complex than was once thought and thus continues to be at the forefront of cancer research.

1.3 *C. elegans* as a model system

The nematode species *Caenorhabditis elegans* has long been used as a model system to help answer some of the greatest questions in biology (Brenner, 2009). *C. elegans* is a hermaphroditic species, adults possess both male and female gametes and are thus capable of self-fertilization. From initial hatching to adulthood takes about 3 days; the worm develops through four larval stages before reaching reproductive capacity (**Fig. 3A**; Riddle et al., 1997). A single adult worm can produce nearly 300 progeny due to a limited number of sperm, however if mated to a male that number increases 4 – 5-fold (Hall and Altun, 2008). This relatively quick generation time, as well as the

ease of genetic manipulation, has made *C. elegans* an attractive model system for a diverse group of fields. In the 40+ years since Sydney Brenner pioneered the use of *C. elegans* as a multi-cellular organism with which to conduct research, myriad breakthroughs in many areas of biological research have occurred. One such field is cell biology, with many researchers employing *C. elegans* to explore the driving force behind such critical processes as mitotic (Oegema and Hyman, 2006) and meiotic (Lui and Colaiácovo, 2013) division of the cell.

1.3.1 The adult *C. elegans* germline

Given the fact that the germline is the sole tissue responsible for the production of gametes, germline development in *C. elegans* is a well-studied process (Hubbard and Greenstein, 2000). The germline develops from two primordial germ cells designated early on in embryogenesis into roughly 1000 cells in the fully formed germline of an adult worm (Hubbard and Greenstein, 2005). The adult *C. elegans* germline (**Fig. 3B**) consists of two identical U-shaped gonad arms. The structure of each arm is a syncitium wherein each nucleus is partially membrane enclosed leaving one side open to the common maternal cytoplasm. The *C. elegans* germline displays spatial organization; mitotic divisions occur in the distal region, which contains the germline stem cells (Kimble and Crittenden, 2005) that generate all the nuclei that undergo meiosis to generate oocytes, which are produced at the proximal end of the gonad. Directly adjacent to the oocytes, at the most proximal edge of the

germline, is the spermatheca. Each spermatheca contains around 150 sperm that were produced during the early L4 larval stage of development when the germline undergoes a limited period of spermatogenesis (L'Hernault, 2006) before permanently switching to the oogenic program.

Of the 1000 nuclei in the adult germline, an estimated 25% makeup the stem cell or mitotic zone located at the distal tip (Crittenden et al., 2006). The size of this region does not diminish over time indicating these nuclei are undergoing constant self-renewal to replenish nuclei that have exited the region and entered into the meiotic program. As nuclei exit the distal tip, they undergo one last round of DNA replication prior to their entry into meiosis. As nuclei travel proximally down the gonad arm they undergo various stages of meiotic prophase I (Greenstein, 2005).

The initial stages of meiotic prophase, leptotene and zygotene, occur in the transition zone directly adjacent to the mitotic tip. During this time chromosomes become tethered to the nuclear envelope, resulting in the distinct crescent nuclear morphology attributed to this region (Penkner et al., 2007). Localization of chromosomes to the nuclear envelope is thought to aid in the homology search and capture process required for proper chromosome pairing and synapsis (Penkner et al., 2009; Sato et al., 2009). *C. elegans* chromosomes are unique in that they pair through a specialized DNA-protein complex called the pairing center (MacQueen et al., 2005; Phillips et al, 2005; Phillips and Dernburg, 2006). The pairing center consists of a repetitive stretch of DNA at one end of the chromosome bound by one of four Zn-finger proteins

(ZIM-1, ZIM-2, ZIM-3 and HIM-8). Once homologous chromosomes pair, the synaptonemal complex begins to polymerize. The synaptonemal complex is a tripartite proteinaceous structure that assembles along the lengths of homologous chromosomes (Colaiácovo, 2006) holding them together to allow for the proper completion of recombination, which is also initiated during the early stages of meiotic prophase I (Dernburg et al., 1998). Recombination is fully complete by the pachytene stage, at which point the synaptonemal complex disassembles and the chromosomes remained linked through their crossover sites, now called chiasmata- a hallmark of the diplotene stage. The chromosomes then maximally condense to become diakinetic nuclei, which are then packaged into oocytes.

1.3.2 Homologous recombination

One of the most important processes in meiosis is the successful completion of homologous recombination (Villeneuve and Hillers, 2001). This is due not only for its ability to introduce genetic diversity into a population but also for its central role in the reductional divisions that generate gametes in sexually reproducing organisms. Meiotic recombination is initiated by deliberate double-strand breaks, which are catalyzed by the type II topoisomerase-like enzyme Spo11 (Keeney et al., 1997). Spo11 is highly evolutionarily conserved and in all species tested is essential for recombination (Keeney, 2001). Immediately following break formation, sets of repair proteins successively localize to the lesion resulting in the resection of

one strand of the double-strand break (Filippo et al., 2008). Once resected, strand exchange proteins, such as Rad51 and accessory factors such as Rad54, localize to the single-strand piece of DNA and promote invasion of the single strand to the homolog for repair (Krejci et al., 2012). Successful completion of this process results in crossover formation between a set of homologous chromosomes. Because the homologs are now physically linked through chiasmata, alignment at metaphase I of meiosis results in homologous chromosomes becoming orientated towards opposite poles (Schvarzstein et al., 2010). This alignment causes a reductional division at anaphase I by separating the homologous chromosomes, followed by an equational division at anaphase II by separating the sister chromatids. Therefore, without the successful completion of homologous recombination, meiotic missegregation will occur and result in the production of inviable, aneuploid gametes.

1.3.3 Germline cell death

Since the germline is tasked with the responsibility of generating the gametes that makeup the next generation, it is crucial that the integrity of the genome in the germline be properly maintained. Just prior to the packaging of nuclei into oocytes, if too many nuclei exist or are somehow unfit these nuclei are removed by programmed cell death (Guimenny et al., 1999). In a unperturbed, wild type background over half of all nuclei produced by the germline are eliminated via programmed cell death in an effort to maintain oocyte quality (Andux and Ellis, 2008). Germline cell death signals through the

same canonical pathway responsible for somatic cell death (**Fig. 4**; Conradt and Xue, 2005). Briefly, cell death is caused by the activation of the caspase-like protein CED-3 by the Apaf-1 homolog CED-4. The Bcl-2 family member CED-9 binds CED-4 and inhibits CED-4's ability to bind to and activate CED-3, thereby protecting cells from death. In somatic cells that are fated to die, the BH3-only protein, EGL-1, is transcriptionally upregulated, binds to CED-9 and inhibits CED-9's ability to bind to CED-4, which allows CED-4 to bind CED-3, thereby promoting cell death; in germline cells fated to die, however, the mechanism by which CED-9 suppression is relieved to activate the pathway still remains unclear. It has been shown though that a functional Ras/MAPK pathway is required for germline cell death (Guimenny et al., 1999).

While a substantial number of nuclei with no discernable defects are removed via programmed cell death in an unperturbed background, it has been shown that nuclei possessing damaged DNA or resulting from defects in meiosis are preferentially eliminated. DNA damaging agents such as hydroxyurea, N-nitroso-N-ethylurea (ENU) and radiation, both ultraviolet and gamma, have all been shown to cause an increase in the levels of cell death in the *C. elegans* germline (Gartner et al., 2000; Garcia-Muse and Boulton, 2005; Stergiou et al., 2007) . DNA damaged-induced cell death signals through a conserved checkpoint (**Fig. 4**). Genes involved in this pathway include kinases ATM-1 and ATL-1, as well as the 9-1-1 complex (HPR-9/MRT-2/HUS-1), CLK-2 and CEP-1^{p53} (Stergiou and Hengartner, 2004). Similar to somatic cell death, yet unlike physiological germline cell death, the DNA

damage checkpoint-induced cell death requires EGL-1. CEP-1^{p53} transcriptionally upregulates both EGL-1 and related BH3-only protein, CED-13, to activate the canonical cell death pathway (Greiss et al., 2008).

In addition to exogenous agents causing in an increase in germline cell death, it has also been shown that failure to properly complete key aspects of meiotic prophase I, such as homologous pairing, synaptonemal complex formation and recombination, results in a similar increase (Gartner et al., 2000; MacQueen et al., 2002; Colaiácovo et al., 2003; Bhalla and Dernburg, 2005; Harper et al., 2011). The death seen in these instances signals either through the DNA damage checkpoint or the pairing/synapsis checkpoint, which is the other germline checkpoint responsible for detecting meiotic errors. As opposed to the DNA damage checkpoint which is activated by unrepaired DNA breaks, the pairing/synapsis checkpoint is more specific in that it requires both the presence of a functional pairing center as well complete chromosome asynapsis (Bhalla and Dernburg, 2005; Harper et al., 2011). The pairing/synapsis checkpoint also signals through a different upstream effector-the AAA-ATPase PCH-2 (Bhalla and Dernburg, 2005). Overall, cell death in the *C. elegans* germline is a well-characterized process and continues to be a great system in which to investigate the how cellular defects are sensed in the context of a complex tissue.

In summary, the fundamental goal of this thesis work is to better understand the consequences of mitotic defects, both in the *C. elegans* germline and in human tissue culture cells. Gaining a more complete

understanding of how errors in mitosis are sensed, especially if and how they signal to cell death, allows for the potential discovery of new, more effective drugs targets in the treatment of cancer.

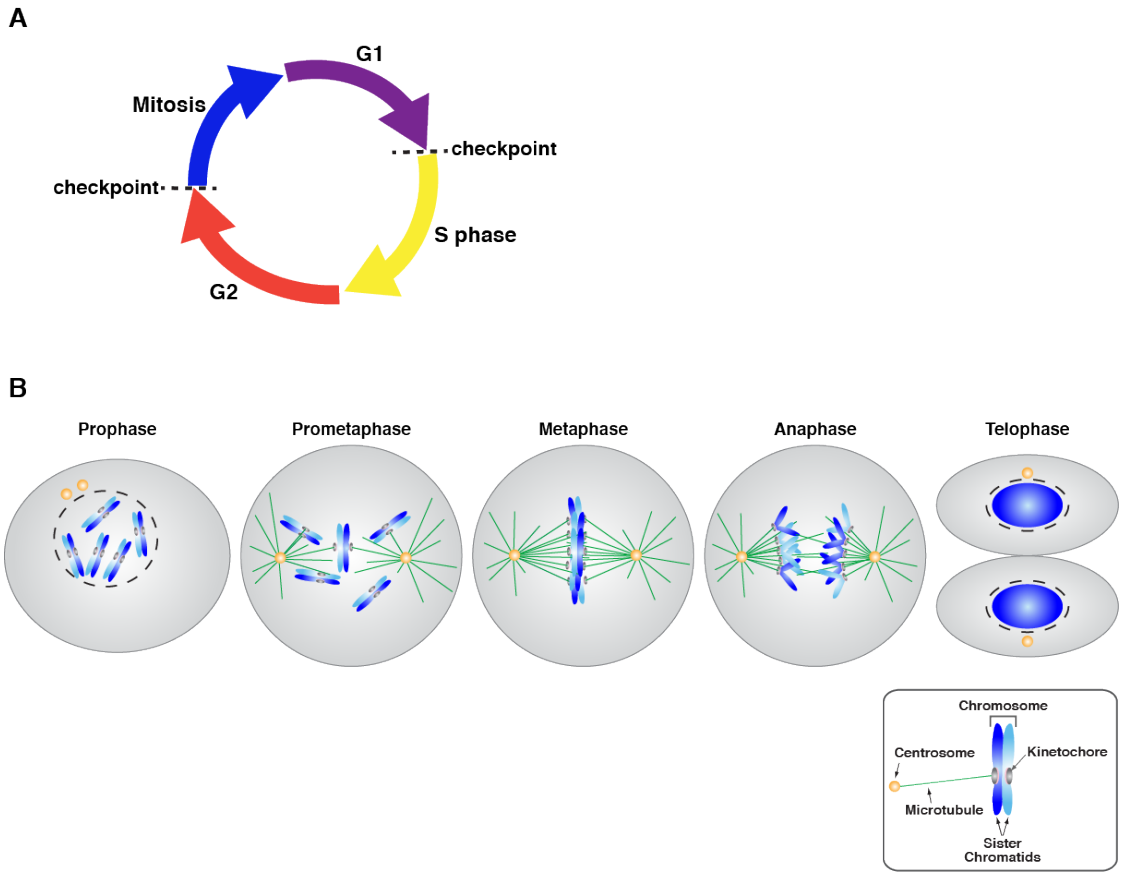

Figure 1.1 The cell cycle and the stages of mitosis. (A) The cell cycle consists of four stages, G1, S, G2 and Mitosis, and two inter-stage checkpoints, at the transition from G1 to S and G2 to M. A newly divided cell undergoes a short growth phase before DNA replication occurs in S phase. After DNA replication, the cell enters another short growth phase before entering mitosis. **(B)** The start of mitosis begins with nuclear envelope breakdown and chromosome condensation in prophase, followed by formation of the bipolar spindle in prometaphase. Metaphase marks the stage at which all chromosomes are properly aligned along the spindle and occurs just before chromosomes are separated in anaphase. At telophase, chromosomes begin to decondense and the nuclear envelope is reformed.

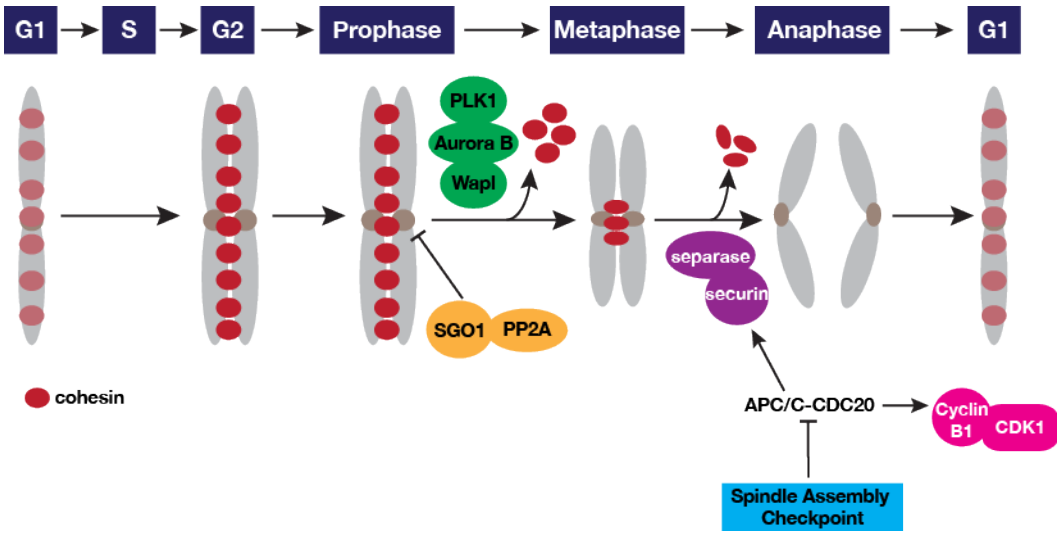

Figure 1.2 Cohesin removal pathways and exit from mitosis. Cohesin begins to associate with chromatin in G1 and is loaded between newly replicated sister chromatids during S phase. Arm cohesion is removed early in mitosis during prophase and requires the activity of PLK1, Aurora B and Wapl. Centromeric cohesin is protected from this removal by Shugoshin (SGO1) and PP2A and is only removed at the metaphase-to-anaphase transition when separase becomes active due to silencing of the spindle assembly checkpoint. Spindle assembly checkpoint silencing activates the APC/C, which then degrades both securin and Cyclin B, allowing for mitotic exit.

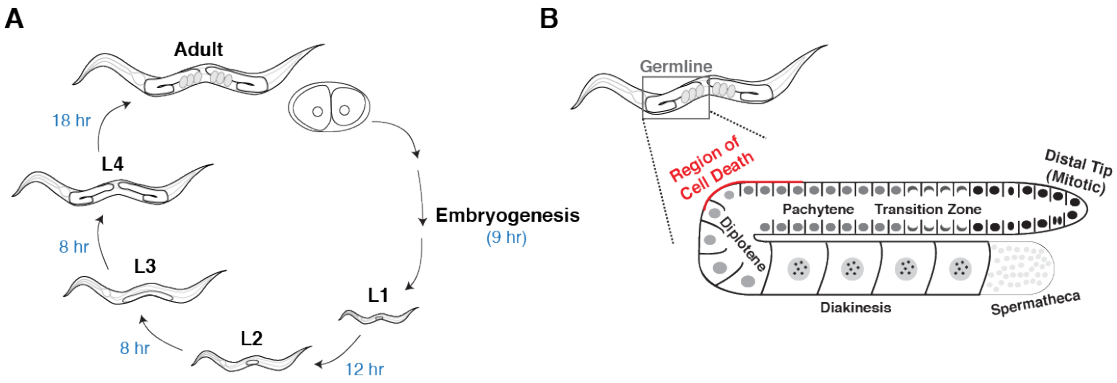

Figure 1.3 The *C. elegans* life cycle and the adult germline. (A) A newly laid embryo takes roughly three days to reach adulthood at 20°C, developing through four discernable larval stages. **(B)** The adult *C. elegans* germline consists of two U-shaped gonad arms. Nuclei at the distal tip are undergoing mitosis and switch to the meiotic program upon exit from this region. The transition zone contains nuclei in the early stages of meiotic prophase I; more proximally, nuclei are in the pachytene stage of meiosis and then pass through diplotene before being packaged into oocytes as diakinetic nuclei. Directly adjacent to the oocytes is the spermatheca. The region of cell death occurs in late pachytene, just prior to oocyte packaging.

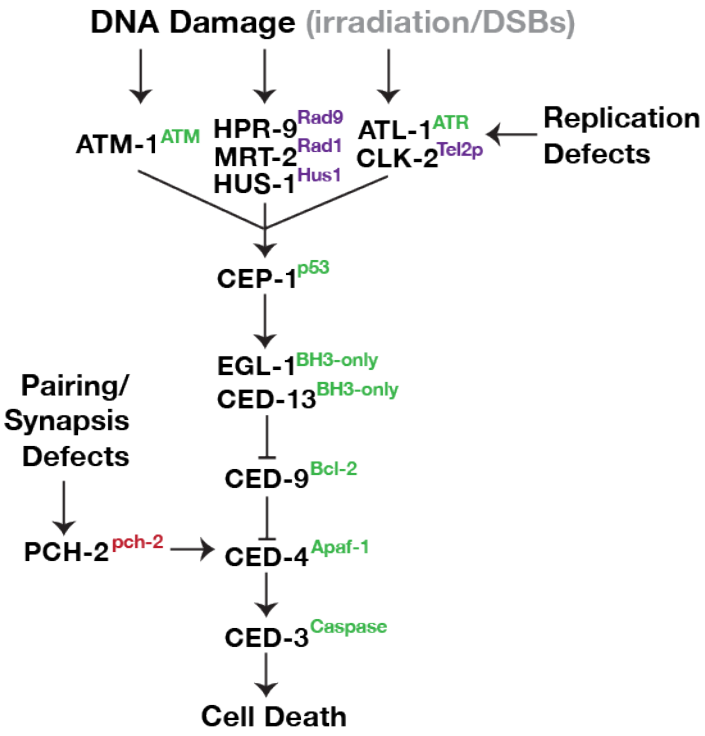

Figure 1.4 Cell death pathways in the *C. elegans* germline. All germline cell death signals through the canonical downstream pathway, CED-9-CED-4-CED-3. The DNA damage pathway can be activated by a variety of upstream sensors, which are not mutually exclusive. Replication defects, however, are only sensed by ATL-1 or CLK-2. All pathways converge at CEP-1, which then transcriptionally upregulates both EGL-1 and CED-13 to promote cell death. Defects in pairing and/or synapsis are sensed by a specific pathway, which requires the activity of the AAA-ATPase PCH-2. Homologues are listed in superscript: green- mammalian, purple- *S. pombe*, red- *S. cerevisiae*.

REFERENCES

Abrieu A, Kahana JA, Wood KW, Cleveland DW (2000) CENP-E as an essential component of the mitotic checkpoint in vitro. Cell 102:817-26.

Andux S, Ellis RE (2008) Apoptosis maintains oocytes quality in aging *Caenorhabditis elegans* females. PLoS Genetics 4:e1000295.

Araki K, Nozaki K, Ueba T, Tatsuka M, Hashimoto N (2004) High expression of Aurora-B/Aurora and Ipl1-like midbody-associated protein (AIM-1) in astrocytomas. Journal of Neurooncology 67:53-64.

Bader JR, Vaughan KT (2010) Dynein at the kinetochore: timing, interactions and functions. Seminars in Cell and Developmental Biology 21:269-75.

Baker DJ, Jeganathan KB, Cameron JD, Thompson M, Juneja S, Kopecka A, Kumar R, Jenkins RB, de Groen PC, Roche P, van Deursen JM (2004) BubR1 insufficiency causes early onset of aging-associated phenotypes and infertility in mice. Nature Genetics 36:744-9.

Bakhoum SF, Compton DA (2012) Chromosomal instability and cancer: a complex relationship with therapeutic potential. Journal of Clinical Investigation 122:1138-43.

Bartek J, Lukas C, Lukas J (2004) Checking on DNA damage in S phase. Nature Reviews Molecular Cell Biology 5:792-804.

Bhalla N, Dernburg AF (2005) A conserved checkpoint monitors meiotic chromosome synapsis in *Caenorhabditis elegans.* Science 310:1683-6.

Biggins S, Murray AW (2001) The budding yeast protein kinase Ipl1/Aurora allows the absence of tension to activate the spindle checkpoint. Genes and Development 15:3118-29.

Bischoff JR, Anderson L, Zhu Y, Mossie K, Ng L, Souza B, Schryver B, Flanagan P, Clairvoyant F, Ginther C, Chan CS, Novotny M, Slamon DJ, Plowman GD (1998) A homologue of *Drosophila* aurora kinase is oncogenic and amplified in human colorectal cancers. EMBO Journal 17:3052-65.

Black BE, Cleveland DW (2011) Epigenetic centromere propagation and the nature of CENP-A nucleosomes. Cell 144:471-79.

Blower MD, Karpen GH (2001) The role of *Drosophila* CID in kinetochore formation, cell-cycle progression and heterochromatin interactions. Nature Cell Biology 3: 730–739.

Bornens M (2012) The centrosome in cells and organisms. Science 335:422-26.

Boyette-Davis JA, Cata JP, Driver LC, Novy DM, Bruel BM, Mooring DL, Wendelschafer-Crabb G, Kennedy WR, Dougherty PM (2013) Persistent chemoneuropathy is patients receiving the plant alkaloids paclitaxel and vincristine. Cancer Chemotherapy and Pharmacology 71:619-26.

Brenner S (2009) In the beginning was the worm. Genetics 182:413-15.

Chabner, B, Roberts, T. (2005) Chemotherapy and the war on cancer. Nature Reviews Cancer 5:65-72.

Chan KS, Koh CH, Li Y (2012) Mitosis-targeted anti-cancer therapies: where they stand. Cell Death and Disease 3:e411.

Chan Y, Fava LL, Uldschmid A, Schmitz MH, Gerlich DW, Nigg E, Santamaria A (2009) Mitotic control of kinetochore-associated dynein and spindle orientation by human Spindly. Journal of Cell Biology 185: 859–874.

Cheeseman IM, Chappie JS, Wilson-Kubalek EM, Desai A (2006) The conserved KMN network constitutes the core microtubule-binding site of the kinetochore. Cell 127:983-97.

Cheeseman IM, Desai A (2008) Molecular architecture of the kinetochore-microtubule interface. Nature Reviews Molecular Cell Biology 9:33-46.

Cheeseman IM, Hori T, Fukagawa T, Desai A (2008) KNL1 and the CENP-H/I/K complex coordinately direct kinetochore assembly in vertebrates. Molecular Biology of the Cell 19:587-94.

Chi YH, Ward JM, Cheng LI, Yasunaga J, Jeang KT (2009) Spindle assembly checkpoint and p53 deficiencies cooperate for tumorigenesis in mice. International Journal of Cancer 124:1483-9.

Chieffi P, Cozzolino L, Kisslinger A, Libertini S, Staibano S, Mansueto G, De Rosa G, Villacci A, Vitale M, Linardopoulous S, Portella G, Tramontano D (2006) Aurora B expression directly correlates with prostate cancer malignancy and influence prostate cancer proliferation. Prostate 66:326-33.

Chieffi P, Troncone G, Caleo A, Libertini S, Linardopoulos S, Tramontano D, Portella G (2004) Aurora B expression in normal testis and seminomas. Journal of Endocrinology 181:263-70.

Cleveland DW, Mao Y, Sullivan KF (2003) Centromeres and kinetochores: from epigenetics to mitotic checkpoint signaling. Cell 112:407-421.

Colaiácovo MP (2006) The many facets of SC function during *C. elegans* meiosis. Chromosoma 115:195-211.

Colaiácovo MP, MacQueen AJ, Martinez-Perez E, McDonald K, Adamo A, La Volpe, A, Villeneuve AM (2003) Synaptonemal complex assembly in *C. elegans* is dispensable for loading strand-exchange proteins but critical for proper completion of recombination. Developmental Cell 5:463-74.

Conradt B, Xue D (2005) Programmed cell death. Wormbook.

Crittenden SL, Leonhard KA, Byrd DT, Kimble J (2006) Cellular analysis of the mitotic region in the *Caenorhabditis elegans* adult germ line. Molecular Biology of the Cell 17:3051-61.

DeLuca JG, Moree B, Hickey JM, Kilmartin JV, Salmon ED (2002) hNuf2 inhibition blocks stable kinetochore-microtubule attachment and induces mitotic cell death in HeLa cells. Journal of Cell Biology 159:549-55.

Desai A, Rybina S, Müller-Reichert T, Shevchenko A, Shevchenko A, Hyman A, Oegema K (2003) KNL-1 directs assembly of the microtubule-binding interface of the kinetochore in *C. elegans*. Genes and Development 17:2421-35.

Diaz-Rodriguez E, Sotillo R, Schvartzman JM, Benezra R (2008) Hec1 overexpression hyperactivates the mitotic checkpoint and induces tumor formation *in vivo*. Proc. Natl Acad. Sci. USA 105:16719–16724.

Feng J, Huang H, Yen TJ (2006) CENP-F is a novel microtubule-binding protein that is essential for kinetochore attachments and affects the duration of the mitotic checkpoint delay. Chromosoma 115:320-29.

Filippo JS, Sung P, Klein H (2007) Mechanisms of eukaryotic homologous recombination. Annual Review of Biochemistry 77:229-57.

Foltz DR, Jansen L, Black BE, Bailey AO, Yates JR, Cleveland DW (2006) The human CENP-A centromeric nucleosome-associated complex. Nature Cell Biology 8:458-69.

Gallant P, Nigg EA (1992) Cyclin B2 undergoes cell cycle-dependent nuclear translocation and, when expressed as a non-destructible mutant, causes mitotic arrest in HeLa cells. Journal of Cell Biology 117:213-224.

García-Higuera I, Manchado E, Dubus P, Cañamero M, Méndez J, Moreno S, Malumbres M (2008) Genomic stability and tumor suppression by the APC/C cofactor Cdh1. Nature Cell Biology 10:802-11.

Garcia-Muse T, Boulton SJ (2005) Distinct modes of ATR activation after replication stress and DNA double-strand breaks in *Caenorhabditis elegans*. EMBO Journal 24:4345-55.

Gascoigne KE, Taylor SS (2008) Cancer cells display profound intra- and interline variation following prolonged exposure to antimitotic drugs. Cancer Cell 14:111-22.

Gassmann R, Essex A, Hu JS, Maddox P, Motegi F, Sugimoto A, O'Rourke S, Bowerman B, McLeod I, Yates J, Oegema K, Cheeseman IM, Desai A (2008) A new mechanism controlling kinetochore-microtubule interactions revealed by comparison of two dynein-targeting components: SPDL-1 and the Rod/Zwilch/Zw10 complex. Genes and Development 22: 2385–2399.

Gassmann R, Holland AJ, Varma D, Wan X, Çivril F, Cleveland DW, Oegema K, Salmon ED, Desai A (2010) Removal of spindly from microtubule-attached kinetochores controls spindle checkpoint silencing in human cells. Genes and Development 24:957-71.

Goshima G, Kiyomitsu T, Yoda K, Yanagida M (2003) Human centromere chromatin protein hMis12, essential for equal segregation, is independent of CENP-A loading pathway. Journal of Cell Biology 160: 25–39.

Grabsch H, Takeno S, Parsons WJ, Pomjanski N, Boecking A, Gabbert HE, Mueller W (2000) Overexpression of the mitotic checkpoint genes BUB1, BUBR1 and BUB3 in gastric cancer- association with tumor cell proliferation. Journal of Pathology 200:16-22.

Greenstein D (2005) Control of oocytes meiotic maturation and fertilization. Wormbook.

Greiss S, Schumacher B, Grandien K, Rothblatt J, Gartner A (2008) Transcriptional profiling in *C. elegans* suggest DNA damage dependent apoptosis as an ancient function of the p53 family. BMC Genomics 9:334.

Griffis ER, Stuurman N, Vale RD (2007) Spindly, a novel protein essential for silencing the spindle assembly checkpoint, recruits dynein to the kinetochore. Journal of Cell Biology 177:1005-15.

Gritsko TM, Coppola D, Paciga JE, Yang L, Sun M, Shelley SA, Fiorica JV, Nicosia SV, Cheng JQ (2003) Activation and overexpression of centrosome

kinase BTAK/Aurora-A in human ovarian cancer. Clinical Cancer Research 9:1420-6.

Grützmann R, Pilarsky C, Ammerpohl O, Lüttges J, Böhme A, Sipos B, Foerder M, Alldinger I, Jahnke B, Schackert HK, Kalthoff H, Kremer B, Klöppel G, Saeger HD (2004) Gene expression profiling of microdissected pancreatic ductual carcinomas using high-density DNA microarrays. Neoplasia 6:611-22.

Guimaraes GJ, DeLuca JG (2009) Connecting with Ska, a key complex at the kinetochore-microtubule interface. EMBO Journal 28:1375-77.

Gumienny TL, Lambie E, Hartwieg E, Horvitz HR, Hengartner MO (1999) Genetic control of programmed cell death in the *Caenorhabditis elegans* hermaphrodite germline. Development 126:1011-22.

Güttinger S, Laurell E, Kutay U (2009) Orchestrating nuclear envelope disassembly and reassembly during mitosis. Nature Reviews Molecular Cell Biology 10:178-91.

Hall DH, Altun ZF (2008) *C. elegans* atlas. Cold Spring Harbor Laboratory Press.

Han S, Park K, Kim HY, Lee MS, Kim HJ, Kim YD, Yuh YJ, Kim SR, Suh HS (2000) Clinical implication of altered expression of Mad1 protein in human breast carcinoma. Cancer 88:1623-32.

Harper NC, Rilo R, Jover-Gill S, Assaf XJ, Bhalla N, Dernburg AF (2011) Pairing centers recruit a polo-like kinase to orchestrate meiotic chromosome dynamics in *C. elegans*. Developmental Cell 21:934-947.

Hauf S, Roitinger E, Koch B, Dittrich CM, Mechtler K et al (2005) Dissociation of cohesin from chromosome arms and loss of arm cohesion during early mitosis depends on phosphorylation of SA2. PLoS Biol 3:e69.

Hauf S, Waizenegger IC, Peters JM (2001) Cohesin cleavage by separase required for anaphase and cytokinesis in human cells. Science 293:1320-1323.

Hayashi T, Fujita Y, Iwasaki O, Adachi Y, Takahashi K, Yanagida M (2004) Mis16 and Mis18 are required for CENP-A loading and deacetylation at centromeres. Cell 118:715-29.

Hernando E, Nahlé Z, Juan G, Diaz-Rodriguez, Alaminos M, Hemann M, Michel L, Mittal V, Gerald W, Benezera R, Lowe SW, Cordon-Cardo C (2004)

Rb inactivation promotes genomic instability by uncoupling cell cycle progression from mitotic control. Nature 430:797-802.

Holland AJ, Cleveland DW (2012) Losing balance: the origin and impact of aneuploidy in cancer. EMBO Reports 13:501-14.

Holloway SL, Gotzer M, King MW, Murray AW (1993) Anaphase is initiated by proteolysis rather than by the inactivation of maturation-promoting factor. Cell 73:1393-1402.

Howman EV, Fowler KJ, Newson AJ, Redward S, MacDonald AC, Kalitsis P, Choo A. (2000) Early disruption of centromeric chromatin organization in centromere protein A (Cenpa) null mice. Proc Natl Acad Sci U S A 97: 1148–1153.

Hoyt MA, Totis L, Roberts BT (1991) *S. cerevisiae* genes required for cell cycle arrest in response to loss of microtubule function. Cell 66:507-17.

Hubbard EJ, Greenstein D (2000) The *Caenorhabditis elegans* gonad: a test tube for cell and developmental biology. Developmental Dynamics 218:2-22.

Hubbard EJ, Greenstein D (2005) Introduction to the germ line. Wormbook.

Hwang A, Maity A, McKenna WG, Muschel RJ (1995) Cell cycle-dependent regulation of the cyclin B1 promoter. Journal of Biological Chemistry 270:28419-24.

Hwang LH, Lau LF, Smith DL, Mistrot CA, Hardwick KG, Hwang ES, Amon A, Murray AW (1998) Budding yeast Cdc20: a target of the spindle checkpoint. Science 279:1041-44.

Iwanaga Y, Chi YH, Miyazato A, Sheleg S, Haller K, Peloponese JM, Li Y, Ward JM, Benezra R, Jeang KT (2007) Heterozygous deletion of mitotic arrest-deficient protein 1 (MAD1) increases the incidence of tumors in mice. Cancer Research 67:160-6.

Izuta H, Ikeno M, Suzuki N, Tomonaga T, Nozaki N, Obuse C, Kisu Y, Goshima N, Nomura F, Nomura N, Yoda K (2006) Comprehensive analysis of the ICEN (Interphase Centromere Complex) components enriched in the CENP-A chromatin of human cells. Genes to Cells 11:673-84.

Jallepalli PV, Lengauer C (2001) Chromosome segregation and cancer: cutting through the mystery. Nature Reviews Cancer 1:109-117.

Jordan MA, Wilson L (2004) Microtubules as a target for anticancer drugs. Nature Reviews Cancer 4:253-265.

Kalitsis P, Fowler KJ, Griffiths B, Earle E, Chow CW, Jamsen K, Choo KH (2005) Increased chromosome instability but not cancer predisposition in haploinsufficient Bub3 mice. Genes, Chromosomes and Cancer 44:29-35.

Kallakury BV, Sheehan CE, Ambros RA, Fisher HA, Kaufman RP Jr, Ross JS (1997) The prognostic significance of p34cdc2 and cyclin D1 protein expression in prostate adenocarcinoma. Cancer 80:753-63.

Kapoor TM, Compton DA (2002) Search for the middle ground: mechanisms of chromosome alignment during mitosis. Journal of Cell Biology 157:551-56.

Karess R (2005) Rod-Zw10-Zwilch: a key player in the spindle checkpoint. Trends in Cell Biology 15:386-92.

Katayama H, Ota T, Jisaki F, Ueda Y, Tanaka T, Odashima S, Suzuki F, Terada Y, Tatsuka M (1999) Mitotic kinase expression and colorectal cancer progression. Journal of the International Cancer Institute 91:1160-2.

Keeney S (2001) Mechanism and control of meiotic recombination initiation. Current Topics in Developmental Biology 52:1-53.

Keeney S, Giroux CN, Kleckner N (1997) Meiosis-specific DNA double-strand breaks are catalyzed by Spo11, a member of a widely conserved protein family. Cell 88:375-84.

Kim SH, Lin DP, Matsumoto S, Kitazono A, Matsumoto T (1998) Fission yeast Slp1: an effector of the Mad2-dependent spindle checkpoint. Science 279:1045-47.

Kimble J, Crittenden SL (2005) Germline proliferation and its control. Wormbook.

Kline-Smith SL, Sandall S, Desai A (2005) Kinetochore-spindle microtubules interactions during mitosis. Current Opinion in Cell Biology 17:35-46.

Ko MA, Rosario CO, Hudson JW, Kulkarni S, Pollett A, Dennis JW, Swallow CJ (2005) Plk4 haploinsufficiency causes mitotic infidelity and carcinogenesis. Nature Genetics 37:883-8.

Komlodi-Pasztor E, Sackett DL, Fojo AT (2012) Inhibitors targeting mitosis: tales of how great drugs against a promising target were brought down by a flawed rationale. Clinical Cancer Research 18:51–63.

Krejci L, Altmannova V, Spriek M, Zhao X (2012) Homologous recombination and its regulation. Nuclei Acids Research 40:5795-818.

L'Hernault SW (2006) Spermatogenesis. Wormbook.

Lara-Gonzalez P, Westhrope FG, Taylor SS (2012) The spindle assembly checkpoint. Current Biology 22:R966-80.

Li D, Zhu J, Firozi PF, Abbruzzese JL, Evans DB, Cleary K, Friess H, Sen S (2003) Overexpression of STK15/BTAK/Aurora A kinase in human pancreatic cancer. Clinical Cancer Research 9:991-7.

Li M, Fang X, Wei Z, York JP, Zhang P (2009) Loss of spindle assembly checkpoint-mediated inhibition of Cdc20 promotes tumorigenesis in mice. Journal of Cell Biology 185:983–994.

Li R, Murray AW (1991) Feedback control of mitosis in budding yeast. Cell 66:519-31.

Lin SF, Lin PM, Yang MC, Liu TC, Chang JG, Sue YC, Chen TP (2002) Expression of hBUB1 in acute myeloid leukemia. Leukemia and Lymphoma 43:385-91.

Lindqvist A, Rodríguez-Bravo V, Medema RH (2009) The decision to enter mitosis: feedback and redundancy in the mitotic network. Journal of Cell Biology 185:193-202.

Longley DB, Johnston PG (2005) Molecular mechanisms of drug resistance. Journal of Pathology 205: 275–292.

Lui DY, Colaiácovo MP (2013) Meiotic development in *Caenorhabditis elegans*. Advances in Experimental Medicine and Biology 757:133-70.

MacQueen AJ, Colaiácovo MP, McDonald K, Villeneuve AM (2002) Synapsis-dependent and -independent mechanisms stabilize homolog pairing during meiotic prophase in *C. elegans*. Genes & Development 16:2428-42.

MacQueen AJ, Phillips CM, Bhalla N, Weiser P, Villeneuve AM, Dernburg AF (2005) Chromosome sites play dual roles to establish homologous synapsis during meiosis in *C. elegans*. Cell 123:1037-50.

Maddox PS, Hyndman F, Monen J, Oegema K, Desai A (2007) Functional genomics identifies a Myb domain-containing protein required for assembly of CENP-A chromatin. Journal of Cell Biology 176:757-63.

Malumbres M, Barbacid M (2001) To cycle or not to cycle: a critical decision in cancer. Nature Reviews Cancer 1:222-31.

Massague J (2004) G1 cell-cycle control and cancer. Nature 432:298-306.

McCleland ML, Gardner RD, Kallio MJ, Daum JR, Gorbsky GJ, Burke DJ, Stukenberg PT (2003) The highly conserved Ndco80 complex is required for kinetochore assembly, chromosome congression and spindle checkpoint activity. Genes and Development 17:101-114.

McGranahan N, Burrell RA, Endesfelder D, Novelli MR, Swanton C (2012) Cancer chromosomal instability: therapeutic diagnostic challenges. EMBO Reports 13:528-38.

Meluh PB, Yang P, Glowczewski L, Koshland D, Smith MM (1998) Cse4p is a component of the core centromere of *Saccharomyces cerevisiae*. Cell 94: 607–613.

Michel LS, Liberal V, Chatterjee A, Kirchwegger R, Pasche B, Gerald W, Dobles M, Sorger PK, Murty VV, Benezra R (2001) MAD2 haplo-insufficieny causes premature anaphase and chromosome instability in mammalian cells. Nature 409:355-9.

Mitchison TJ, Salmon ED (2001) Mitosis: a history of division. Nature Cell Biology 3:E17-21.

Miyoshi Y, Iwao K, Egawa C, Noguchi S (2001) Association of centrosomal kinase STK15/BTAK mRNA expression with chromosomal instability in human breast cancers. International Journal of Cancer 92:370-3.

Moreno-Bueno G, Sánchez-Estévez C, Cassia R, Rodríguez-Perales S, Díaz-Uriarte R, Domínguez O, Hardisson D, Andujar M, Prat J, Matias-Guiu X, Cigudosa JC, Palacios J (2003) Differential gene expression profile in endometrioid and nonendometrioid endometrial carcinoma: STK15 is frequently overexpressed and amplified in nonendometrioid carcinomas. Cancer Research 63:5697-702.

Murray AW, Kirschner MW (1989) Cyclin synthesis drives the early embryonic cell cycle. Nature 339:275-80.

Musacchio AW, Salmon ED (2007) The spindle-assembly checkpoint in space and time. Nature Reviews Molecular and Cell Biology 8:379-93.

Nishigaki R, Osaki M, Hiratsuka M, Toda T, Murakami K, Jeang KT, Ito H, Inoue T, Oshimura M (2005) Proteomic identification of differentially-expressed genes in human gastric carcinomas. Proteomics 5:3205-13.

Obuse C, Yang H, Nozaki N, Goto S, Okazaki T, Yoda K (2004) Proteomics analysis of the centromere complex from HeLa interphase cells: UV-damaged DNA binding protein 1 (DDB-1) is a component of the CEN-complex, while BMI-1 is transiently co-localized with the centromeric region in interphase. Genes to Cells 9:105-120.

Oegema K, Desai A, Rybina S, Kirkham M, Hyman AA (2001) Functional analysis of kinetochore assembly in *Caenorhabditis elegans*. Journal of Cell Biology 153: 1209–1226.

Oegema K, Hyman AA (2006) Cell division. Wormbook.

Onn I, Heidinger-Pauli JM, Guacci V, Unal E, Koshland DE (2008) Sister chromatid cohesion: a simple concept with a complex reality. Annual Reviews in Cell and Developmental Biology 24:105-29.

Penkner AM, Fridkin A, Gloggnitzer J, Baudrimont A, Machacek T, Woglar A, Csaszar E, Pasierbek G, Gruenbaum Y, Jantsch V (2009) Meiotic chromosome homology search involved modifications of the nuclear envelope protein Matefin/SUN-1. Cell 139:920-33.

Penkner AM, Tang L, Novatchkova M, Ladurner M, Fridkin A, Gruenbaum Y, Schweizer D, Loidl J, Jantsch V (2007) The nuclear envelope protein Matefin/SUN-1 is required for homologous pairing in *C. elegans* meiosis. Developmental Cell 12:873-85.

Pérez de Castro I, de Cárcer G, Malumbres M (2007) A census of mitotic cancer genes: new insights into tumor cell biology and cancer therapy. Carcinogenesis 28:899-912.

Peters JM (2006) The anaphase promoting complex/cyclosome: a machine designed to destroy. Nature Reviews Molecular and Cell Biology 7:644-56.

Peters JM, Tedeschi A, Schmitz J (2008) The cohesion complex and its roles in chromosome biology. Genes and Development 22:3089-3114.

Petrovic A, Pasqualato S, Dube P, Krenn V, Santaguida S, Cittaro D, Monzani S, Massimiliano L, Keller J, Tarricone A, Maiolica A, Stark H, Musacchio A (2010) The MIS12 complex is a protein interaction hub for outer kinetochore assembly. Journal of Cell Biology 190:835-52.

Phillips CM, Dernburg AF (2006) A family of zinc-finger proteins is required for chromosome-specific pairing and synapsis during meiosis in *C. elegans*. Developmental Cell 11:817-829.

Phillips CM, Wong C, Bhalla N, Carlton PM, Weiser P, Meneely PM, Dernburg AF (2005) HIM-8 binds to the X chromosome pairing center and mediates chromosome-specific meiotic synapsis. Cell 123:1051-63.

Pimkhaokham A, Shimada Y, Fukuda Y, Kurihara N, Imoto I, Yang ZQ, Imamura M, Nakamura Y, Amagasa T, Inazawa J (2000) Nonrandom chromosomal imbalances in esophageal squamous cell carcinoma cell lines: possible involvment of the ATF3 and CENPF genes in the 1q32 amplicon. Japanse Journal of Cancer Research 91:1126-33.

Pines J (2006) Mitosis: a matter of getting rid of the right protein at the right time. Trends in Cell Biology 16:55-63.

Rao CV, Kurkjian CD, Yamada HY (2012) Mitosis-targeting natural products for cancer prevention and therapy. Current Drug Targets 13:1820-30.

Regnier V, Vagnarelli P, Fukagawa T, Zerjal T, Burns E, Trouche D, Earnshaw W, Brown W. (2005) CENP-A is required for accurate chromosome segregation and sustained kinetochore association of BubR1. Molecular and Cellular Biology 25: 3967–3981.

Ren B, Cam H, Takahashi Y, Volkert T, Terragni J, Young RA, Dynlacht BD (2002) E2F integrates cell cycle progression with DNA repair, replication and G(2)/M checkpoints. Genes and Development 16:245-56.

Riddle DL, Blumenthal T, Meyer BJ, Priess JR (eds.) (1997) *C. elegans* II, 2nd edition. Cold Spring Harbor Laboratory Press.

Rieder CL, Cole RW, Khodiakov A, Sluder G (1995) The checkpoint delaying anaphase in response to chromosome monoorientation is medicated by an inhibitory signal produced by unattached kinetochores. Journal of Cell Biology 130:941-8.

Rieder, C. (2004) Stuck in division or passing through: what happens when cells cannot satisfy the spindle assembly Checkpoint. Developmental Cell 7(5):637-51.

Sakakura C, Hagiwara A, Yasuoka R, Fujita Y, Nakanishi M, Masuda K, Shiomomura K, Nakamura Y, Inazawa J, Abe T, Yamagishi H (2001) Tumor-amplified kinase BTAK is amplified and overexpressed in gastric cancers with

possible involvement in aneuploid formation. British Journal of Cancer 84:824-31.

Sato A, Issac B, Phillips CM, Rilo R, Carlton PM, Wynne DJ, Kasad RA, Dernburg AF (2009) Cytoskeletal forces span the nuclear envelope to coordinate meiotic chromosome pairing and synapsis. Cell 139:907-19.

Schliekelman M, Cowley DO, O'Quinn R, Oliver TG, Lu L, Salmon ED, Van Dyke T (2009) Impaired Bub1 function in vivo compromises tension-dependent checkpoint function leading to aneuploidy and tumorigenesis. Cancer Research 69:45-54.

Schmidt M, Bastians H (2007) Mitotic drug targets and the development of novel anti-mitotic anticancer drugs. Drug Resistance Updates 10:162-81.
Schvartzman JM, Sotillo R, Benezra R (2010) Mitotic chromosomal instability and cancer: mouse modeling of the human disease. Nature Reviews Cancer 10:102-115.

Schvarzstein M, Wignall SM, Villeneuve AM (2010) Coordinating cohesion, co-orientation and congression during meiosis: lessons from holocentric chromosomes. Genes and Development 24:219-28.

Screpanti E, De Antoni A, Alushin GM, Petrovic A, Melis T, Nogales E, Musacchio A (2011) Direct binding of Cenp-C to the Mis12 complex joins the inner and outer kinetochore. Current Biology 21:391-8.

Sen S, Zhou H, Zhang RD, Yoon DS, Vakar-Lopez F, Ito S, Jiang F, Johnston D, Grossman HB, Rulfrok AC, Katz RL, Brinkley W, Czerniak B (2002) Amplication/overexpression of a mitotic kinase gene in human bladder cancer. Journal of the International Cancer Institute 94:1320-1329.

Sherr CJ (2000) The Pezcoller lecture: cancer cell cycles revisited. Cancer Research 60:3689-95.

Shintomi K, Hirano T (2009) Releasing cohesin from chromosome arms in early mitosis: opposing actions of Wapl-Pds5 and Sgo1. Genes & Dev 23:2224-2236.

Smith SL, Bowers NL, Betticher DC, Gautschi O, Ratschiller D, Hoban PR, Booton R, Santibáñez-Koref MF, Heighway J (2005) Overexpression of aurora B kinase (AURKB) in primary non-small lung carcinoma is frequent, generally driven from one allele and correlates with the level of genetic instability. British Journal of Cancer 93:719-29.

Soria JC, Jang SJ, Khuri FR, Hassan K, Liu D, Hong WK, Mao L (2000) Overexpression of cyclin B1 in early-stage non-small cell lung cancer and its clinical implication. Cancer Research 60:4000-4.

Sorrentino R, Libertini S, Pallante PL, Troncone G, Palombini L, Bavetsias V, Spalletti-Cernia D, Laccetti P, Linardopoulos S, Chieffi P, Fusco A, Portella G (2005) Aurora B overexpression associates with the thyroid carcinoma undifferentiated phenotype and is required for thyroid carcinoma cell proliferation. Journal of Clinical Endocrinology and Metabolism 90:928-35.

Sotillo R, Schvartzman JM, Socci ND, Benezra R (2010) Mad2-induced chromosome instability leads to lung tumor relapse after oncogene withdrawal. Nature 464:436-40.

Stergiou L, Doukoumetzidis K, Sendoel A, Hengartner MO (2007) The nucleotide excision repair pathway is required for UV-C-induced apoptosis in *Caenorhabditis elegans*. Cell Death and Differentiation 14:1129-38.

Stergiou L, Hengartner MO (2004) Death and more: DNA damage response pathways in the nematode C. elegans. Cell Death and Differentiation 11:21-28.

Strebhardt K, Ullrich A (2006) Targeting polo-like kinase 1 for cancer theraphy. Nature Reviews Cancer 6:321-30.

Sullivan M, Morgan DO (2007) Finishing mitosis, one step at a time. Nature Reviews Molecular and Cell Biology 8:894-903.

Takahashi K, Chen ES, Yanagida M (2000) Requirement of Mis6 centromere connector for localizing a CENP-A-like protein in fission yeast. Science 288: 2215–2219.

Takeno S, Noguchi T, Kikuchi R, Uchida Y, Yokoyama S, Müller W (2002) Prognostic value of cyclin B1 in patients with esophageal squamous cell carcinoma. Cancer 94:2874-81.

Tanaka K (2013) Regulatory mechanisms of kinetochore-microtubule interactions in mitosis. Cellular and Molecular Life Sciences 70:559-79.

Tanenbaum ME, Medema RH (2010) Mechanisms of centrosome separation and bipolar spindle assembly. Developmental Cell 19:797-806.

Thronton BR, Toczyski DP (2003) Securing and B-cyclin/CDK are the only essential targets of the APC. Nature Cell Biology 5:1090-4.

Tomkiel J, Cooke CA, Saitoh H, Bernat RL, Earnshaw WC (1994) CENP-C is required for maintaining proper kinetochore size and for a timely transition to anaphase. Journal of Cell Biology 125:531-45.

Tooley J, Stukenberg PT (2011) The Ndc80 complex: integrating the kinetochore's many movements. Chromosome Research 19:377-91.

Uhlmann F (2009) A matter of choice: the establishment of sister chromatid cohesion. EMBO Reports 10:1095-1102.

van den Boom J, Wolter M, Kuick R, Misek DE, Youkilis AS, Wechsler DS, Sommer C, Reifenberger G, Hanash SM (2003) Characterization of gene expression profiles associated with glioma progression using oligonucleotide-based microarray analysis and real-time reverse transcription-polymerase chain reaction. American Journal of Pathology 163:1033-43.

Villeneuve AM, Hillers KJ (2001) Whence meiosis? Cell 106:647-50.

Wang X, Zhou YX, Qiao W, Tominaga Y, Ouchi M, Ouchi T, Deng CX (2006) Overexpression of aurora kinase A in mouse mammary epithelium induces genetic instability preceding mammary tumor formation. Oncogene 25:7148-58.

Weaver BA, Silk AD, Montagna C, Verdier-Pinard P, Cleveland DW (2007) Aneuploidy acts both oncogenically and as a tumor suppressor. Cancer Cell 11:25-36.

Weiss E, Winey M (1996) The *Saccharomyces cerevisiae* spindle pole body duplication gene *MPS1* is part of a mitotic checkpoint. Journal of Cell Biology 132:111-23.

Wigge PA, Kilmartin JV (2001) The Ndc80p complex from *Saccharomyces cerevisiae* contains conserved centromere components and has a function in chromosome segregation. Journal of Cell Biology 152:349-60.

Woodcock CL, Ghosh RP (2010) Chromatin higher-order structure and dynamics. Cold Spring Harbor Perspectives in Biology 2:a000596.

Yamada, H, Gorbsky, G. (2006) Spindle checkpoint function and cellular sensitivity to antimitotic drugs. Molecular Cancer Therapeutics 5(12):2963-69.

Yamamoto T, Watanabe S, Essex A, Kitagawa R (2008) SPDL-1 functions as a kinetochore receptor for MDF-1 in *Caenorhabditis elegans*. Journal of Cell Biology 183: 187–194.

Yuan B, Xu Y, Woo JH, Wang Y, Bae YK, Yoon DS, Wersto RP, Tully E, Wilsbach K, Gabrielson E (2006) Increased expression of mitotic checkpoint genes in breast cancer cells with chromosomal instability. Clinical Cancer Research 12:405-10.

Zhou J, Giannakakou P (2005) Targeting microtubules for cancer chemotherapy. Current Medicinal Chemistry – Anticancer Agents 5:65-71.

Zirn B, Hartmann O, Samans B, Krause M, Wittmann S, Mertens F, Graf N, Eilers M, Gessler M (2006) Expression profiling of Wilms tumors reveals new candidate genes for different clinical parameters. International Journal of Cancer 118:1954-62.

Chapter 2. Meiotic double-strand breaks act as a surveillance mechanism to uncover mitotic errors in the *C. elegans* germline

ABSTRACT

The genomic integrity of gametes is critical for successful reproduction. In the *C. elegans* germline, gametes are generated in an assembly line-like process: mitotic divisions in the germline stem cell niche generate nuclei that enter into meiosis and progress through meiotic prophase. Here we show that perturbing mitoses in the stem cell niche triggers elimination of nuclei by programmed cell death during meiotic prophase. Targeting of nuclei harboring mitotic errors for cell death does not require the spindle checkpoint, but instead depends on p53 and upstream components of the DNA damage response pathway. Detection of mitotic errors also requires Spo11, the enzyme that creates double-strand breaks to initiate meiotic recombination. Thus, Spo11 not only promotes recombination but also monitors the chromosome content of nuclei entering meiosis, generating breaks that trigger cell death in the presence of an incorrect chromosome complement.

INTRODUCTION

In sexually reproducing multi-cellular organisms, genetic information is propagated via the germline, the specialized tissue that generates haploid gametes. Defects in gametogenesis result in aneuploidy, the leading genetic cause of miscarriages and birth defects in humans (Hassold et al., 2007). Due to the central importance of the germline in the transfer of genetic information, understanding the mechanisms that ensure genome integrity in the germline is a prominent area of investigation, with important insights emerging from studies in model organisms such as *C. elegans* (Saito et al., 2012; Xu et al., 2012).

The germline in the adult *C. elegans* worm consists of two identical U-shaped gonad arms with ~1000 nuclei arranged in a syncitium (Kimble and Crittenden, 2005). Each nucleus is partially enclosed by membrane in a pseudo cell that is open on one side to the common maternal cytoplasm. The distal tip of the germline acts as the stem cell niche, generating, via mitotic divisions, all of the nuclei that enter into the meiotic pipeline to generate oocytes (Byrd and Kimble, 2009). After exit from the distal tip, nuclei progress through pre-meiotic S phase, homolog pairing, synaptonemal complex formation and recombination as they migrate towards the proximal end of the gonad. Meiotic recombination is initiated by double-strand breaks (DSBs) catalyzed by the type II DNA topoisomerase-like enzyme Spo11 (Keeney, 1997). Typically only one double-strand break per homolog develops into a successful crossover, even though more than one break per pair is made

(Martinez-Perez and Colaiácovo, 2009). At the most proximal end of the gonad, individual nuclei are packaged into oocytes and become fertilized by the spermatheca, triggering the start of embryogenesis.

Prior to their packaging into oocytes, a large proportion of meiotic nuclei (~50%) are removed via programmed cell death (Gumienny et al., 1999) in order to maintain oocyte quality (Andux and Ellis, 2008). While a majority of these nuclei lack any obvious defects, nuclei with DNA damage or meiotic defects are preferentially eliminated (Gartner et al., 2000; MacQueen et al., 2002; Colaiácovo et al., 2003; Bhalla and Dernburg, 2005). For example, in mutants that prevent completion of recombination, DSBs persist and trigger programmed cell death through the DNA damage checkpoint (Gartner et al, 2000; Jantsch et al., 2007). Direct irradiation of the germline also strongly increases cell death and has been a common approach used to investigate DNA damage response pathways in the germline (Gartner et al., 2000; Deng et al., 2004; Garcia-Muse and Boulton, 2005; Quevedo et al., 2007; Greiss et al., 2008; Lee et al., 2010).

Here, we determine how the germline responds to mitotic errors in the stem cell niche and investigate the mechanism that prevents propagation of these nuclei as defective gametes. We examine the effects of different perturbations that cause chromosome segregation defects during mitosis and find that all significantly elevate the number of nuclei eliminated via programmed cell death during meiotic prophase. This cell death is independent of the spindle checkpoint, the major pathway responsible for

monitoring errors in mitosis. Instead, it requires p53 and upstream activators of the DNA damage checkpoint and is correlated with presence of excess DSBs in the meiotic nuclei generated following defective mitotic divisions. Inhibition of Spo11, the enzyme that initiates meiotic recombination by generating double strand breaks, eliminates both the increase in cell death and the excess DSBs. Thus, Spo11-mediated double-strand break formation, which is integral to the mechanism of meiotic recombination, also serves as a surveillance system by creating DSBs to mark nuclei entering meiosis with an incorrect chromosome complement for programmed cell death. These findings reveal how defective precursor nuclei are detected and eliminated following entry into meiosis to prevent formation of aneuploid gametes.

RESULTS

The cell death pathway in the proximal germline detects mitotic errors occurring in the distal stem cell niche

The cell death pathway surveys nuclei at the proximal end of the germline (Gumienny et al., 1999; **Fig. 1A**). To determine if this pathway specifically detects nuclei that have undergone mitotic errors in the stem cell niche in the distal germline, we inhibited key proteins required for mitosis and monitored cell death by visualizing the cell corpse engulfment marker CED-1::GFP (**Fig. 1A;** Zhou et al., 2001). Soaking-based RNAi interference (RNAi) was used to deplete six proteins required for three different aspects of mitosis: kinetochore formation (KNL-1 and CENP-C^{HCP-4}; Desai et al., 2003), mitotic

microtubule assembly (HCP-1/2 and ZYG-9; Cheeseman et al., 2005; Matthews et al., 1998) and centrosome duplication (ZYG-1 and SAS-6; O'Connell et al., 2001; Dammermann et al., 2004; Leidel et al., 2005)—none of these proteins have any known functions during meiotic prophase. The experimental protocol (**Fig. 1B**) provides sufficient recovery time after soaking in dsRNA to allow nuclei to migrate from the distal tip to the region of cell death (Crittenden et al., 2006; Jaramillo-Lambert et al., 2007). Compared to controls, a significant increase (1.5 – 2-fold; $p<0.001$) in germline cell death was observed following each individual inhibition of the six components tested (**Fig. 1B**). The magnitude of the increase was similar to that previously observed following inhibition of synaptonemal complex formation or homolog pairing (MacQueen et al., 2002; Colaiacovo et al., 2003; Bhalla and Dernburg, 2005). Thus, perturbing mitoses at the germline distal tip triggers the elimination of nuclei by the cell death pathway in the proximal germline.

To further study how mitotic errors are detected by the cell death pathway, we first sought to develop a consistent genetic means for perturbing distal germline mitoses without directly affecting subsequent meiotic events. Inhibition of centrosome duplication is ideally suited for this purpose; centrosomes are critical for germline mitosis but are inactivated upon meiotic entry and degraded as nuclei travel proximally through the germline (Mikeladze-Dvali et al., 2012). To disrupt centrosome duplication, we capitalized on a temperature-sensitive mutation in the kinase ZYG-1 (*zyg-1(b1)*, referred to here as *zyg-1*^{ts}; O'Connell et al., 2001). When shifted to the

restrictive temperature for 24 – 48 hours, *zyg-1*^{ts} worms displayed a robust 2.5 – 3-fold increase in germline cell death compared to controls (**Fig. 1C,D, S1A;** $p<0.0001$). To validate that the observed CED1::GFP circles represent programmed cell death, we analyzed *zyg-1*^{ts}*;ced-3(n717)* double mutants; CED-3/caspase is the downstream effector in the pathway and is required for all programmed cell death. In the double mutant, the number of CED-1::GFP circles was reduced to nearly zero (**Fig. 1C**). To confirm that the increase in cell death seen upon ZYG-1 inactivation is a consequence of errors in mitosis as opposed to a direct result of loss of ZYG-1 function, we analyzed cell death 6h after upshift to the restrictive temperature. This duration of inactivation is sufficient to inhibit centrosome duplication but does not allow enough time for nuclei from the distal tip to travel to the proximal germline. In contrast to the 24h and longer inactivation experiments, 6h inactivation had no effect on cell death (**Fig. S1A**). This observation supports the idea that rather than being a direct consequence of ZYG-1 inactivation, the increase in cell death results from defects in distal mitoses that are detected as the defective nuclei progress through meiotic prophase. Thus, conditional inhibition of centrosome duplication is a convenient and reproducible means to induce distal mitotic errors that result in a robust elevation of programmed cell death in the proximal germline.

Nuclei resulting from errors in mitosis progress into meiosis after a delay

To directly assess the consequences of perturbing mitosis in the distal tip of the germline, we analyzed fixed, extruded gonads, which were labeled to visualize chromosomes, microtubules and centrosomes. Analysis of the distal tip in *zyg-1*^{ts} worms, revealed the presence of defective mitotic figures, the most notable of which were monopolar spindles (**Fig. 1D**); less frequently observed (20%) defects include abnormalities in spindle structure and unaligned or lagging chromosomes. Defective mitotic figures were also observed following RNAi-mediated inhibition of kinetochore assembly or mitotic microtubule formation (**Fig. S1B**).

To determine if mitotic defects delay the cell cycle by activating the spindle checkpoint, we scored for the mitotic index by visualizing mitosis-associated phosphorylation on Serine 10 of histone H3 (phospho-H3S10; Hendzel et al, 1997). Compared to controls, both *zyg-1*^{ts} upshift and the other mitotic perturbations led to a significant increase in the number of phospho-H3S10 nuclei in the distal tip of the germline (**Fig. 1E; Fig. S1C**). In *zyg-1*^{ts} worms the number of phospho-H3S10 positive nuclei did not further increase between 24h and 48h after ZYG-1 inactivation suggesting that spindle checkpoint activation leads to a 2.5 – 3-fold increase in the duration of mitosis rather than a permanent mitotic arrest. Consistent with the idea that nuclei with mitotic defects exit mitosis and progress into meiosis, in *zyg-1*^{ts} worms we observed nuclei lacking phospho-H3S10 staining and/or outside the distal tip that exhibited enhanced DAPI staining (**Fig. 1F**), as well as the presence of micronuclei, defined as small, round DAPI-stained dots (**Fig. S1D**). Aside from

aberrantly DAPI-stained nuclei, no major defects in germline structure were observed upon inactivation of ZYG-1 (**Fig. 1F**). These results suggest that the spindle checkpoint delays cell cycle progression, but does not grossly affect the ability of the distal tip to supply nuclei for entry into the meiotic program.

To more directly test whether nuclei with mitotic defects progress into meiosis, we labeled *zyg-1*^{ts} mutant gonads for HTP-3, a protein whose recruitment to the axial elements of the synaptonemal complex requires the pre-meiotic S-phase-associated loading of cohesin (Goodyer et al., 2008). In germlines dissected from *zyg-1*^{ts} worms, HTP-3 localization was observed on aberrant DAPI-stained nuclei (arrow, **Fig. 1G**) supporting the conclusion that nuclei with mitotic defects in *zyg-1*^{ts} worms enter meiosis. Injection of fluorescent nucleotides to pulse label S-phase nuclei at the distal tip and monitor their progression over time further confirmed that ZYG-1 inhibition had no major effect on the ability of the nuclei to travel proximally through the gonad (**Fig. S2**). Collectively, these observations suggest that while ZYG-1 inhibition prolongs mitosis, nuclei with incorrect chromosomal complements exit mitosis and enter the meiotic program.

The spindle checkpoint is dispensable for mitotic error-induced cell death in the proximal germline

The results above show that perturbing mitosis triggers a transient mitotic delay in the distal germline and an elevation of cell death during meiotic prophase in the proximal germline. We next explored the relationship between

these two phenomena. In particular, we determined whether activation of the spindle checkpoint during distal mitoses marks nuclei for subsequent elimination by programmed cell death in the proximal germline (**Fig. 2A**). For this purpose, we inhibited the essential spindle checkpoint components Mad1^{MDF-1}, Mad2^{MDF-2} and Mad3^{MDF-3}, and monitored the consequences on both the *zyg-1*^{ts}-induced mitotic delay, measured by the number of phospho-H3S10-labeled nuclei in the distal tip, as well as the increase in cell death during meiotic prophase, measured by the number of CED-1::GFP circles near the turn of the gonad arm. This analysis showed that inhibition of the spindle checkpoint eliminated the *zyg-1*^{ts}-induced mitotic delay—the number of phospho-H3S10 positive nuclei was equivalent to controls (**Fig. 2B**)—but had no effect on the elevation in cell death (**Fig. 2C**). In control worms with no induced mitotic defects, inhibition of the spindle checkpoint did not significantly affect either the number of phospho-H3S10 nuclei or the number of corpses at the gonad turn (**Fig. 2B,C**). Thus, the spindle checkpoint is responsible for the mitotic delay triggered by division defects in the distal germline but is not required for the subsequent elimination of the defective nuclei by programmed cell death.

The DNA damage checkpoint is required for the increase in cell death observed following defective mitoses in the distal tip

We next focused on the DNA damage checkpoint, which has been well studied in the *C. elegans* germline (**Fig. 3A**; Gartner et al., 2000; Stergiou and

Hengartner, 2004). We first tested p53^{CEP-1}, the DNA damage responder directly upstream of the canonical cell death pathway. A null mutant of p53^{CEP-1}, *cep-1(gk138)*, is viable but fails to elevate cell death following induction of DNA damage (Schumacher et al., 2001). A comparison of *zyg-1^{ts};cep-1(gk138)* double mutants to *zyg-1^{ts}* mutants alone at the restrictive temperature revealed that loss of p53^{CEP-1} suppressed the elevation in cell death triggered by inactivation of ZYG-1 (**Fig. 3B**). RNAi-mediated inhibition of the kinetochore proteins KNL-1 and CENP-C^{HCP-4} also failed to elevate cell death in the *cep-1* deletion strain (**Fig. 3C**), indicating loss of p53^{CEP-1} generally suppresses the ability of the germline to detect mitotic defects in nuclei emanating from the distal tip. Similar to loss of p53^{CEP-1}, loss of HUS-1, a subunit of the 911 complex that is recruited to the site of double-strand breaks and functions upstream of p53^{CEP-1} (Hofmann et al., 2002), also suppressed the cell death induced by ZYG-1 inhibition (**Fig. 3B**). Thus, cell division defects in the distal germline are detected by the DNA damage checkpoint, which activates programmed cell death to trigger removal of the defective nuclei. Consistent with previous work showing that the DNA damage checkpoint is required for the cell cycle delay seen in the distal tip of germlines exposed to ionizing radiation (Gartner et al., 2000), both the *zyg-1^{ts};cep-1(gk138)* and the *zyg-1^{ts};hus-1(op241)* double mutants showed a mild reduction in the number of phospho-H3S10 positive nuclei (**Fig. 3D**). However this reduction cannot underline the suppression of cell death given our previous results following inhibition of the spindle checkpoint (**Fig. 2B,C**).

Thus, cell division defects in the distal germline are detected by the DNA damage checkpoint, which activates programmed cell death to trigger removal of defective nuclei.

Meiotic nuclei generated following defective mitotic divisions harbor persistent double-strand breaks

The DNA damage checkpoint typically senses broken DNA ends. We therefore tested whether nuclei with mitotic errors generated by inhibition of ZYG-1 displayed abnormal numbers of DNA double-strand breaks. To this end, we performed immunofluorescence for the RecA-related strand exchange protein, RAD-51, which concentrates at sites of double-strand breaks to promote strand invasion (Shinohara et al., 1992). In an unperturbed germline, RAD-51 foci transiently appear in meiotic nuclei undergoing recombination in the transition zone (Alpi et al., 2003). In cases where DNA damage or recombination defects are present, RAD-51 foci increase in both frequency and persistence, making it a commonly used marker for DNA damage (Craig et al., 2012). ZYG-1 inhibition caused a significant increase in both the number of nuclei with RAD-51 foci as well as the average number of RAD-51 foci per nucleus (**Fig. 3E,F**), suggesting DNA damage or recombination defects are triggered under these conditions. Consistent with this idea, RAD-51-positive nuclei persisted longer in *zyg-1*^{ts} gonads, as evidenced by detection of RAD-51 staining well into the pachytene stage of meiotic prophase where RAD-51 foci are not detectable in controls (**Fig. 3F**). However, inhibition of ZYG-1 did

not lead to an accumulation of RAD-51 foci in the distal tip or in the oocytes; this is in contrast to other perturbations that result in double-strand breaks, such as ionizing radiation, which leads to RAD-51 foci throughout the entire germline, or inhibition of the cohesin subunit REC-8, which leads to RAD-51 during meiotic prophase, including in oocytes (Alpi et al., 2003). Cumulatively, these results suggest that nuclei with mitotic errors accumulate DNA breaks in meiotic prophase that in turn trigger DNA damage checkpoint-dependent cell death.

Spo11 is required for the increase in cell death and the double-strand breaks induced by defective distal tip mitoses

We next investigated the mechanism by which the double-strand breaks were generated to mark the defective nuclei for programmed cell death. The fact that DNA breaks did not accumulate in the distal tip following ZYG-1 inhibition suggested that nuclei with mitotic defects accumulate double-strand breaks due to an event following mitotic exit. As strong accumulation of RAD-51 foci was not observed before the transition zone (**Fig. 3F**), which marks the start of homologous recombination, we tested if recombination itself was involved in creating the excess double-strand breaks that mark the defective nuclei for death. Meiotic recombination requires the topoisomerase-related enzyme Spo11, which catalyzes the formation of double-strand breaks to initiate the process (Keeney, 2001). We therefore tested if inhibition of Spo11 could suppress the elevated cell death induced by defective distal tip

mitoses. Analysis of *zyg-1^{ts};spo-11(ok79)* double mutants revealed a complete suppression of the elevated cell death observed in the *zyg-1^{ts}* mutant (**Fig. 4A**).

RNAi-mediated inhibition of the kinetochore components KNL-1 and CENP-C^{HCP-4} also failed to elevate cell death in the *spo-11(ok79)* background (**Fig. 4B**), indicating that suppression is not specific to ZYG-1 inhibition. The number of phospho-H3S10 nuclei in the *zyg-1^{ts};spo-11(ok79)* double mutants was similar to that in the *zyg-1^{ts}* mutant alone (**Fig. 4C**), consistent with the prior conclusion that reduction in cell death is not linked to whether nuclei experience a mitotic delay. Finally, the double-strand breaks visualized as RAD-51 foci were significantly decreased in *zyg-1^{ts};spo-11(ok79)* double mutants compared to the *zyg-1^{ts}* mutant alone (**Fig. 4D**). Thus, Spo11, well-studied for its role in initiation of homologous recombination, creates double strand breaks in nuclei resulting from defective divisions in the distal germline to target nuclei with mitotic errors for removal by programmed cell death.

DISCUSSION

Sexually reproducing organisms must carefully safeguard the genomic integrity of their germline. Although the molecular mechanisms that protect the germline against errors in meiosis are becoming clear (Hochwagen and Amon, 2006), how the germline protects itself against mitotic errors remains relatively uncharacterized. The work described here uses *C. elegans* as a model to gain insight into this question.

A key aspect of our study was to examine the role of the spindle checkpoint in detection of mitotic errors in the germline. One hypothesis is that the spindle checkpoint arrests nuclei with mitotic defects in the distal stem cell niche, preventing them from entering the meiotic program (Buttner et al, 2007). Through examination of the number of nuclei undergoing mitosis over time and analysis of nuclear travel through the germline in upshifted *zyg-1*^{ts} worms, we show that this hypothesis is incorrect. Although the spindle checkpoint prolongs the duration of mitosis, defective nuclei eventually overcome this delay and enter the meiotic program. Furthermore, our data shows that inhibition of the spindle checkpoint had no effect on the ability of the germline to eliminate nuclei with mitotic defects. This finding discounts the idea that activation of the checkpoint in the distal tip marks nuclei for subsequent removal. Therefore, although the spindle checkpoint extends mitosis in an effort to attenuate errors, it does not play a role in eliminating nuclei with mitotic defects once they have occurred.

Our data supports an alternative hypothesis to explain how the germline protects itself from passing on gametes with mitotic errors. We find that nuclei resulting from a mitotic missegregation event are targeted for programmed cell death by a mechanism that depends on the production of unrepaired Spo11-induced double-strand breaks and subsequent activation of the DNA damage response. While Spo11 is known to promote recombination, this finding reveals a previously undiscovered role for Spo11 as a critical component of the mechanism that surveys the genome to ensure the presence of a correct chromosome complement.

We propose that nuclei containing an incorrect complement of chromosomes generated by mitotic defects activate the DNA damage pathway because chromosomes are unable to properly pair and synapse, which in turn prevents repair of recombinigenic breaks (**Fig. 4E**). This hypothesis seems likely, given the fact that both pairing and the initial licensing step in synaptonemal complex formation are dependent on homology (MacQueen et al., 2005). Consistent with this idea, worms lacking synaptonemal complex proteins SYP-1 or SYP-2 have previously been shown to result in a Spo11-dependent increase in cell death (MacQueen et al., 2002; Colaiácovo et al., 2003). In addition, worms in which individual chromosomes remain unpaired yet somehow synapse back on themselves result in persistent double-strand breaks and an increase in cell death that is dependent on the DNA damage pathway (Harper et al., 2011). A key role for Spo11 in genome surveillance may also explain why double-strand breaks occur in excess to the number of

crossovers (Martinez-Perez and Colaiácovo, 2009). Recent work also suggests that in the absence of proper pairing, Spo11-dependent breaks continue to form (S. Keeney, personal communication), thereby amplifying the number of breaks created to potentially trigger the DNA damage response.

How mitotic defects are linked to cell death is a topic of great interest, particularly in the context of chromosomal instability and cancer (Schvartzman et al., 2010; Bakhoum and Compton, 2012; Holland and Cleveland, 2012). The idea that an abnormal mitosis can trigger DNA damage is a common theme emerging from this work (Ganem and Pellman, 2012); the damage can occur either directly, through the action of the cleavage furrow (Janssen et al., 2011), or indirectly via the formation of micronuclei (Crasta et al., 2012). Here we present a third way, involving the action of a developmentally controlled double-strand break program. In the context of the germline, this purposeful induction of breaks, essential for recombination, also functions to weed out mitotic errors, thereby protecting the genomic integrity of the gametes.

EXPERIMENTAL PROCEDURES

C. elegans strains

All strains were maintained at 16°C. Mutant alleles used were *zyg-1(b1)*, *ced-3(n717)*, *ced-4(n1162)*, *cep-1(gk138)*, *hus-1(op241)* and *spo-11(ok79)*. All strains were propagated in the homozygous state, except for strains carrying the *spo-11(ok79)* allele, which were balanced with the nT1 balancer and propagated as previously described (Dernburg et al., 1998). The transgene insertions used, CED-1::GFP and HistoneH2b::mCherry, are from strains MD701 and OD95, respectively. Upshift experiments were performed by taking mid-to-late L4 larval stage worms and placing them at 25°C for the indicated time.

RNA Interference & Live imaging

Production of dsRNA, soaking RNAi and live imaging of the gonad was done as previously described (Green et al., 2011).

Immunofluorescence of fixed gonads

To extrude the gonad, 20-30 worms were placed in a depression slide containing 10 μL of egg salts (118 mM NaCl, 48 mM KCl, 2 mM $CaCl_2$ and 5 mM HEPES pH 7.5) with 1 mg/mL levamisole. Using 2, 27 gauge ½' needles, the head was severed just under the pharynx, allowing for full extrusion of one arm of the gonad. Gonads were fixed in 4% PFA for 20 mins, post-fixed in cold methanol for 10 mins. All antibody incubations were performed in 1.5 ml siliconized tubes- overnight at 4°C for primary antibodies and 1h at RT for secondary antibodies. Fixed and stained gonads were then mounted on poly-

lysine coated slides. Primary antibodies and dilutions used: α tubulin 1:500 (DM1α – Sigma), γ tubulin 1 μg/mL (A. Desai), phospho-HistoneH3^{Ser10} 1:500 (Sigma), HTP-3 1:500 (gift of A. Dernburg) and RAD-51 1:1000 (Novus Biologicals). Images were recorded on a Deltavision microscope at 1 x 1 or 2 x 2 binning with a 40x, 60x or 100x objective. Z-stacks (0.2-μm sections) were deconvolved using softWorRx (Applied Precision), analyzed in ImageJ and imported into Adobe Photoshop CS4 (Adobe) for further processing.

ACKNOWLEDGMENTS

We thank Abby Dernburg for the anti-HTP-3 antibody, the Caenorhabditis Genetics Center and Michael Hengartner for strains and Becky Green for comments on the manuscript. This work was supported by an NIH grant (GM074215) to A.D. D.S. was supported in part by an Institutional NRSA Award from NIGMS to the UCSD Genetics Training Program (T32 GM008666). A.D. and K.O. receive salary and other support from the Ludwig Institute for Cancer Research.

Chapter 2, in full, has been submitted for publication. It may appear as Deanna Stevens, Karen Oegema and Arshad Desai. *Meiotic double-strand breaks act as a surveillance mechanism to uncover mitotic errors in the C. elegans germline*. The dissertation author was the primary researcher and author of this paper.

REFERENCES

Alpi A, Pasierbek P, Gartner A, Loidl J (2003) Genetic and cytological characterization of the recombination protein RAD-51 in *Caenorhabditis elegans*. Chromosoma 112:6-16.

Andux S, Ellis RE (2008) Apoptosis maintains oocytes quality in aging *Caenorhabditis elegans* females. PLoS Genetics 4:e1000295.

Bakhoum SF, Compton DA (2012) Chromosomal instability and cancer: a complex relationship with therapeutic potential. Journal of Clinical Investigation 122:1138-43.

Berry LW, Westlund B, Schedl T (1997) Germ-line tumor formation caused by *glp-1*, a *Caenorhabditis elegans* member of the *Notch* family of receptors. Development 124:925-36.

Bhalla N, Dernburg AF (2005) A conserved checkpoint monitors meiotic chromosome synapsis in *Caenorhabditis elegans.* Science 310:1683-6.

Byrd DT, Kimble J (2009) Scratching the niche that control *C. elegans* germline stem cells. Seminars in Cell and Developmental Biology 20:1107-13.

Cheeseman IM, McLeod I, Yates JR, Oegema K, Desai A (2005) The CENP-F-like proteins HCP-1 and HCP-2 target CLASP to kinetochores to mediate chromosome segregation. Current Biology 15: 771-777.

Colaiácovo MP, MacQueen AJ, Martinez-Perez E, McDonald K, Adamo A, La Volpe, A, Villeneuve AM (2003) Synaptonemal complex assembly in *C. elegans* is dispensable for loading strand-exchange proteins but critical for proper completion of recombination. Developmental Cell 5:463-74.

Couteau F, Nabeshima K, Villeneuve A, Zetka M (2004) A component of the *C. elegans* meiotic chromosome axes at the interface of homolog alignment, synapsis, nuclear reorganization and recombination. Current Biology 14:585-92.

Craig AL, Moser SC, Bailly AP, Gartner A (2012) Methods for studying the DNA damage response in the *Caenorhabditis elegans* germ line. Methods in Cell Biology 107:321-52.

Crasta K, Ganem NJ, Dagher R, Lantermann AB, Ivanova EV, Pan Y, Nezi L, Protopopov A, Chowdhury D, Pellman D (2012) DNA breaks and chromosome pulverization from errors in mitosis. Nature 482:53-58.

Crittenden SL, Leonhard KA, Byrd DT, Kimble J (2006) Cellular analysis of the mitotic region in the *Caenorhabditis elegans* adult germ line. Molecular Biology of the Cell 17:3051-61.

Dammermann A, Müller-Reichert T, Pelletier L, Habermann B, Desai A, Oegema K (2004) Centriole assembly requires both centriolar and pericentriolar material proteins. Developmental Cell 7:815-29.

Deng XZ, Hofmann ER, Villanueva A, Hobert O, Capodieci P, Veach DR, Yin XL, Campodonico L, Glekas A, Cordon-Cardo C, Clarkson B, Bornmann WG, Fuks Z, Hengartner MO, Kolesnick R (2004) *Caenorhabditis elegans* ABL-1 antagonizes p53-mediated germline apoptosis after ionizing irradiation. Nature Genetics 36:906-12.

Desai A, Rybina S, Müller-Reichert T, Shevchenko A, Shevchenko A, Hyman A, Oegema K (2003) KNL-1 directs assembly of the microtubule-binding interface of the kinetochore in *C. elegans*. Genes & Development 17:2421-2435.

Ganem NJ, Pellman D (2012) Linking abnormal mitosis to the acquisition of DNA damage. Journal of Cell Biology 199:871-81.

Garcia-Muse T, Boulton SJ (2005) Distinct modes of ATR activation after replication stress and DNA double-strand breaks in *Caenorhabditis elegans*. EMBO Journal 24:4345-55.

Gartner A, Milstein S, Ahmed S, Hodgkin J, Hengartner MO (2000) A conserved checkpoint pathway mediates DNA damage-induced apoptosis and cell cycle arrest in *C. elegans*. Molecular Cell 5:435-43.

Goodyer W, Kaitna S, Couteau F, Ward JD, Boulton SJ, Zetka M (2008) HTP-3 links DSB formation with homolog pairing and crossing over during *C. elegans* meiosis. Developmental Cell 14:263-74.

Green RA, Kao HL, Audhya A, Arur S, Mayers JR, Fridolfsson HN, Schulman M, Schloissnig S, Niessen S, Laband K, Wang S, Starr DA, Hyman AA, Schedl T, Desai A, Piano F, Gunsalus KC, Oegema K (2011) A high-resolution *C. elegans* essential gene network based on phenotypic profiling of a complex tissue. Cell 145:470-82.

Greiss S, Hall J, Ahmed S, Gartner A (2008) *C. elegans* SIR-2.1 translocation is linked to a proapoptotic pathway parallel to cep-1/p53 during DNA damage-induced apoptosis. Genes & Development 22:2831-42.

Gumienny TL, Lambie E, Hartwieg E, Horvitz HR, Hengartner MO (1999) Genetic control of programmed cell death in the *Caenorhabditis elegans* hermaphrodite germline. Development 126:1011-22.

Harper NC, Rillo R, Jover-Gill S, Assaf ZJ, Bhalla N, Dernburg AF (2011) Pairing centers recruit a polo-like kinase to orchestrate meiotic chromosome dynamics in *C. elegans*. Developmental Cell 21:934-947.

Hassold T, Hall, H, Hunt, P (2007) The origin of human aneuploidy: where we have been, where we are going. Human Molecular Genetics 16:R203-208.

Hendzel MJ, Wei Y, Mancini MA, Van Hooser A, Ranalli T, Brinkley BR, Bazett-Jones DP, Allis CD (1997) Mitosis-specific phosphorylation of histone H3 initiates primarily within pericentromeric heterochromatin during G_2 and spreads in an ordered fashion coincide with mitotic chromosome condensation. Chromosoma 106:348–60.

Hochwagen A, Amon A (2006) Checking your breaks: surveillance mechanisms of meiotic recombination. Current Biology 16:R217-228.

Hofmann ER, Milstein S, Boulton SJ, Ye M, Hofmann JJ, Stergiou L, Gartner A, Vidal M, Hengartner MO (2002) *Caenorhabditis elegans* HUS-1 is a DNA damage checkpoint protein required for genome stability and EGL-1-mediated apoptosis. Current Biology 12:1908-18.

Holland AJ, Cleveland DW (2012) Losing balance: the origin and impact of aneuploidy in cancer. EMBO Reports 13:501-14.

Janssen A, van der Burg M, Szuhai K, Kops G, Medema RH (2011) Chromosome segregation errors as a cause of DNA damage and structural chromosome aberrations. Science 333:1895-98.

Jantsch V, Tang L, Pasierbek P, Penker A, Nayak S, Baudrimont A, Schedl T, Gartner A, Loidl J (2007) *Caenorhabditis elegans prom-1* is required for meiotic prophase progression and homologous chromosome pairing. Molecular Biology of the Cell 18:4911-20.

Jaramillo-Lambert A, Ellefson M, Villeneuve AM, Engebrecht J (2007) Differential timing of S phase, X chromosome replication and meiotic prophase in the *C. elegans* germ line. Developmental Biology 308:206-21.

Keeney S (2001) Mechanism and control of meiotic recombination initiation. Current Topics in Developmental Biology 52:1-53.

Keeney S, Giroux CN, Kleckner N (1997) Meiosis-specific DNA double-strand breaks are catalyzed by Spo11, a member of a widely conserved protein family. Cell 88:375-84.

Kimble J, Crittenden SL (2005) Germline proliferation and its control. Wormbook.

Kimble J, Crittenden SL (2007) Controls of germline stem cells, entry into meiosis and the sperm/oocytes decision in *Caenorhabditis elegans*. Annual Reviews in Developmental Biology 23:405-33.

Lee SJ, Gartner A, Hyun M, Ahn B, Koo HS (2010) *Caenorhabditis elegans* Werner Syndrome protein functions upstream of ATR and ATM in response to DNA replication inhibition and double-strand breaks. PLoS Genetics 6:e1000801.

Leidel S, Delattre M, Cerutti L, Baumer K, Gönczy P (2005) SAS-6 defines a protein family required for centrosome duplication in C. elegans and in human cells. Nature Cell Biology 7:115-25.

Lemmens BB, Tijsterman M (2011) DNA double-strand break repair in *Caenorhabditis elegans*. Chromosoma 120:1-21.

MacQueen AJ, Colaiácovo MP, McDonald K, Villeneuve AM (2002) Synapsis-dependent and -independent mechanisms stabilize homolog pairing during meiotic prophase in *C. elegans*. Genes & Development 16:2428-42.

MacQueen AJ, Phillips CM, Bhalla N, Weiser P, Villeneuve AM, Dernburg AF (2005) Chromosome sites play dual roles to establish homologous synapsis during meiosis in C. elegans. Cell 123:1037–50.

Martinez-Perez E, Colaiácovo MP (2009) Distribution of meiotic recombination events: talking to your neighbors. Current Opinion in Genetics & Development 19:105-112.

Matthews LR, Carter P, Thierry-Mieg D, Kemphues K (1998) ZYG-9, a *Caenorhabditis elegans* protein required for microtubule organization and function, is a component of meiotic and mitotic spindle poles. Journal of Cell Biology 141:1159-68.

Mikeladze-Dvali T, von Tobel L, Stmad P, Knott G, Leonhardt H, Schermelleh L, Gönczy P (2012) Analysis of centriole elimination during *C. elegans* oogenesis. Development 139:1670-9.

O'Connell KF, Caron C, Kopish KR, Hurd DD, Kempheus KJ, Li Y, White JG (2001) The *C. elegans zyg-1* gene encodes a regulator of centrosome duplication with distinct maternal and paternal roles in the embryo. Cell 105:547-58.

Phillips CM, Wong C, Bhalla N, Carlton PM, Weiser P, Meneely PM, Dernburg AF (2005) HIM-8 binds to the X chromosome pairing center and mediates chromosome-specific meiotic synapsis. Cell 123:1051-63.

Quevedo C, Kaplan DR, Derry, WB (2007) AKT-1 regulates DNA damage-induced germline apoptosis in *C. elegans*. Current Biology 17:286-92.

Rieder CL, Maiato H (2004) Stuck in division or passing through: what happens when cells cannot satisfy the spindle assembly checkpoint. Developmental Cell 7:637-51.

Saito TT, Mohideen F, Meyer K, Harper JW, Colaiácovo MP (2012) SLX-1 is required for maintaining genomic integrity and promoting meiotic noncrossover in the *Caenorhabditis elegans* germline. PLoS Genetics 8:e1002888.

Schumacher B, Hofmann K, Boulton S, Gartner A (2001) The *C. elegans* homolog of p53 tumor suppressor is required for DNA damage-induced apoptosis. Current Biology 11:1722-7.

Schvartzman JM, Sotillo R, Benezra R (2010) Mitotic chromosomal instability and cancer: mouse modeling of human disease. Nature Reviews Cancer 10:102-15.

Shinohara A, Ogawa H, Ogawa T (1992) RAD51 protein involved in repair and recombination in *Saccharomyces cerevisiae* is a RECA-like protein. Cell 69:457-70.

Stergiou L, Hengartner MO (2004) Death and more: DNA damage response pathways in the nematode C. elegans. Cell Death and Differentiation 11:21-28.

Xu J, Sun X, Jing Y, Wang M, Liu K, Jian Y, Yang M, Cheng Z, Yang C (2012) MRG-1 is required for genomic integrity in *Caenorhabditis elegans* germ cells. (2012) Cell Research 22:886-902.

Zhou Z, Hartwieg E, Horvitz HR (2001) CED-1 is a transmembrane receptor that mediates cell corpse engulfment in *C. elegans*. Cell 104:43-56.

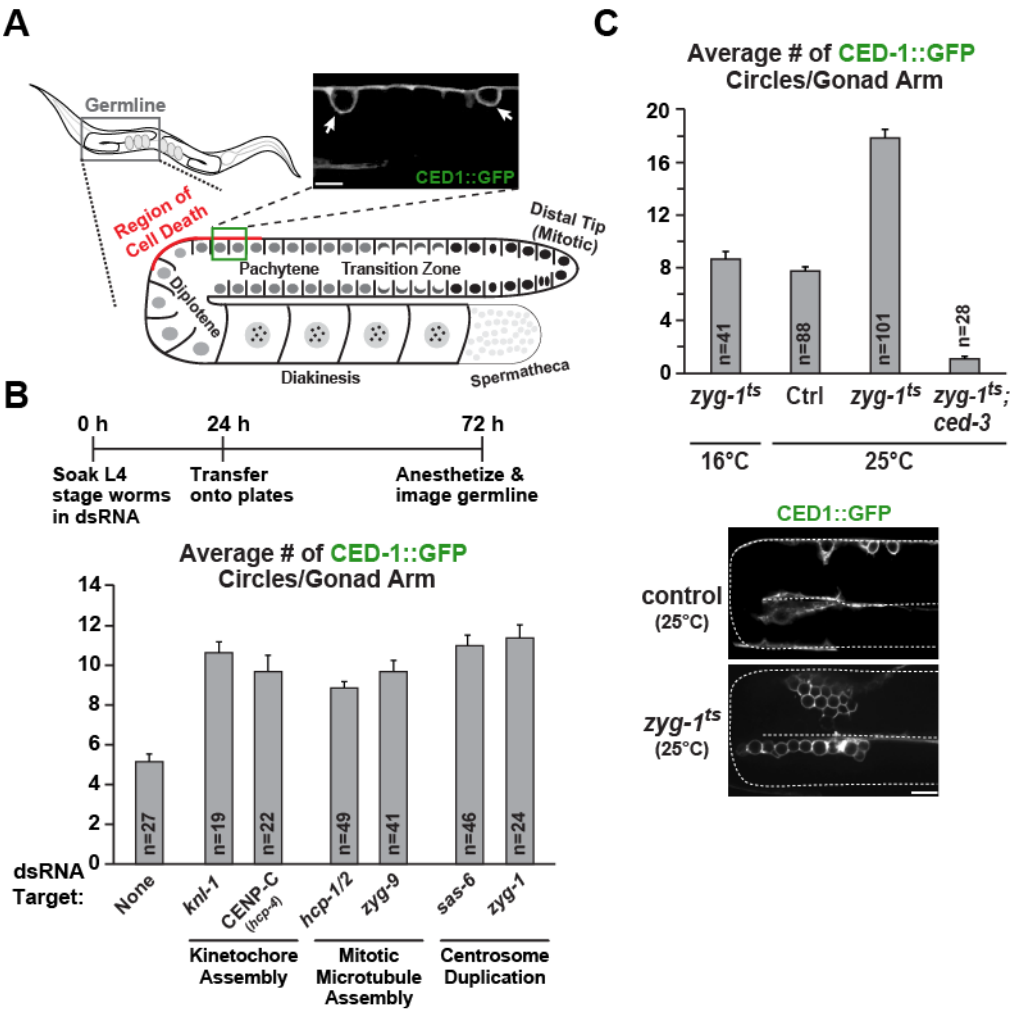

Figure 2.1 (A-C) Perturbation of mitosis in distal tip of the germline results in an increase in cell death. (A) Schematic of an adult hermaphrodite gonad and a representative image of CED-1::GFP signal; arrows denote nuclei undergoing programmed cell death. Scale bar=5 μm. **(B)** Quantification of cell death for the indicated conditions. Error bars are SEM; unpaired *t* test show high significance ($p<0.001$) between control and each individual inhibition. Experimental scheme is shown above the graph. **(C)** Quantification of cell death in the *zyg-1*^{ts} mutant and example images of the region of cell death in a *zyg-1*^{ts} mutant. The values plotted are the average number of CED-1::GFP circles at the following times: for *zyg-1*^{ts};ced-3, 24h after upshift of L4 larvae; for *zyg-1*^{ts} at 16°C, adults age-matched to 24h at 25°C; for control and *zyg-1*^{ts} at 25°C the compiled average from 24, 36 and 48h post-upshift of L4 larvae, which have similar individual values (*Fig. S1A*). Error bars are SEM; unpaired *t* test shows high significance ($p<0.0001$) between control and *zyg-1*^{ts} at 25°C. Scale bar=10 μm.

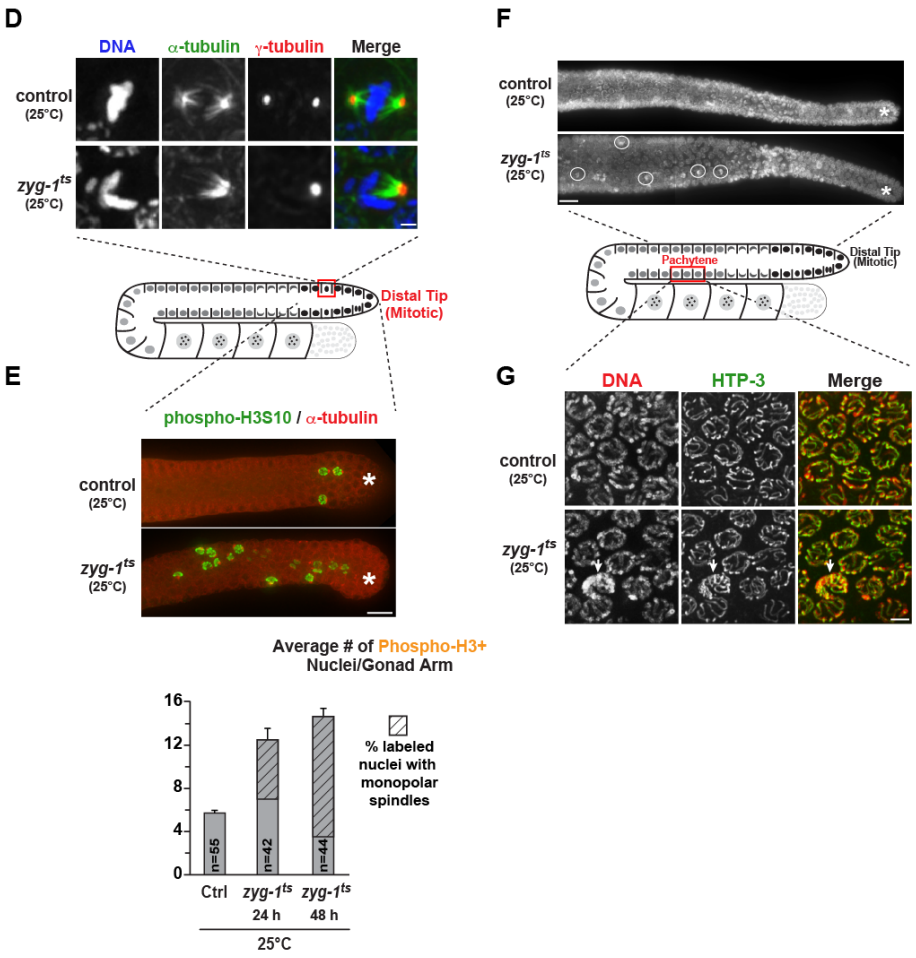

Figure 2.1 (D-G) Perturbation of mitosis in distal tip of the germline results in an increase in cell death. (D) Immunofluorescence images of the distal tip of extruded gonads labeled for DNA, α-tubulin and γ-tubulin 24h post upshift of L4 larvae. Images are partial z stack projections. Scale bar=2 μm. **(E)** Images and quantification of phospho-H3S10 positive nuclei in the distal gonad region 24h post-upshift of L4 larvae; the prevalence of monopolar spindles in the labeled nuclei is also plotted. Each bar represents the average value for each condition. Errors bars are SEM; unpaired *t* test shows high significance ($p<0.0001$) between control and *zyg-1*^{ts}. Asterisk denotes the distal most end of the mitotic tip. Images are partial z stack projections. Scale bar=10 μm. **(F)** Images of extruded gonads 48h post-upshift of L4 larvae stained with DAPI to visualize overall germline morphology. Images are partial z stack projections; asterisk denotes the distal end of the gonad and the circles highlight abnormal DAPI-stained nuclei. Scale bar=10 μm. **(G)** Immunofluorescence images of the pachytene region of extruded gonads stained for DNA and HTP-3 24h post upshift. Images are partial z stack projections; arrow denotes an abnormal nucleus positive for HTP-3. Scale bar=2 μm.

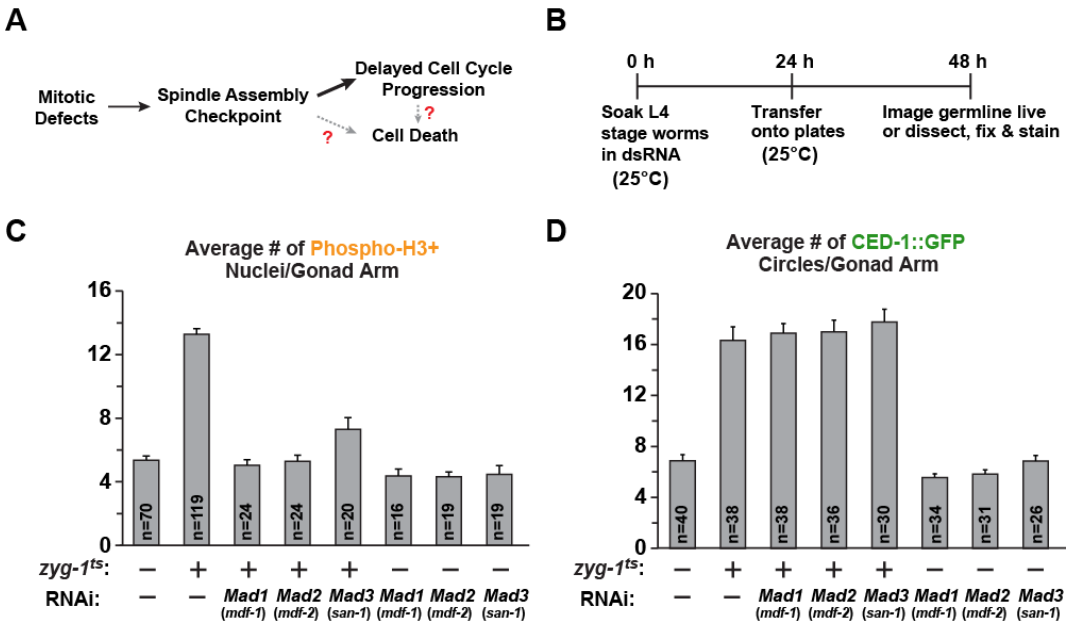

Figure 2.2 The spindle assembly checkpoint is required for the delay in mitosis, but not for the increase in cell death. (A) Schematic summarizing the function of the spindle checkpoint in delaying the cell cycle and hypothetical links between checkpoint activation and cell death. **(B)** Experimental scheme for both (C) and (D). **(C)** Quantification of the number of phospho-H3S10 positive nuclei for the indicated conditions. Errors bars are SEM; unpaired *t* test shows high significance ($p<0.0001$) comparing *zyg-1*^{ts} alone to *zyg-1*^{ts} in combination with each individual checkpoint protein inhibition. **(D)** Quantification of cell death following inhibition of the spindle checkpoint. Error bars are SEM.

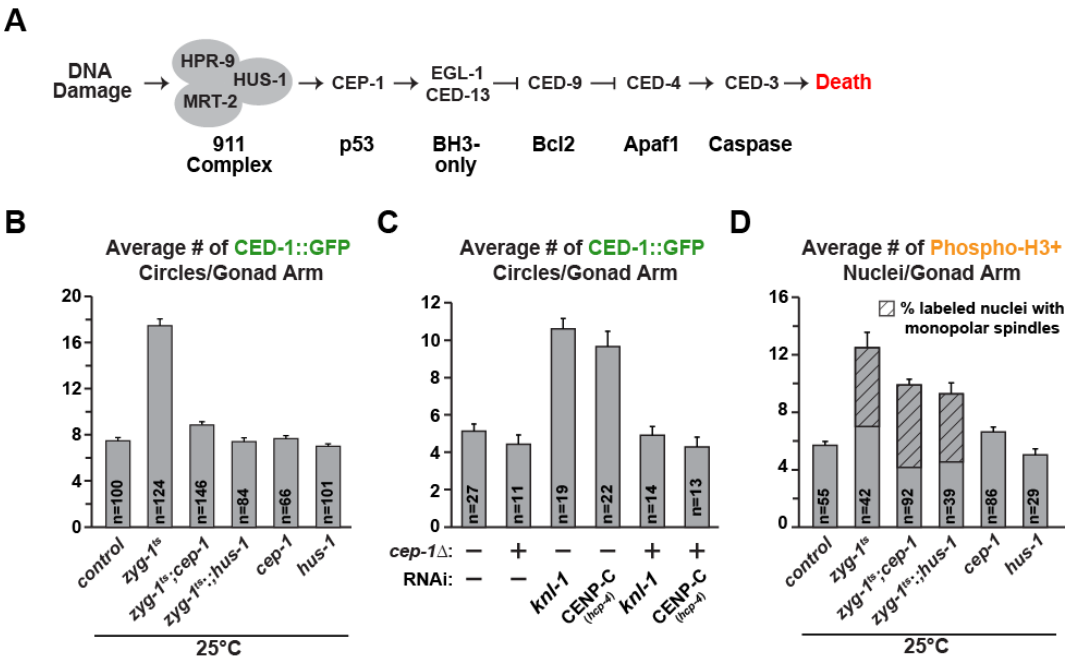

Figure 2.3 (A-D) The DNA damage checkpoint mediates the elevation in cell death induced by defective mitoses in the distal tip. (A) Simplified schematic of the DNA damage checkpoint pathway in the *C. elegans* germline. **(B)** Quantification of cell death following inhibition of the DNA damage checkpoint components $p53^{CEP-1}$ and HUS-1, in both control and *zyg-1*^{ts} worms. Each bar represents the average number of CED-1::GFP positive circles 24 - 48h post upshift of L4 larvae. Error bars are SEM; unpaired *t* test shows high significance ($p<0.001$) between *zyg-1*^{ts} alone and the double mutants. **(C)** Quantification of cell death for the indicated conditions using the experimental scheme shown in Fig. 1B. Each bar represents the average number of CED-1::GFP positive circles. Error bars are SEM; unpaired *t* test shows high significance ($p<0.001$) between RNAi in controls versus RNAi in the *cep-1* deletion. **(D)** Quantification of the number of phospho-H3S10 positive nuclei and the prevalence of monopolar spindles 24h post upshift (data for the control and *zyg-1*^{ts} is the same as in *Fig. 1E*). Error bars are SEM; unpaired *t* test shows high significance ($p<0.001$) between *zyg-1*^{ts} alone and the double mutants.

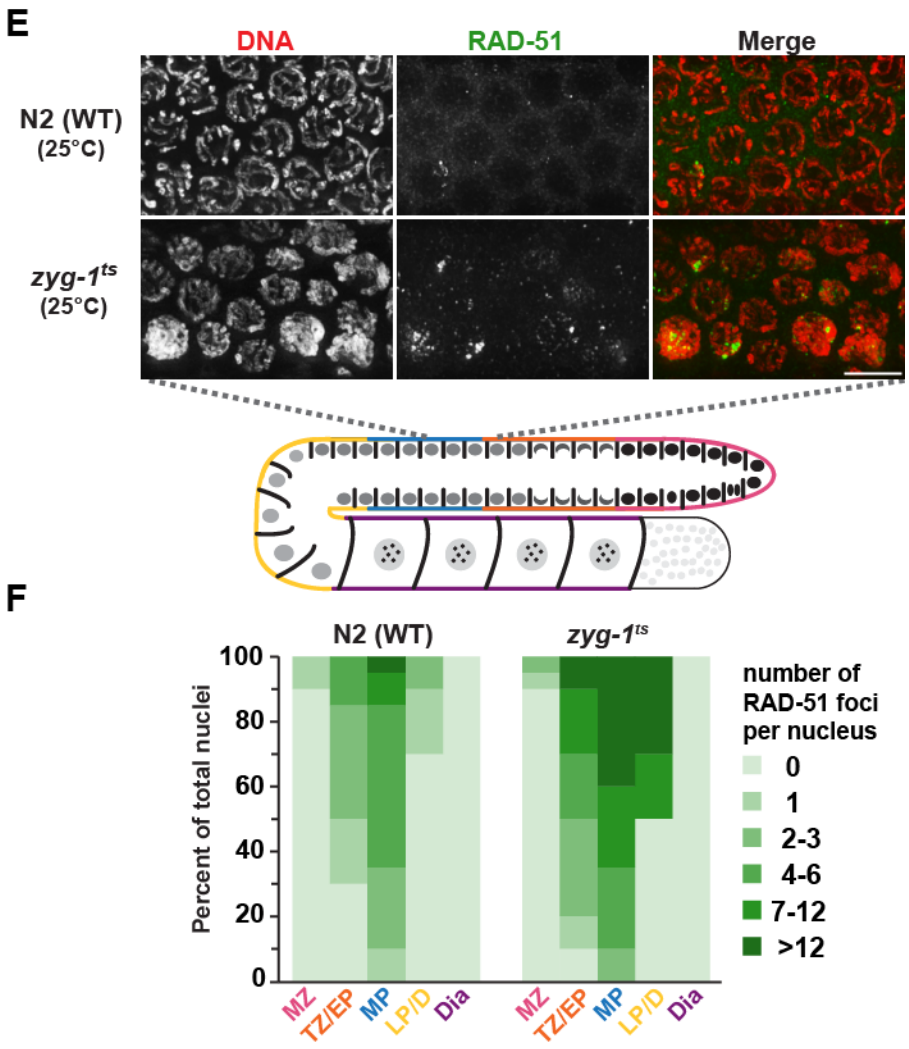

Figure 2.3 (E and F) The DNA damage checkpoint mediates the elevation in cell death induced by defective mitoses in the distal tip. (E) Immunofluorescence images of the late pachytene region of extruded gonads stained with DAPI and RAD-51. Images are a partial z stack projection. Scale bar=5 μm. **(F)** Quantification of the number and prevalence of RAD-51 foci for both control and *zyg-1*^{ts} 48h post upshift. Each gonad was divided into 5 distinct zones and the number of nuclei labeled with RAD-51 as well as the number of foci per nucleus was counted; at least 10 gonads were analyzed per genotype. (MZ=mitotic zone; TZ/EP=transition zone/early pachytene; MP=mid-pachytene; LP/D=late pachytene/diplotene; Dia=diakinesis)

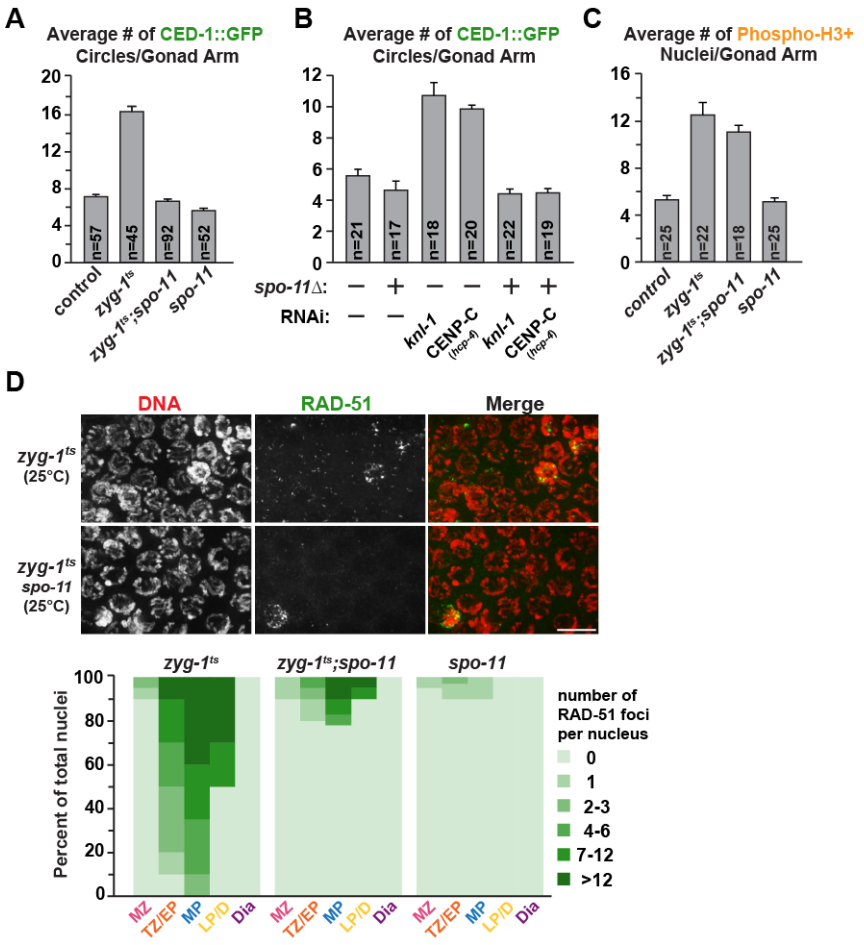

Figure 2.4 (A-D) Meiotic recombination-initiating double-strand breaks are responsible for the elevated cell death observed following errors in mitosis. (A) Quantification of cell death following inhibition of *spo-11* in both control and *zyg-1*^{ts} 24h post upshift. Error bars are SEM; unpaired *t* test shows high significance (p<0.0001) between *zyg-1*^{ts} alone and the double mutant. **(B)** Quantification of cell death following inhibition of *spo-11* in both control and indicated mitotic inhibitions (same experimental scheme as *Fig. 1B*). Error bars are SEM; unpaired *t* test shows high significance (p<0.001) between RNAi in controls versus RNAi in the *spo-11* deletion. **(C)** Quantification of the number of phospho-H3S10 positive nuclei following inhibition of *spo-11* in both control and *zyg-1*^{ts} 24h post upshift of L4 larvae. Error bars are SEM; unpaired *t* test shows no significant difference (p=0.27) between *zyg-1*^{ts} alone and the double mutant. **(D)** Immunofluorescence images of the late pachytene region of extruded gonads for both *zyg-1*^{ts} and *zyg-1*^{ts};*spo-11* 48h post upshift stained with DAPI and RAD-51. Images are a partial z stack projection. Scale bar=5 μm. Quantification of the RAD-51 foci is shown below the images (*zyg-1*^{ts} values are the same as in *Fig. 3F*).

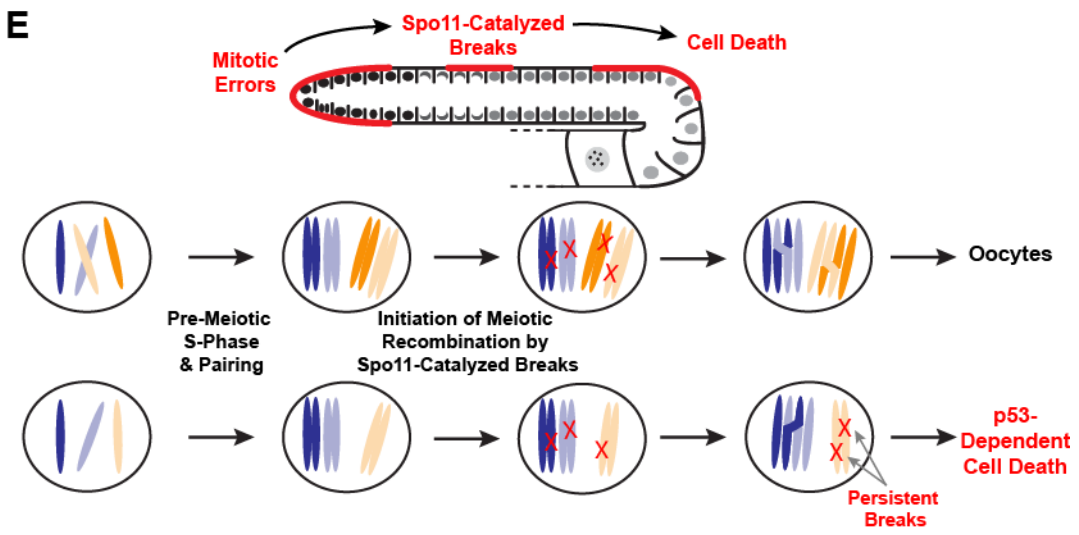

Figure 2.4 (E) Meiotic recombination-initiating double-strand breaks are responsible for the elevated cell death observed following errors in mitosis. (E) Schematic summarizing the role of Spo11-catalyzed breaks in the detection of mitotic errors that occurred in the distal tip. The individual nucleus cartoons below show a normal nucleus with 2 pairs of homologous chromosomes (*top*) and a defective nucleus in which one of the chromosomes is missing due to missegregation (*bottom*).

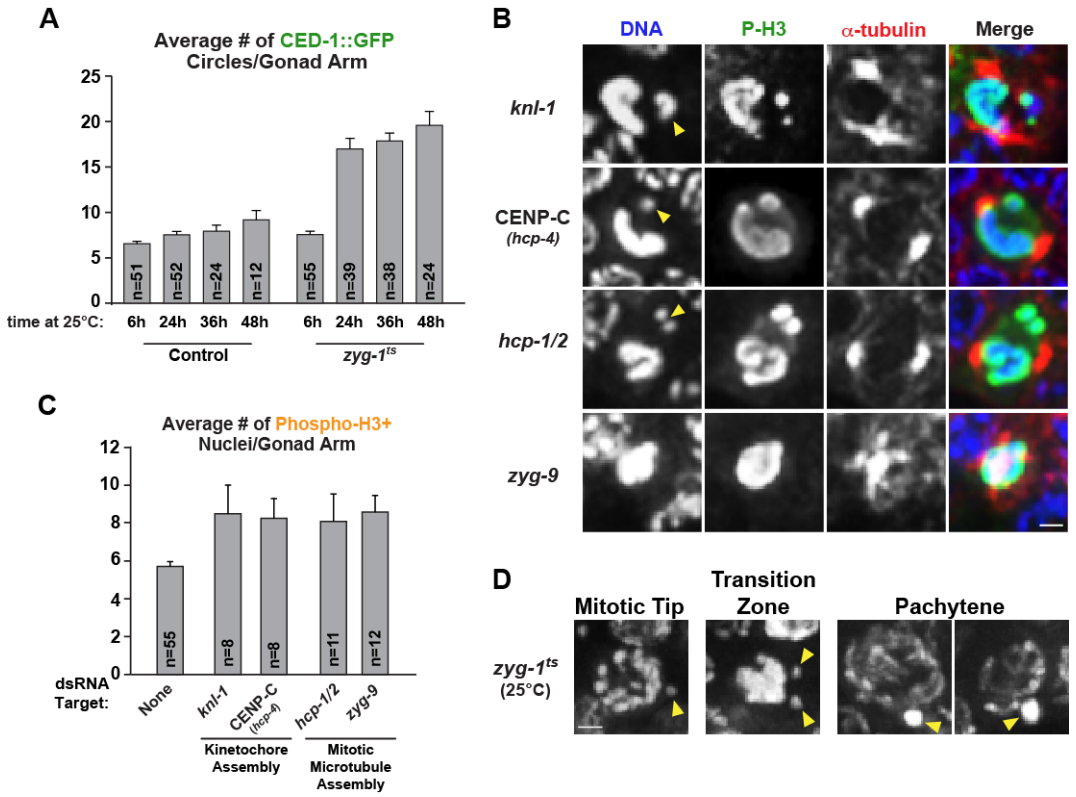

Figure S2.1 (related to Figure 2.1) Defects in distal tip cells observed following inhibition of mitotic subprocesses. (A) Quantification of each individual timepoint from the data presented in *Fig. 1C*. Each bar represents the average number of CED-1::GFP positive circles per condition. Error bars are SEM; one-way ANOVA analysis shows no significance between the 24, 36 and 48h time points for either control or *zyg-1*^{ts} (p=0.23 and p=0.33, respectively). **(B)** Immunofluorescence images of the distal tip of extruded gonads stained with DAPI, α tubulin and γ tubulin for both the control and mitotic inhibitions (*knl-1*, CENP-C^{hcp-4}, *hcp-1/2* and *zyg-9* RNAi). Images are a partial z stack projection; arrowheads denote misaligned chromosomes. Scale bar=2 μm. **(C)** Quantification of the number of phospho-H3S10 positive nuclei upon inhibition of mitosis in the distal germline. Experimental scheme is the same as is presented in Fig. 1B, but instead of live imaging, gonads were extruded, fixed and stained. Error bars are SEM; unpaired *t* test shows high significance (p<0.001) between control and each individual inhibition. **(D)** DAPI-stained nuclei in *zyg-1*^{ts} germlines 24h post upshift of L4 larvae showing the presence of micronuclei. Image 1 is from the mitotic/distal tip, image 2 the transition zone and images 3 and 4 pachytene. Scale bars= 2 μm.

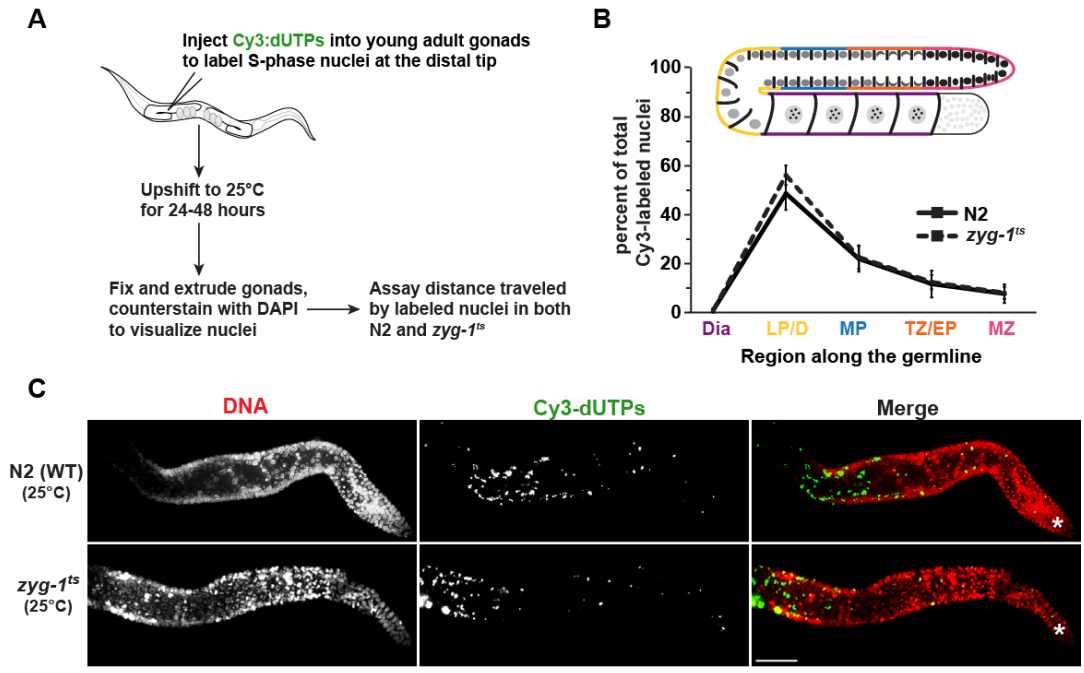

Figure S2.2 (related to Figure 2.1) Disruption of mitotic cell divisions in the distal tip does not affect travel of nuclei through the gonad. (A) Schematic of the experimental procedure presented in (B) and (C). Injection of Cy3-dUTP was done as previously described (Jaramillo-Lambert et al., 2007). **(B)** Quantification of the distance traveled by Cy3-dUTP labeled nuclei in both control and *zyg-1*^{ts}. The number of labeled nuclei was counted in each of the 5 different zones (MZ=mitotic zone; TZ/EP=transition zone/early pachytene; MP=mid-pachytene; LP/D=late pachytene/diplotene; Dia=diakinesis), the data points represent 24h post upshift, averaged for 10 worms per genotype. Error bars are SEM. **(C)** Representative immunofluorescence images for the data presented in (B), counterstained with DAPI. Images are a maximum projection z stack. The single asterisk denotes the distal tip. Scale bar=10 μm.

Chapter 3. Uncoordinated loss of chromatid cohesion is a common outcome of extended metaphase arrest

ABSTRACT

Chromosome segregation requires coordinated separation of sister chromatids following biorientation of all chromosomes on the mitotic spindle. Chromatid separation at the metaphase-to-anaphase transition is accomplished by cleavage of the cohesin complex that holds chromatids together. Here we show using live-cell imaging that extending the metaphase bioriented state using five independent perturbations (expression of non-degradable Cyclin B, expression of a Spindly point mutant that prevents spindle checkpoint silencing, depletion of the anaphase inducer Cdc20, treatment with a proteasome inhibitor, or treatment with an inhibitor of the mitotic kinesin CENP-E) leads to eventual scattering of chromosomes on the spindle. This scattering phenotype is characterized by uncoordinated loss of cohesion between some, but not all sister chromatids and subsequent spindle defects that include centriole separation. Cells with scattered chromosomes persist long-term in a mitotic state and eventually die or exit. Partial cohesion loss-associated scattering is observed in both transformed cells and in karyotypically normal human cells, albeit at lower penetrance. Suppressing microtubule dynamics reduces scattering, suggesting that cohesion at centromeres is unable to resist dynamic microtubule-dependent pulling forces on the kinetochores. Consistent with this view, strengthening cohesion by

inhibiting the two pathways responsible for its removal significantly inhibits scattering. These results establish that chromosome scattering due to uncoordinated partial loss of chromatid cohesion is a common outcome following extended arrest with bioriented chromosomes in human cells. These findings have important implications for analysis of mitotic phenotypes in human cells and for development of anti-mitotic chemotherapeutic approaches in the treatment of cancer.

INTRODUCTION

Accurate passage through mitosis is a highly orchestrated process that relies on the timely coordination of multiple events to ensure proper segregation of genetic material. Errors in chromosome segregation lead to aneuploidy, a well-known hallmark of human cancers. A key mechanism that ensures each daughter cell receives the correct chromosome content is the maintenance of the physical links between sister chromatids until all chromosomes become properly bioriented on the mitotic spindle (Nasmyth and Haering, 2009). Sister chromatids are held together by cohesin, a multisubunit protein complex that is loaded along the length of each pair concomitant with replication in S phase (Sherwood et al., 2010). A majority of the cohesin resides on the chromosome arms and is removed at the beginning of mitosis, whereas centromeric cohesin remains bound until the metaphase-to-anaphase transition (Waizenegger et al., 2000). The prophase removal of cohesin involves the activity of the kinases Plk1 and Aurora B (Losada et al., 2002; Sumara et al., 2002) as well as the physical interaction of the protein Wapl with the cohesin complex (Gandhi et al., 2006; Kueng et al., 2006). In contrast, the removal of cohesin at the onset of anaphase requires the protease separase, which cleaves the cohesin subunit Scc1 (Uhlmann et al., 1999; Hauf et al., 2001). Separase is activated at anaphase onset when the anaphase promoting complex/cyclosome (APC/C), an E3 ubiquitin ligase, targets its inhibitor securin for degradation and reduces Cdk1 activity (Zachariae et al., 1999; Stemmann et al., 2001). The APC/C activity targeting

securin is inhibited by the spindle assembly checkpoint until all chromosomes are fully aligned on the metaphase plate. When the last pair of chromatids properly aligns, the checkpoint is turned off, which leads to APC/C-mediated degradation of securin, and in turn activates separase. Separase then cleaves the centromeric cohesin in a coordinated manner so that cohesin is lost from all sister chromatids as the cell enters anaphase. Previous studies have investigated the consequences of uncoupling these regulated events and have shown how important their coordination is for proper chromosome segregation and progression through mitosis (Jallepalli et al., 2001; McGuinness et al., 2005; Wirth et al., 2006).

Under conditions where the checkpoint signal is sustained in the presence of fully aligned chromosomes, cells persist in mitosis for a variable amount of time before the metaphase plate begins to break down. This phenotype, termed chromosome scattering, was initially described as a result of inhibition of the spindle and kinetochore associated protein Ska3 (Daum et al., 2009) and was later observed in cells expressing a point mutant of the kinetochore protein Spindly (Gassmann et al., 2010). Since both perturbations cause the checkpoint to remain active without interfering with chromosome alignment, we hypothesized that chromosome scattering is not perturbation specific, but rather a general result of prolonged arrest in metaphase. In the present study we set out to determine how frequently cells scatter their chromosomes after a persistent arrest in a relatively unperturbed mitosis and to investigate the factors contributing to this phenotype. Using both live cell

and fixed image analyses we found chromosome scattering to occur in a wide variety of conditions that prevent exit from mitosis with a completely or near-completely aligned metaphase plate. Cells with scattered chromosomes had partial loss of chromatid cohesion and defects in spindle structure. Scattering was inhibited by either stabilizing microtubules or by preventing the removal of cohesion. These results establish that uncoordinated loss of chromatid cohesion is a common outcome of extended metaphase arrest in human cells.

RESULTS

Prolonged Metaphase Arrest Induced by Five Distinct Treatments Leads to Chromosome Scattering

To assess whether chromosome scattering is a general consequence of a prolonged metaphase arrest, we tested whether this phenotype is induced by multiple perturbations used to hold cells in a metaphase-like state. For this purpose, HeLa FRT cells (harboring a single FRT recombination site that was either empty or integrated with tetracycline-regulated transgenes expressing either the Spindly F258A or Cyclin B Δ86 mutants (Gassmann et al., 2010)) expressing fluorescent histone H2b were exposed to five distinct conditions that prevent anaphase entry. Chromosomes aligned fully with normal kinetics in four of these conditions—expression of non-degradable Cyclin B Δ86 (Gallant et al., 1992; Holloway et al., 1993), expression of a Spindly F258A mutant following endogenous Spindly depletion, Cdc20 depletion, or proteasome inhibitor treatment; in the fifth condition, treatment with a CENP-E kinesin inhibitor (Qian et al., 2008; Wood et al., 2010) the majority of chromosomes aligned but a few persisted at the poles. Live imaging revealed that chromosome scattering is eventually observed for the aligned chromosomes with all five perturbations (Fig. 1A; Movie S1 and S2).

In four out of the five conditions, 100% of the cells exhibited scattering. Following Cdc20 knockdown, half of the cells that entered mitosis scattered their chromosomes; the remainder progressed through mitosis with a mild delay (51 ± 30 mins from NEBD to anaphase compared to 34 ± 5 mins for the

control), most likely due to partial penetrance of the RNAi-mediated knockdown (Huang et al., 2009). The time from NEBD to scattering was variable between the different conditions, ranging from 44 to 360 mins (Fig. 1B). Chromosomes remained condensed during the scattered state indicating a persistent mitotic arrest; for the Spindly mutant, prior work showed persistence of securin and Cyclin B in the scattered state (Gassmann et al., 2010). We also observed securin and Cyclin B persistence in scattered cells knocked down for Cdc20 or treated with the CENP-E inhibitor (Fig. S1A and B). Scattered cells expressing Cyclin B Δ86 exhibited high securin levels (Fig. S1B), indicating that the single copy Cyclin B Δ86 insertion does not robustly activate the anaphase promoting complex and trigger an anaphase-like state with high Cdk1 kinase activity (Holloway et al., 1993; Gallant et al., 1992). We did observe a small proportion (~10%) of the cells expressing Cyclin B Δ86 that were in an anaphase-like state with reduced securin levels (Fig. S1C); these cells are morphologically distinct from the scattered cells, as they show equal separated chromosome masses, and were not included in analysis of the scattered state. These observations indicate that when progression into anaphase is prevented in HeLa FRT cells, chromosome scattering is a frequent outcome irrespective of the precise means used to prevent anaphase entry.

Chromosome Scattering is Initiated by Uncoordinated Loss of Sister Chromatid Cohesion

We next investigated the scattering phenotype at higher resolution using both live imaging and fixed analysis. High-resolution live imaging revealed initial dispersion of a few fluorescent H2b masses from the metaphase plate, followed by increasing dispersion of chromosomes and rotation of the spindle within the cell (Fig. 1C; Movie S3). High-resolution fixed analysis revealed the frequent presence of single chromatids in the scattered state, indicating loss of sister chromatid cohesion on some of the chromosomes in the cell. In the same cells, sisters at the spindle equator remained paired (Fig. 1D). This result suggests that scattering induced loss of cohesin is uncoordinated, in contrast to anaphase onset in which cohesin is removed from all sister chromatids simultaneously.

The above observations suggest that partial and uncoordinated loss of chromatid cohesion is the trigger for entry into the scattered state. To assess if weakened cohesion could be detected prior to the onset of scattering, we analyzed the inter-kinetochore distance in cells with fully aligned chromosomes prior to visible scattering for arrests generated using Cyclin B Δ86 or the Spindly F258A mutant. Control cells were mock transfected and treated with tetracycline in parallel. In this experiment, which involved fixed analysis of an asynchronous population of cells, each cell analyzed had spent a variable and undetermined amount of time with fully aligned chromosomes. A mild but statistically significant increase is observed for the average inter-kinetochore distance for the two perturbations (unpaired *t* test, $p = 0.0001$ for Cyclin B Δ86 and 0.0005 for the Spindly F258A mutant when compared to

control). However, we observed the presence of a number of hyper-stretched sister kinetochores in cells expressing either the Spindly F258A or Cyclin B Δ86 mutants (Fig. 1E), which are not detected in the control cells. We suggest this extended stretch reflects weakened sister cohesion that is less able to resist the outward pulling forces generated on the kinetochores and will soon after lead to dispersion of chromatids from the metaphase plate and entry into the scattered state. These measurements support the notion that uncoordinated loss of cohesion underlies the scattering phenotype.

Spindle Defects are a Secondary Consequence of Entry into the Scattered State

Analysis in fixed cells revealed that the scattered state is frequently correlated with spindle defects that include extra spindle poles and disengaged centrioles (Fig. 2A and B). Live imaging of a HeLa cell line expressing mRFP:histone H2b and YFP:α-tubulin that was transfected to transiently express nondegradable Cyclin B Δ86 revealed that chromosomes scattered from the plate prior to the emergence of spindle defects and spindle rotation (Fig. 2C, n=14 cells). The time in which spindle defects arose after cells scattered their chromosomes was variable, ranging from 60 to 344 mins after the first visible sign of scattering. In 5/6 cells where spindle rotation was clearly visible, rotation preceded the appearance of extra spindle poles. In fixed analysis, the spindle rotation phenotype appears as spindle malorientation relative to the cell substrate. These results suggest that partial

and uncoordinated loss of chromatid cohesion is the initiating event in scattering, followed by subsequent spindle defects.

Karyotypically Normal Human Cells are Susceptible to Chromosome Scattering After An Extended Metaphase Arrest

The observation that entry into the chromosome scattering state is a frequent response to a prolonged metaphase arrest in HeLa FRT cells prompted us to test whether this phenotype is also observed in a karyotypically normal human cell line. For this purpose, we analyzed telomerase-immortalized RPE1 cells (hTERT-RPE1) expressing fluorescent histone H2b. We initially attempted Cdc20 RNAi in these cells to generate a metaphase arrest but low transfection efficiency prevented significant knockdown and extended arrest in metaphase. We therefore treated hTERT-RPE1 cells with the CENP-E inhibitor and imaged them over time (Fig. 3A). Of the treated cells, 35% exhibited chromosome scattering following an extended arrest (Class II), 35% delayed in mitosis and progressed into anaphase (Class I) and 30% remained arrested in mitosis for the duration of the 10 hr time lapse without scattering, but did exhibit a large number of polar chromosomes that had never congressed to the metaphase plate (Class III). When compared to HeLa FRT cells, the Class II hTERT-RPE1 cells took over twice as long to scatter their chromosomes (362 ± 62 mins after NEBD for hTERT-RPE1 and 164 ± 50 mins for HeLa FRT, Fig. 3B). Fixed analysis of both cell lines treated with the CENP-E inhibitor revealed the presence of

single chromatids in cells with scattered chromosomes (Fig. 3C), confirming the idea that scattering results from the uncoordinated loss of cohesion.

These results establish that scattering is also observed at a significant frequency in karyotypically normal human cells following an extended metaphase arrest, albeit at lower penetrance and after a longer arrest time than in the highly aneuploid HeLa FRT cells.

The Spindle Checkpoint is Reactivated in the Scattered State and Leads to Long-Term Persistence in Mitosis

The spindle checkpoint is silenced by removal of checkpoint proteins from the kinetochore following microtubule attachment (Hardwick and Shah, 2010). Uncoordinated loss of chromatid cohesion is expected to reactivate the checkpoint on the individual chromatids that are no longer stably attached to the spindle. Consistent with this, we observed Mad1 labeling on kinetochores of single chromatids in scattered Cyclin B Δ86-expressing cells (no Mad1 labeling is observed on metaphase aligned chromosomes prior to scattering onset, Fig. 4A).

We next assessed the long-term consequences of entry into the scattered state. For this purpose, we filmed HeLa FRT cells or hTERT-RPE1 cells for 48 hrs following treatment with the CENP-E inhibitor. For both cell lines, the scattered cells persisted in their aberrant state for 10-25 hrs and then exhibited one of two fates: mitotic exit (characterized by chromosome decondensation and separation of the chromatin into two or three distinct

masses) or death (characterized by the presence of hypercondensed chromatin masses) (Fig. 4B). For both cell lines, the predominant long-term outcome of chromosome scattering via inhibition of CENP-E was mitotic exit. A portion of the cells that exited the scattering state subsequently died in interphase (50% for HeLa FRT cells and 4% for hTERT-RPE1 cells); the remaining population of cells neither died nor entered another round of mitosis during the 48 hr filming period.

We also filmed HeLa FRT cells expressing the Spindly F258A mutant or Cyclin B Δ86 for 48 hrs. For these two conditions, which lock the spindle checkpoint into an active state or prevent mitotic exit, respectively (Gassmann et al., 2010; Gallant and Nigg, 1992) cells persisted with condensed, scattered chromosomes and eventually died 10-25 hrs after initial entry into mitosis (Fig. 4C).

We next assessed whether the long-term persistence in the scattered state required spindle checkpoint activity. We first treated HeLa FRT cells with the CENP-E inhibitor and filmed them for 5 hrs. We then added the Mps1 inhibitor reversine (Santaguida et al., 2010) and assessed the outcome in cells that had already been in a scattered state for 1-5 hrs. We also performed a similar experiment with scattered cells generated using the Spindly F258A mutant. Without reversine addition, scattered cells generated by either perturbation spent 8-14 hrs in mitosis before exiting or undergoing cell death (Fig. 4D). For both perturbations, treatment with reversine led to rapid exit from the scattered mitotic state, as determined by chromosome

decondensation (Fig. 4E and F). This result, together with the presence of checkpoint proteins on the kinetochores of scattered chromatids, suggests that spindle checkpoint activity maintains the cells in the long-term scattered mitotic state.

Overall, the long-term filming revealed that once cells enter the scattered state, they persist in this state for minimally 8 hrs and either exit in a non anaphase-like manner or die in the scattered state. In the cells that do exit the scattered state interphase cell death is frequently observed. The long-term persistence of this aberrant mitotic state is likely due to activation of the spindle checkpoint following partial loss of chromatid cohesion. Given that, under our conditions, normal mitotic duration (from NEBD to anaphase) in HeLa FRT cells is ~34 mins and in hTERT-RPE1 cells is ~29 mins, the persistence of the scattered state for over 10-25 hrs indicates that, once cells scatter their chromosomes, they are effectively in a terminal state and are unable to recover and proliferate.

Prolonged Biorientation With Dynamic Microtubules Promotes Chromosome Scattering

Prior to the onset of chromosome scattering, cells spend a significant amount of time arrested with most, or all, chromosomes aligned on the metaphase plate. In bioriented chromosomes, pulling forces from the dynamic spindle microtubules bound to kinetochores are resisted by cohesion between the sisters, placing sister chromatids under tension (Bloom and Yeh, 2010). To

determine if the action of dynamic microtubules contributes to the chromosome scattering phenotype, taxol was added to cells expressing Cyclin B Δ86 following full alignment in metaphase in order to stabilize microtubules and decrease tension across sisters. Asynchronously cycling cells induced for Cyclin B Δ86 expression were imaged live and monitored for entry into mitosis and alignment of chromosomes. Taxol was added after 30 minutes; enough time to allow for completion of, but not significant arrest in, metaphase. Continued long-term live imaging of these cells revealed that addition of taxol effectively inhibits chromosome scattering. After the addition of taxol, cells expressing Cyclin B Δ86 remain arrested with a metaphase plate without scattering (Fig. 5A). After a variable amount of time, the plate did begin to breakdown and collapse, however this is due to the effect of taxol on spindle structure, as the same phenotype is observed in control cells not expressing Cyclin B Δ86 (data not shown).

Since the average time a cell spends in mitosis prior to scattering is at least twice as long as the normal mitotic duration, it is possible that the amount of time a cell stays in mitosis, not just the forces from dynamic microtubules, contributes to the onset of chromosome scattering. To address this possibility, HeLa FRT cells, hTERT-RPE1 cells and HeLa cells expressing mRFP:histone H2b and YFP:α-tubulin were treated with monastrol, which arrests cells in mitosis with very little to no tension across sisters (average interkinetochore distance as measured by ACA staining: 0.42 ± 0.07 μm in cells treated with monastrol compared to 1.41 ± 0.15 μm in untreated cells fully aligned in

metaphase). The cells were incubated in the presence of the drug for 6 hrs, given fresh, drug-free media and subsequently imaged live for 10 hrs. The majority of hTERT-RPE1 cells entered anaphase after washout (Fig. 5B and C), indicating that extended time in mitosis without tension across sisters does not induce scattering in this cell line. The HeLa FRT cells, however, responded in one of two ways: 50% entered anaphase after washout whereas the other 50% remain arrested with what appear to be scattered chromosomes (Fig. 5B and C). Since a proportion of the cells that did progress through mitosis did so with multipolar spindles (three or four distinct chromatin masses segregating at anaphase), it appeared that spindle defects were arising during the prolonged drug treatment in the HeLa FRT cells. We speculated that in the 50% of these cells that did not progress into anaphase, spindle defects as opposed to uncoordinated cohesion loss, was responsible for the progression defect. To test this, we directly imaged spindles and chromosomes under the same experimental regime in a different HeLa line stably expressing mRFP:histone H2b and YFP:α-tubulin. In this line, we observed that at the time of washout 40% of the cells had more than two α-tubulin foci, indicating aberrant spindle formation. Of the cells with multipolar spindles, 50% failed to progress into anaphase (Fig. 5B and C), supporting the view that spindle defects can arise during prolonged treatment in monastrol and perturb progression after washout.

Overall, these results suggest that spending an extended time in mitosis without tension across sisters does not promote uncoordinated

cohesion loss to the same extent as when tension is present. However, depending on the cell line, different levels of spindle defects may be present at the time of drug washout, which greatly decreases the frequency of normal progression into anaphase. Cumulatively, the analysis of acute taxol treatment and monastrol treatment followed by washout suggests that uncoordinated cohesion loss during extended metaphase arrest is promoted by the action of dynamic microtubules pulling on bioriented kinetochores.

Strengthening Cohesion Inhibits Chromosome Scattering

The above results suggest that chromatid cohesion is lost in an uncoordinated manner during an extended mitotic arrest and this loss is promoted by dynamic microtubules exerting tension on the paired sisters. To test this model, we decided to strengthen cohesion by perturbing its cleavage during anaphase and/or its non-proteolytic removal during prophase. In an unperturbed mitosis, the majority of cohesin is removed in prophase by a non-proteolytic pathway involving the conserved Wapl protein and Polo-like kinase 1 (Hauf et al., 2005; Shintomi and Hirano, 2009). Centromeric cohesion is protected during prophase and removed at the metaphase-to-anaphase transition by the protease separase, whose activity is inhibited by the spindle assembly checkpoint until all of the chromosomes are properly bioriented (Hauf et al., 2001). We inhibited separase via RNAi in HeLa FRT cells expressing Cyclin B Δ86 (Fig. S2). Live imaging of these cells revealed that inhibition of separase led to a delay in the onset of chromosome scattering

(NEBD to scattering: 119 ± 51 mins with Cyclin B Δ86 + separase RNAi versus 78 ± 25 mins with Cyclin B Δ86 alone, Fig. 6A and C). However, all of the cells that entered mitosis scattered their chromosomes (Fig. 6B). In cells not expressing Cyclin B Δ86, separase knockdown caused two different phenotypes, 50% of the cells either progressed through anaphase, albeit with both a delay in timing (NEBD to anaphase onset: 51 ± 12 mins versus 34 ± 5 mins for the control) and the appearance of lagging chromosomes, whereas the other 50% remain arrested in mitosis with what appear to be scattered chromosomes (data not shown). Inhibition of Wapl by RNAi (Fig. S2) also led to a delay in the onset of chromosome scattering (NEBD to scattering: 134 ± 47 mins with Cyclin B Δ86 + Wapl RNAi, Fig. 6A and C). Similar to separase inhibition, all of the cells that entered mitosis with reduced Wapl function scattered their chromosomes (Fig. 6B). Reducing the function of both separase and Wapl together had a strongly synergistic effect. Only one-third of the cells that entered mitosis scattered their chromosomes in the double RNAi, whereas the remaining cells either died or persisted in mitosis with an observable metaphase plate (Fig. 6A and B). Of the cells that scattered, the time spent in mitosis prior to chromosome scattering increased nearly 3-fold (200 ± 91 mins) compared to the control cells (78 ± 25 mins) (Fig. 6C). 65% of the cells that persisted with a metaphase plate showed no signs of spindle rotation, as assessed by the orientation of the metaphase plate; the remaining 35% exhibited mild spindle rocking but not the full rotations observed in scattered cells. These results suggest that strengthening cohesion by

blocking both cohesin removal pathways significantly inhibits the scattering phenotype.

DISCUSSION

In this study, we describe an aberrant mitotic state that is induced in karyotypically normal and abnormal human cells by multiple perturbations that prevent normal progression into anaphase. Entry into this state is triggered by partial and uncoordinated loss of sister chromatid cohesion on chromosomes aligned at the metaphase plate. Spindle checkpoint activation on the single chromatids leads to persistence in a mitotic state with increasing loss of cohesion and subsequent spindle defects, followed by an eventual non anaphase-like exit and/or cell death. These results suggest that chromatid cohesion is placed under stress in an attached bi-oriented state and extending this state can lead to cohesion failure. Discovery of this phenotype as a general result of prolonged metaphase arrest has implications for the interpretation of mitotic defects following perturbation of specific components and for the mechanistic analysis of anti-mitotic chemotherapeutic strategies.

Distinction Between Scattering and Anaphase

Both scattering and anaphase are associated with loss of chromatid cohesion. Anaphase onset is tightly coupled to biorientation of all chromosomes in the cell (Rieder et al., 1995). In contrast, scattering is observed with perturbations where all of the chromosomes are aligned as well as with perturbations where some chromosomes fail to align at the plate. Thus, it appears that too much time spent in a bioriented state initiates entry into the scattered state. Another key distinction between scattering and

anaphase is that in the scattering phenotype, cohesion loss is partial and uncoordinated; a hallmark of anaphase is coordinated removal of cohesion that is coupled to Cdk1 inactivation. The lack of coordination in the presence of Cdk1 activity leads to reactivation of the spindle checkpoint on single chromatids following their dispersal from the plate. We propose that this traps the cell in an increasingly unstable mitotic state, leading to further cohesion loss (Fig. 7). The onset of scattering is also followed by spindle defects and spindle rotation within the cell (Fig. 7). At metaphase, biorientation of chromosomes and forces in the spindle are poised to coordinate separation of sister chromatids (Matos et al., 2009). The partial loss of cohesion during scattering may lead to an imbalance in these forces and subsequent spindle structure defects.

The comparison between scattering and anaphase onset suggests that cohesion is a potential weak link during mitosis and rapid alignment and progression are important to avoid entering into the scattered state. It is currently unclear what features make a subset of chromosomes initiate scattering. Either a differential force depending on spindle location underlies susceptibility to scattering or there is chromosome-autonomous susceptibility, potentially dictated by the amount of cohesin present at individual centromeres.

Mechanism of Scattering

There are two possible explanations for the dysregulation that leads to the partial uncoordinated cohesion loss that underlies scattering. The first explanation is that the separase-mediated cleavage reaction, which normally acts to trigger anaphase, is weakly activated in an extended mitotic arrest. The second possibility is that cohesion mediated by the cohesin ring is unable to mechanically resist microtubule-dependent pulling forces over an extended time. Prior work has suggested that weak separase activation may occur in nocodazole-arrested cells over time (Nakajima et al., 2007). Using separase RNAi, we weakly delayed but did not inhibit the onset of scattering. However, this weak effect may reflect partial penetrance of the RNAi knockdown. The strongly synergistic suppression of scattering by Wapl RNAi and separase RNAi, as well as observation of centriole disengagement which involves separase activity (Tsou et al., 2009), suggests that separase activation does indeed contribute to the scattering phenotype. However, this does not exclude the possibility that independently of cleavage, cohesin is unable to maintain cohesion over an extended period under mechanical load. A recent study similar to ours also reported partial loss of cohesion following extended metaphase arrest (Daum et al., 2011). In that study, the authors proposed that cohesion fatigue induced by extended biorientation accounts for the loss of cohesion; however, neither they nor we can conclusively eliminate weak activation of normal cohesin removal pathways as the origin of the uncoordinated cohesion loss. Further work will be necessary to elucidate the mechanistic origins of the scattered phenotype.

Implications of the Scattering Phenotype for Characterization of Mitotic Phenotypes

The prevalence of the scattering phenotype has significant implications for RNAi-based phenotypic analysis of mitotic mechanisms in human cells. Numerous knockdowns reported in the literature, when analyzed using fixed assays, show the hallmarks of this phenotype (e.g. (Cho et al., 2006; Ban et al., 2007; Thein et al., 2007; Woolner et al., 2008; Yang et al., 2008; Wu et al., 2008; Fang et al., 2009; Mattiuzzo et al., 2011)). As control cells treated in parallel do not show the phenotype, the observed defects are interpreted to reflect the function(s) of the targeted protein(s). Our observations suggest that future work must consider the possibility that defects observed in fixed assays may either reflect a function of the targeted protein or secondary consequences of entry into the scattered state. As scattering is observed with multiple perturbations that permit full or partial biorientation of chromosomes, many perturbations are likely to lead to eventual scattering. One approach that may help avoid confusion would be to perform live imaging from NEBD onward following knockdowns. In addition to revealing the primary phenotype, such an approach will also reveal if an extended metaphase arrest is occurring and whether this eventually results in scattering.

Implications of the Scattering Phenotype for Evaluation and Design of Anti-Mitotic Agents

Anti-mitotic agents targeting tubulin are a mainstay of modern cancer chemotherapy. Increased mechanistic understanding of mitosis has led to significant interest and investment in the development of new highly specific anti-mitotic agents. The existence of the scattering phenotype in cells used to assess such agents has implications for these efforts. For example, recent work testing for the efficacy of taxol-mediated killing of cells suggested that cells held in metaphase by depletion of Cdc20 RNAi were more susceptible to taxol (Huang et al., 2009). In that study, spindle defects were evident in the Cdc20 RNAi-mediated arrest but the chromosome behavior was not analyzed. We suggest that the Cdc20 RNAi may be causing these cells to enter the scattered state, and this in turn enhances their sensitivity to taxol. This example indicates how monitoring of entry into the scattered state may prove useful in evaluation of anti-mitotic agents.

A corollary to the above is the terminal nature of the scattered state and, in our comparison of HeLa FRT cells and hTERT-RPE1 cells, the significantly higher susceptibility of the former to scattering. This observation suggests that highly aneuploid cancer cells may be more susceptible to scattering than normal cells. Testing this idea will require high-resolution analysis of a large number of cell lines and quantitative analysis of their scattering properties using a uniform means for inducing metaphase arrest. If such an effort reveals that cancer cells show significantly higher susceptibility to scattering then development of therapeutic agents that induce scattering,

potentially by holding cells in a metaphase-like state, may provide a new avenue for anti-mitotic chemotherapy.

ACKNOWLEDGMENTS

We thank Andy Holland and Don Cleveland for cell lines and small molecule inhibitors, Tim Gahman and Andy Shiau for the CENP-E inhibitor, John Daum and Gary Gorbksy (Oklahoma Medical Research Foundation) for sharing unpublished work, and Chris Campbell for useful discussions and comments on the manuscript. This work was supported by a grant from the NIH to A.D. (GM074215) and D.S. was supported in part by an Institutional Ruth L. Kirschstein National Research Service Award from the National Institute for General Medical Sciences to the UCSD Genetics Training Program (T32 GM008666). K.O. and A.D. receive salary and additional support from the Ludwig Institute for Cancer Research.

Chapter 3, in full, is a reprint of the material as it appears in the journal Public Library of Science One. Deanna Stevens, Reto Gassmann, Karen Oegema and Arshad Desai. *Uncoordinated loss of chromatid cohesion is a common outcome of extended metaphase arrest* PLoS One 6(8): e22969. The dissertation author was the primary researcher and author of this paper.

MATERIALS AND METHODS

Cell lines and drugs

Stable isogenic HeLa Flp-In T-Rex (HeLa FRT) cell lines expressing the nondegradable Cyclin B1 (lacking the N-terminal 86 amino acids) and the Spindly point mutant, both stably expressing H2b:mRFP, were previously generated (Gassmann et al., 2010; Tighe et al., 2004). Stable expression of H2b:mRFP, and mRFP:H2b and YFP:α-tubulin, in hTERT-RPE1 and HeLa cells respectively, was done by retroviral delivery as previously described (Shah et al., 2004). hTERT-RPE1 and HeLa cells were obtained from the ATCC (American Type Culture Collection, www.atcc.org). The CENP-E inhibitor used was a close analog of GSK923295 (Qian et al., 2008; Wood et al., 2010) and was a gift from D. Cleveland and A. Shiau. For all experiments it was used at a final concentration of 1 μM. Reversine (Santaguida et al., 2010) was used at a final concentration of 0.5 μM. MG132 (Sigma) was used at a final concentration of 20 μM.

Cell culture and RNAi

Cells were maintained at 37°C in a 5% CO_2 atmosphere. HeLa cells were maintained in Dulbecco's modified Eagle's medium (Gibco), hTERT-RPE1 cells were maintained in DMEM/F12+Glutamax (Gibco) and both were supplemented with 10% tetracycline-free fetal bovine serum (Clontech), 100 U/mL penicillin and 100 U/mL streptomycin. For immunofluorescence, cells were seeded on 12-mm poly-L-lysine coated coverslips in 12-well plates 24 h prior to treatment. For live-cell imaging experiments, cells were seeded in a

35-mm glass-bottom dish coated with poly-D-lysine (MatTek). Cells were transfected using Oligofectamine and reduced-serum Opti-MEM (Invitrogen) according to manufacturer's instructions. A predesigned (Dharmacon/Thermo Scientific) siRNA for Spindly (GAAAGGGUCUCAAACUGAA), ESPL1/separase (GCUUGUGAUGCCAUCCUGAUU) or a nontargeting control (UGGUUUACAUGUCGACUAA) was used at a final concentration of 100 nM. ON-TARGETplus SMARTpool siRNA (Dharmacon/Thermo Scientific) was used for knockdown of Cdc20 (L-003225-00) and Wapl (L-026287-01) at a final concentration of 100 nM. After incubation for 5-6 hrs, 1 vol of medium and fetal bovine serum (10% final) was added. After 24 hrs, the transfection mixture was replaced with fresh medium. For live imaging of HeLa Flp-In T-Rex cells, transgene expression was induced with tetracycline (0.2 mg/mL) 24 hrs after transfection, and the filming session was initiated 8 hrs later.

Live-cell imaging

For live-cell imaging, medium was replaced with CO_2-independent medium (Gibco) supplemented with 10% tetracycline-free fetal bovine serum, 100 U/mL penicillin and 100 U/mL streptomycin. Tetracycline (0.2 mg/mL) was added to maintain transgene expression, and the medium was covered with mineral oil immediately before filming. Time-lapse images were recorded (every 4 minutes for the 10 hr filming, every 12 minutes for the 48 hr filming and every 30 sec for the 3 hr imaging) on a Deltavision microscope (Applied Precision) equipped with an environmental chamber heated to 37°C. Images were acquired with a CoolSnap charge-coupled device camera (Roper

Scientific) and a 40x NA 1.35 U-planApo objective (Olympus) at 2 x 2 binning. Images were viewed and analyzed with MetaMorph software (Molecular Dynamics).

Indirect Immunofluorescence

Cells were washed once with PBS and fixed with 4% paraformaldehyde in PBS for 10-15 min at room temperature, then permeabilized for 3-5 min with 0.1% Triton X-100 in PBS. Primary antibodies and dilutions used: ACA 1:500 (Antibodies Incorporated), α-tubulin 1:500 (DM1α – Sigma), Sas4 1:500 (A. Dammermann, K. Oegema Lab), Mad1 1:40 (a gift from A. Musacchio), Cyclin B 1:100 (Santa Cruz) and securin 1:100 (Abcam). Images were recorded on a Deltavision microscope at 1 x 1 binning with a 100x NA 1.3 U-planApo objective. Z-stacks (0.2-μm sections) were deconvolved using softWorRx (Applied Precision) and maximum intensity projections were imported into Adobe Photoshop CS4 (Adobe) for further processing. Determination of interkinetochore stretched was done as previously described (Gassmann et al., 2010).

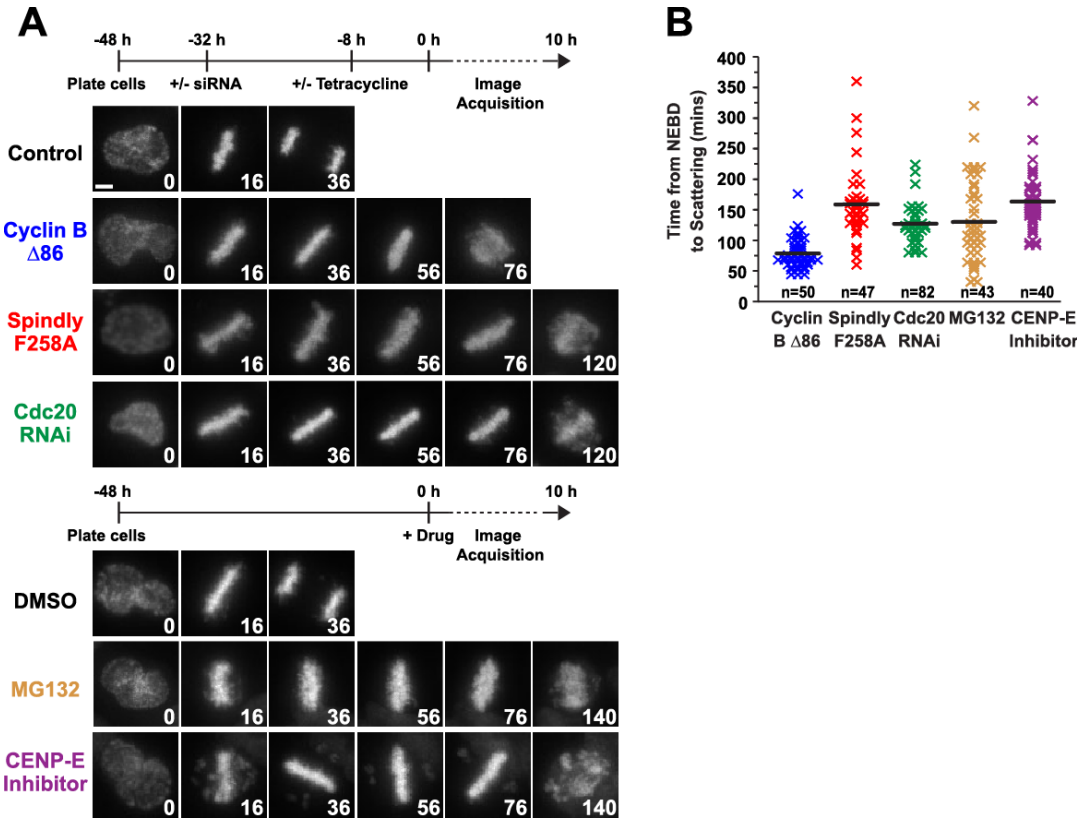

Figure 3.1 (A-B) Chromosome scattering results from a prolonged metaphase arrest and is characterized by uncoordinated loss of chromatid cohesion. (A) Selected images from time-lapse imaging sequences of cells expressing histone H2b:mRFP. Time (in mins) is indicated on the lower right of each panel; time 0 indicates NEBD. The scheme for each set of experiments is depicted above the images. Both Cyclin B Δ86 and the Spindly motif mutant are under regulated expression, induced by Tetracycline. For Spindly F258A, endogenous Spindly was knocked down via RNAi prior to expression of the mutant. Scale bar, 5 μm. **(B)** Quantification of the experiments in (A) for the time cells spent in mitosis prior to scattering. Each mark represents one cell and the black line indicates the average. For MG132, the average time spent in mitosis was calculated from metaphase alignment to scattering since no new cells entered mitosis after addition of the drug and a majority of the cells were fully aligned at the beginning of filming.

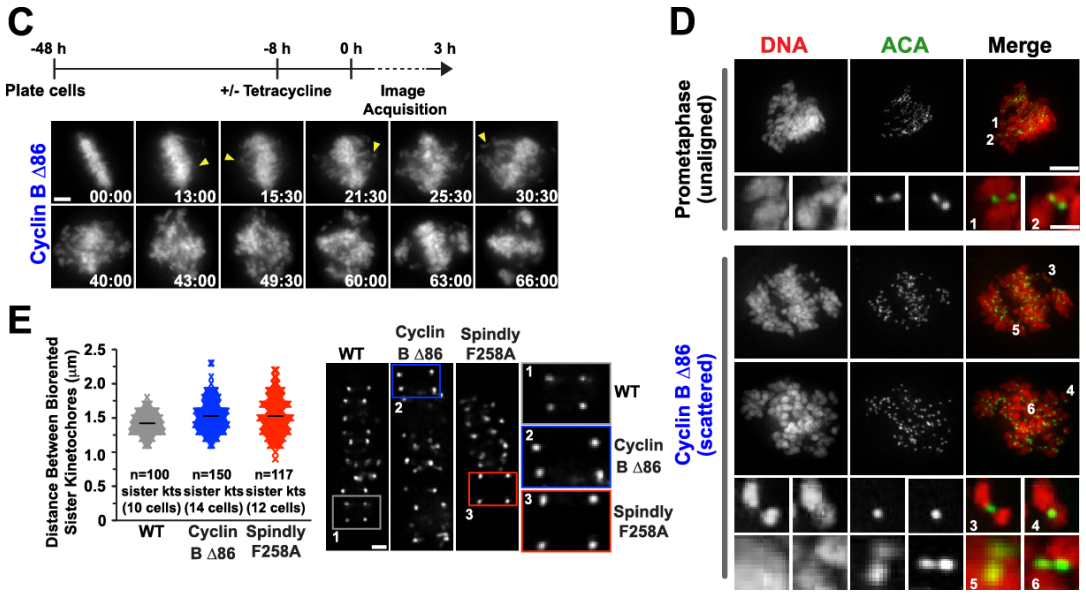

Figure 3.1 (C-E) Chromosome scattering results from a prolonged metaphase arrest and is characterized by uncoordinated loss of chromatid cohesion. (C) Selected images from a time-lapse imaging sequence of cells expressing histone H2b:mRFP. Images were acquired every 30 seconds, time (in mins:secs) is indicated on the lower right of each panel; time 0 represents the fully aligned metaphase plate just prior to the onset of visible scattering. Arrowheads indicate chromatids that have escaped from the metaphase plate. Scale bar, 5 μm. **(D)** Immunofluorescence images of cells that are either unaligned in prometaphase or have scattered their chromosomes, stained for DNA and centromere marker ACA. Paired sister chromatids are seen off the plate in prometaphase, whereas single chromatids are seen off the plate in scattered cells. Scale bar, 5 μm; magnified image 1 μm. **(E)** Distance between the ACA signals at sister kinetochores at metaphase for the indicated conditions. Each mark represents one pair of sister kinetochores, and the black line indicates the average. Immunofluorescence of a single Z plane of a metaphase cell stained for ACA for each condition is shown highlighting the difference in interkinetochore distance. Scale bar, 1 μm.

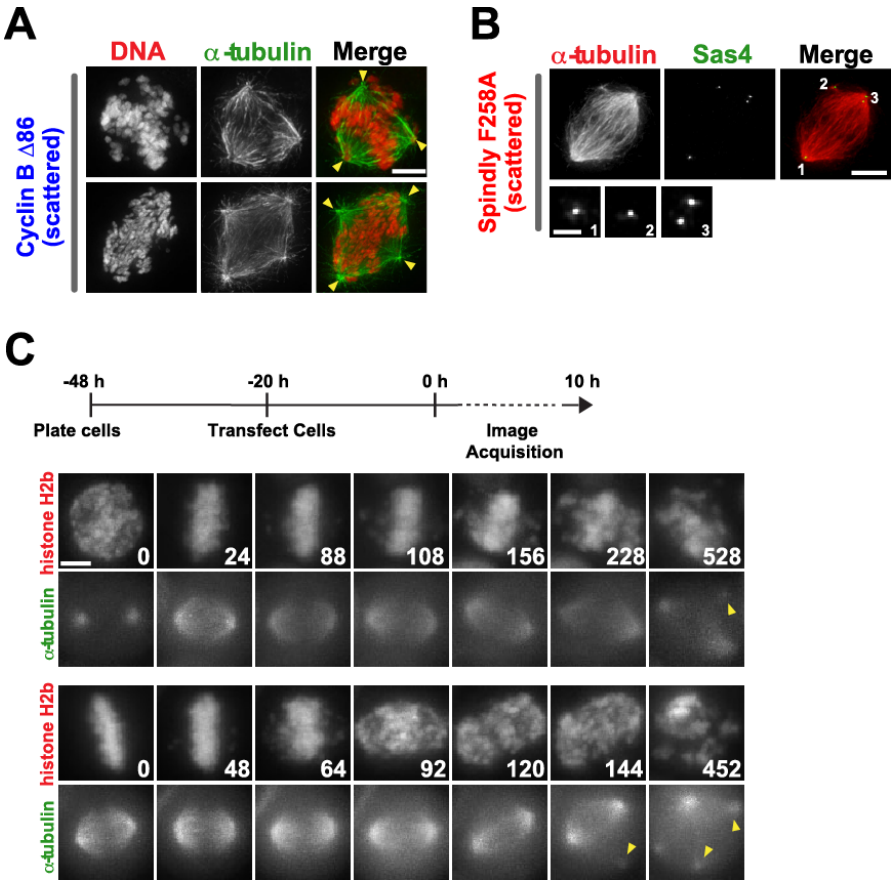

Figure 3.2 Chromosome scattering results in spindle defects that are secondary to loss of cohesion. (A, B) Immunofluorescence images of scattered cells stained with DNA and (A) α-tubulin [arrowheads denote all spindle poles] and (B) centriole marker Sas4. Scale bar, 5 μm; magnified image 1 μm. **(C)** Selected images from time-lapse imaging sequences of cells expressing mRFP:histone H2b and YFP:α-tubulin. The experimental scheme is depicted above the images. Time (in mins) is indicated on the lower right of each panel; time 0 for panel set 1 is NEBD and for panel set 2 full alignment in metaphase. Arrowheads indicated the appearance of extra spindle poles. Scale bar, 5 μm.

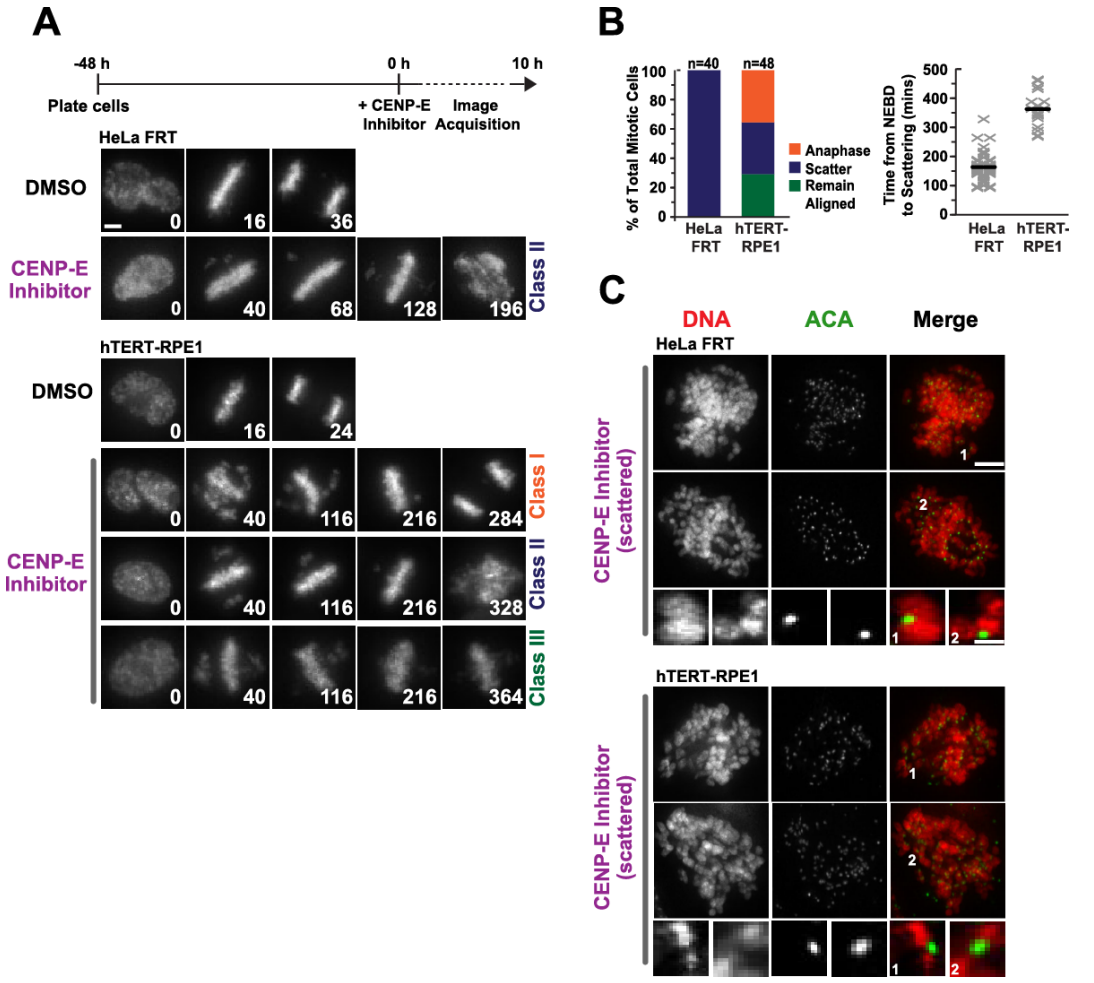

Figure 3.3 Chromosome scattering occurs in karotypically normal cells
(A) Selected images from time-lapse imaging sequences of cells expressing histone H2b:mRFP for HeLa FRT and hTERT-RPE1 cells treated with a CENP-E inhibitor. Time (in mins) is indicated on the lower right of each panel; time 0 is NEBD. The experimental scheme is depicted above the images. Scale bar, 5 μm. **(B)** Comparison and quantification of the cellular response to the CENP-E inhibitor. **(C)** Immunofluorescence images of scattered cells that are stained for DNA and centromere marker ACA. Individual chromatids are seen off the plate in the scattered state for both cells lines treated with the CENP-E inhibitor. Scale bar, 5 μm; magnified image 1 μm.

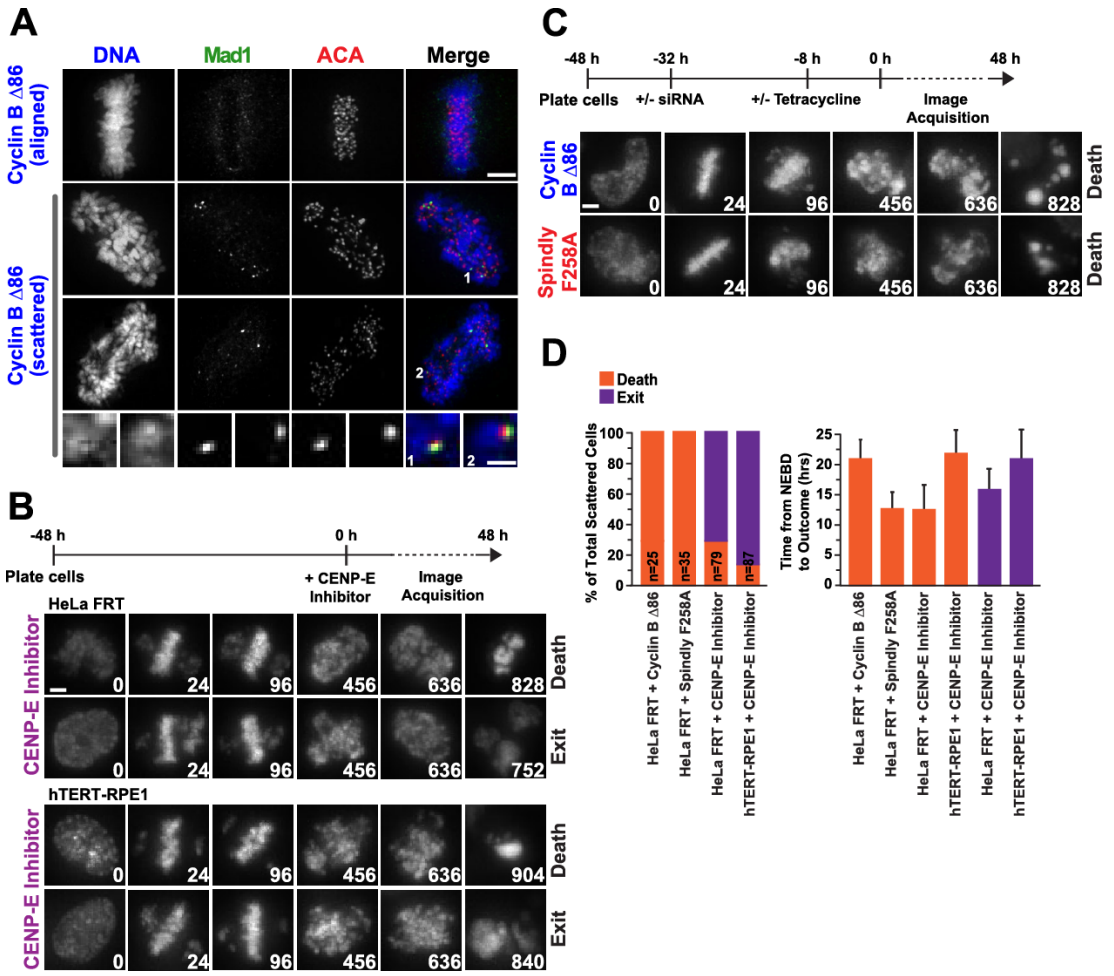

Figure 3.4 (A-D) The spindle assembly checkpoint is reactivated upon loss of cohesion and is required to maintain the scattered state (A) Immunofluorescence images of metaphase-aligned and scattered cells expressing Cyclin B Δ86 stained for DNA, Mad1 and ACA. No Mad1 is seen on fully aligned chromosomes, whereas Mad1 relocalizes to kinetochores of single chromatids upon scattering. Scale bar, 5 μm; magnified image 1 μm. **(B and C)** Selected images from time-lapse imaging sequences of cells expressing histone H2b:mRFP for (B) HeLa FRT and hTERT-RPE1 cells treated with a CENP-E inhibitor and (C) HeLa FRT cells expressing either Cyclin B Δ86 or the Spindly motif mutant. The scheme for each set of experiments is depicted above the images. Time (in mins) is indicated on the lower right of each panel; time 0 is NEBD. Scale bar, 5 μm. **(D)** Determination and quantification of the endpoint of cells in the scattered state. All error bars represent SD.

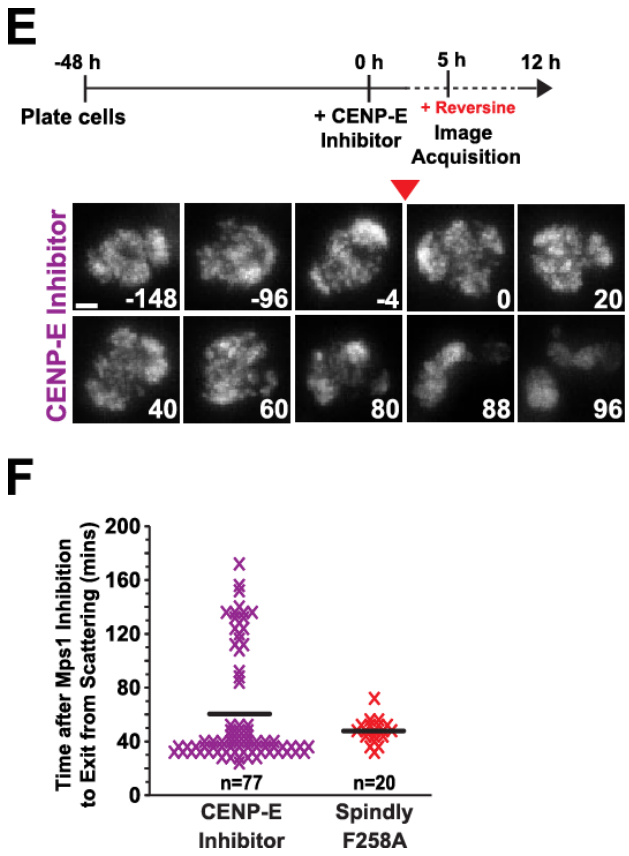

Figure 3.4 (E and F) The spindle assembly checkpoint is reactivated upon loss of cohesion and is required to maintain the scattered state (E) Selected images from time-lapse imaging sequences of cells expressing histone H2b:mRFP. HeLa FRT cells were imaged for 5 hours in the presence of the CENP-E inhibitor prior to the addition of 0.5 μM reversine. The red arrowhead indicates the frame after which reversine was added for that cell. Time (in mins) is indicated in the lower right of each panel; time 0 is directly after drug addition. Scale bar, 5 μm. **(F)** Quantification of the results for (E). Each mark represents one cell and the black line indicates the average.

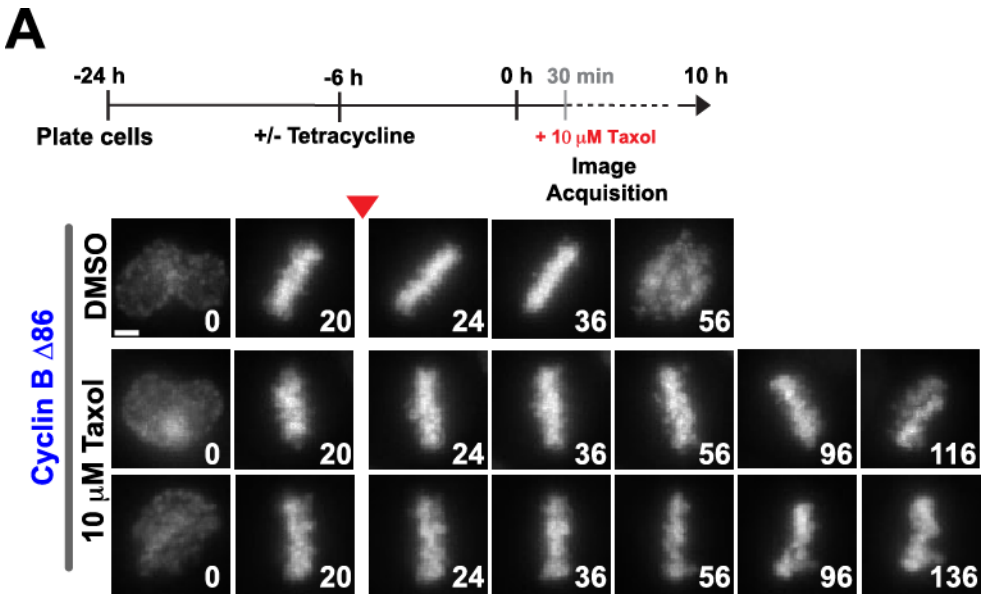

Figure 3.5 (A) Biorientation with dynamic microtubule-dependent tension at kinetochores contributes to the onset of chromosome scattering (A) Selected images from time-lapse imaging sequences of Cyclin B Δ86 HeLa FRT cells expressing histone H2b:mRFP. The experimental scheme is depicted above the images. Taxol was added to an asynchronous population of cells after the initial 30 minutes of filming. The red arrowhead denotes the frame after which the drug was added. Time (in mins) is indicated on the lower right of each panel; time 0 is NEBD. Scale bar, 5 μm.

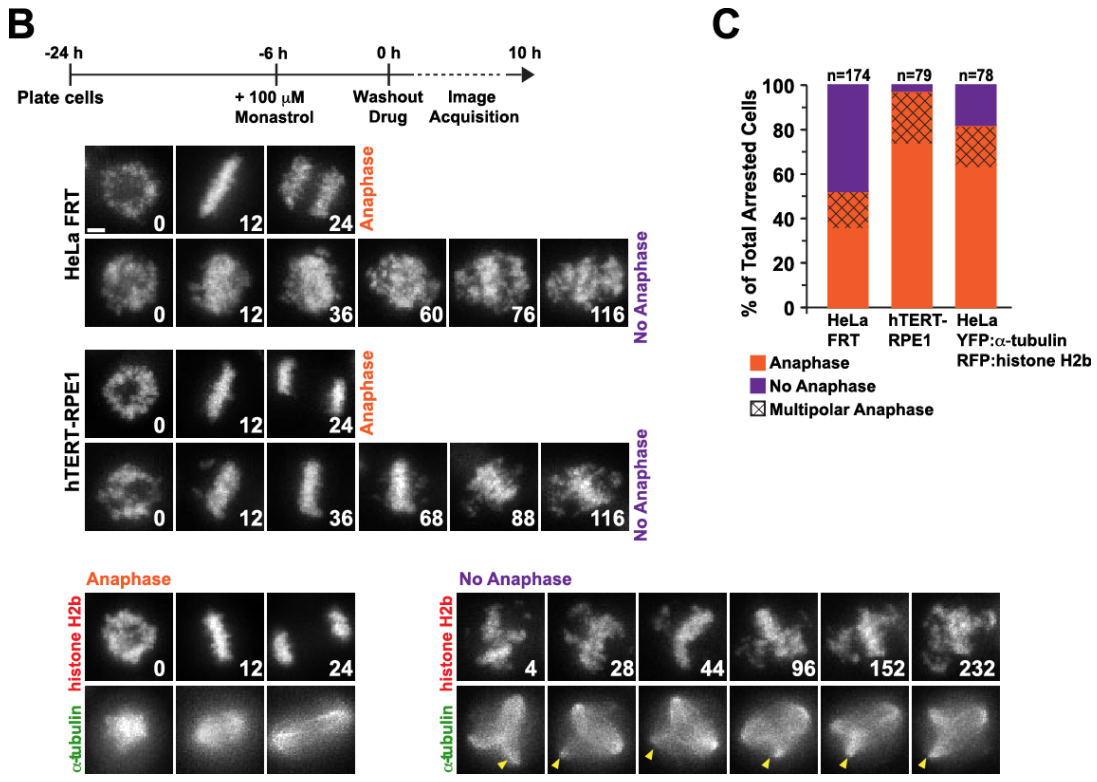

Figure 3.5 (B and C) Biorientation with dynamic microtubule-dependent tension at kinetochores contributes to the onset of chromosome scattering (B) Selected images from time-lapse imaging sequences of cells expressing H2b:mRFP (HeLa FRT and hTERT-RPE1) or mRFP:histone H2b and YFP:α-tubulin. The scheme used for monastrol addition and washout is indicated on top. Time (in mins) is indicated on the lower right of each panel; time 0 is the start of filming, directly after monastrol washout. The arrowhead indicates the persistence of an extra spindle pole. Scale bar, 5 μm. **(C)** Quantification of the experiments in (B).

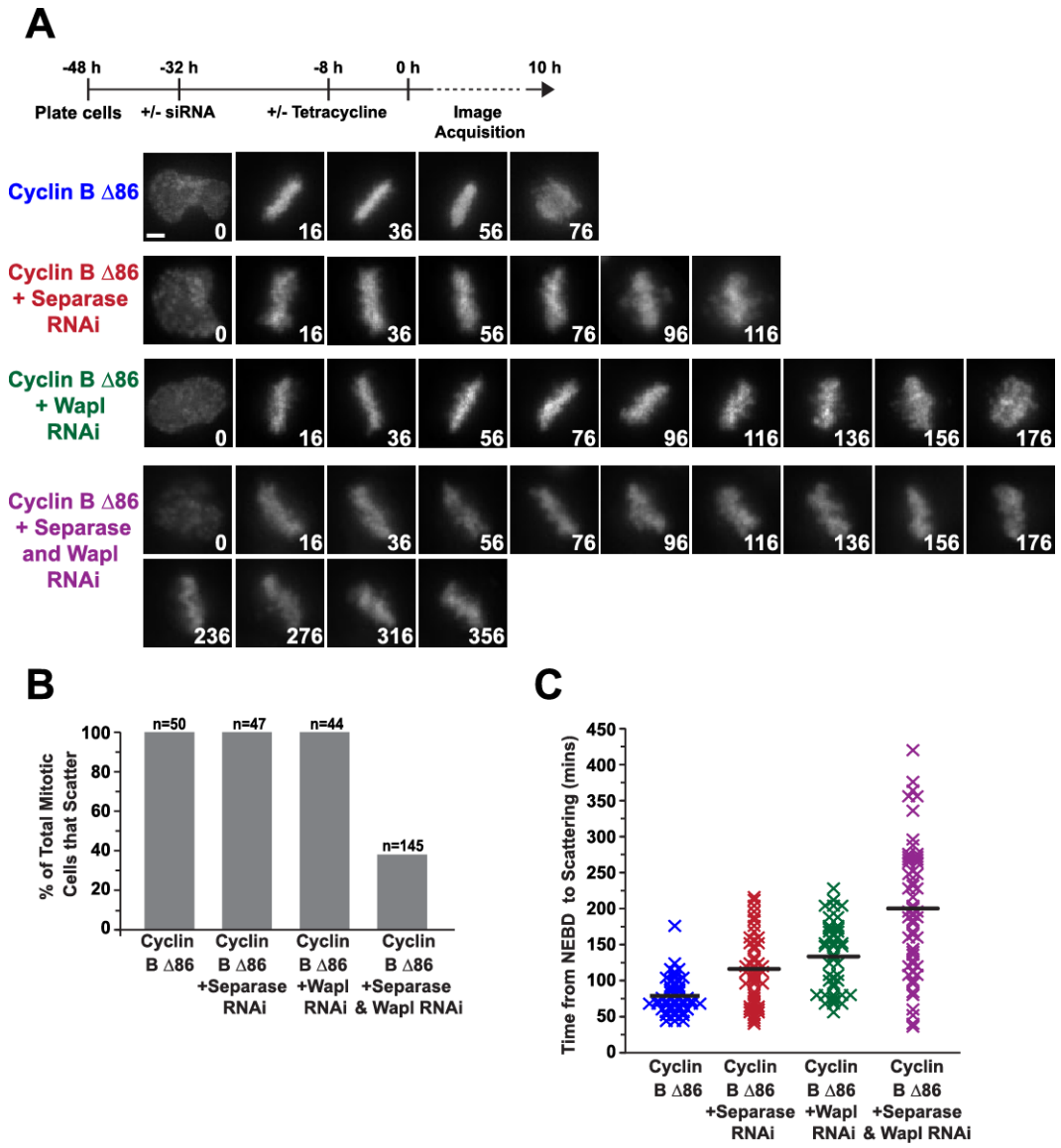

Figure 3.6 Chromosome scattering is prevented by inhibition of the two pathways that remove cohesin (A) Selected images from time-lapse imaging sequences of Cyclin B Δ86 HeLa FRT cells expressing histone H2b:mRFP and subjected to the indicated perturbations. The experimental scheme is depicted on top. Time (in mins) is indicated on the lower right of each panel; time 0 is NEBD. Scale bar, 5 μm. **(B and C)** Quantification of the experiments in (A); (B) the percentage of total cells in mitosis that scatter for each condition and (C) the time that those cells remain in mitosis before scattering is plotted (only cells that scattered were analyzed for the double separase/Wapl inhibition); each mark represents one cell and the black line indicates the average.

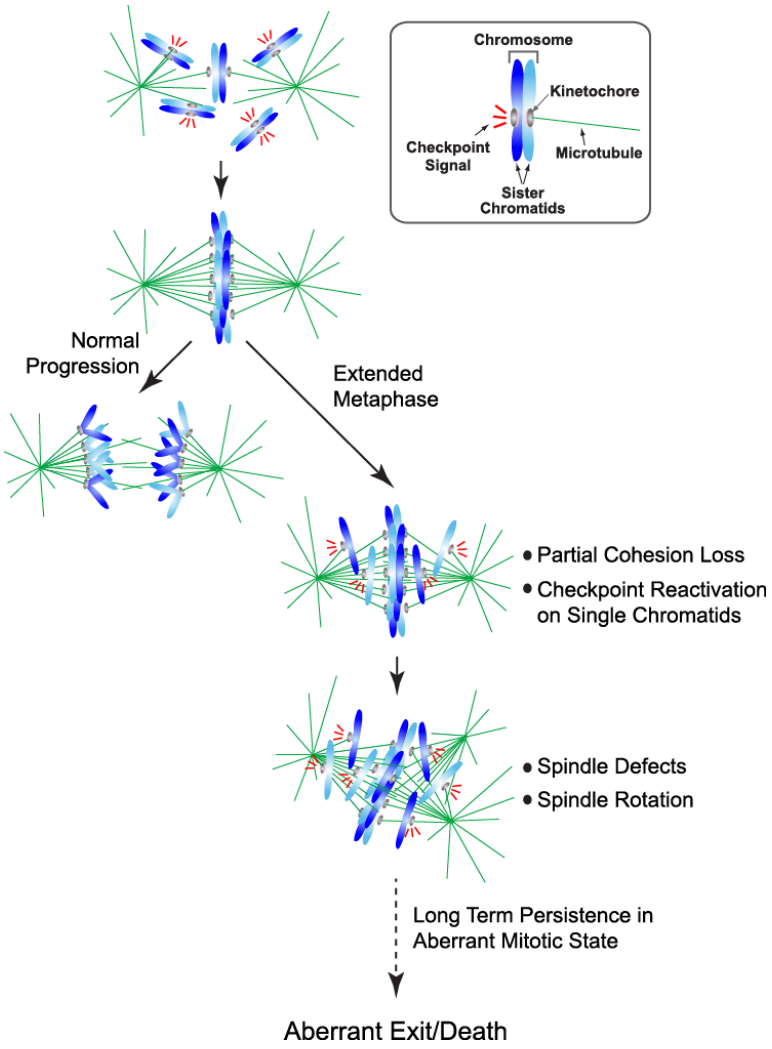

Figure 3.7 Model describing the chromosome scattering phenotype
In an unperturbed mitosis, sister chromatids align along the metaphase plate and lose their cohesion in a coordinated manner such that all sisters are separated simultaneously. In contrast, during a prolonged metaphase arrest, single unpaired sister chromatids escape from the plate while a majority of the chromosomes still remain paired. These single sister chromatids activate the spindle assembly checkpoint and hold the cell in an extended mitotic arrest during which further cohesion loss and spindle defects occur. Cells with scattered chromosomes remain in a long-term mitotic state and eventually escape via a non-anaphase like exit or cell death.

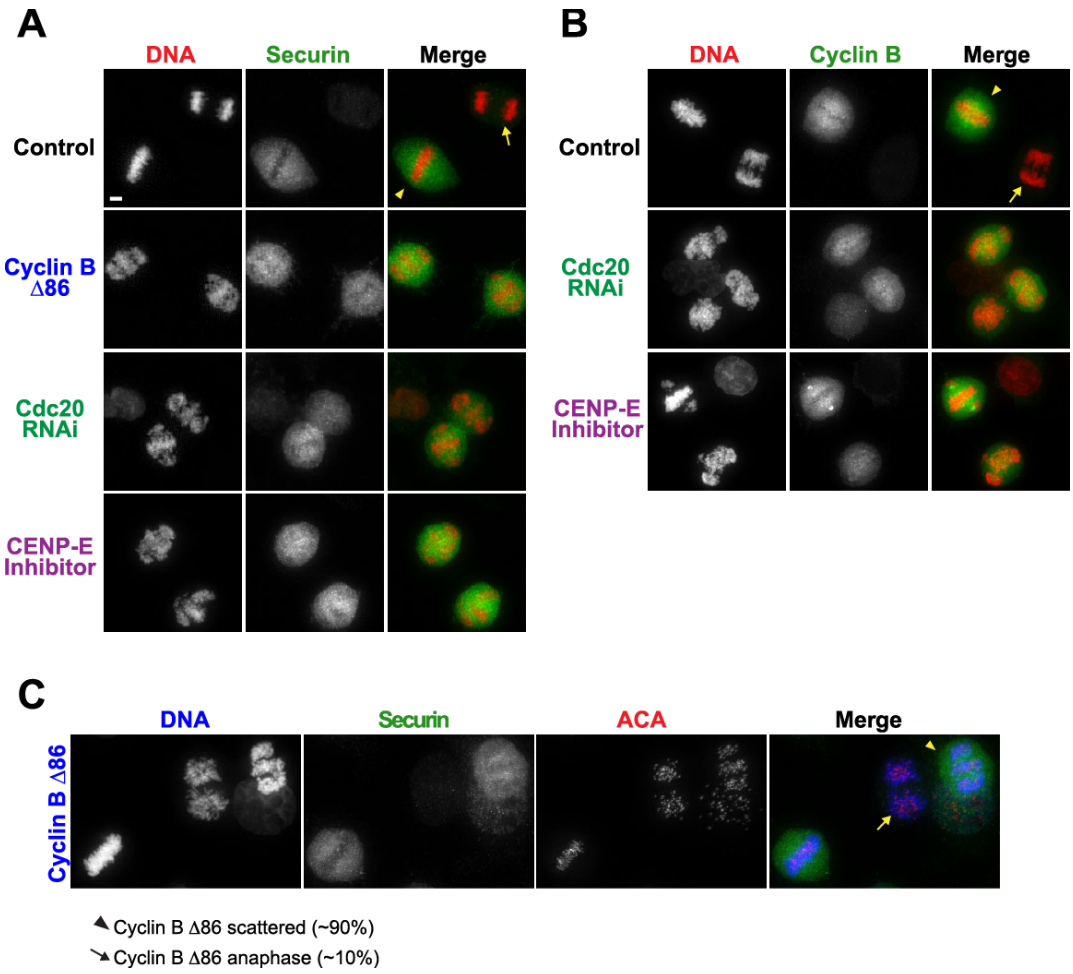

Figure S3.1 (related to Figure 3.1) Cells with scattered chromosomes maintain the hallmarks of mitosis (A, B, C) Immunofluorescence images of control or scattered cells for (A and C) securin and (B) Cyclin B. For (A and B) the arrowhead indicates cells in metaphase, the arrow indicates cells in anaphase. In (C), the arrowhead indicates a scattered cell, the arrow indicates a cell that has entered an anaphase-like state. Scale bar, 5 μm.

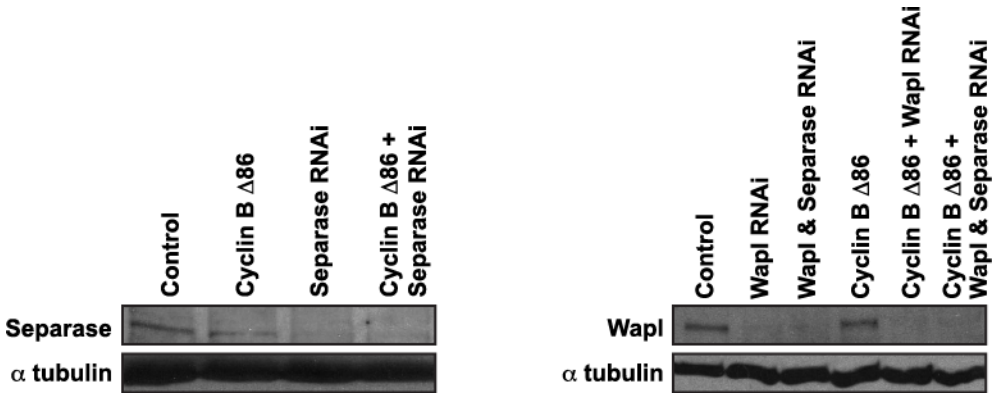

Figure S3.2 (related to Figure 3.6) Immunoblot of protein inhibition via RNAi Whole cell lysates were probed for either separase or Wapl for the various conditions.

REFERENCES

Ban KH, Torres JZ, Miller JJ, Mikhailov A, Nachuary MV et al (2007) The END network couples spindle pole assembly to inhibition of the anaphase-promoting complex/cyclosome in early mitosis. Developmental Cell 13:29-42.

Bloom K, Yeh E (2010) Tension management at the kinetochore. Current Biology 20:R1040-1048.

Cho JH, Chang CJ, Chen CY, Tang TK (2006) Depletion of CPAP by RNAi disrupts centrosome integrity and induces multipolar spindles. Biochemical and Biophysical Research Communications 339:742-747.

Daum JR, Wren JD, Daniel JJ, Sivakumar S, McAvoy JN et al (2009) Ska3 is required for spindle checkpoint silencing and the maintenance of chromosome cohesion in mitosis. Current Biology 19:1467-1472.

Daum JR, Potapova TA, Sivakumar S, Daniel JJ, Flynn JN et al (2011) Cohesion fatigue induces chromatid separation in cells delayed at metaphase. Current Biology 21:1018-1024.

Fang L, Seki A, Fan G (2009) SKAP associates with kinetochores and promotes the metaphase-to-anaphase transition. Cell Cycle 8:2819-2827.

Gallant P, Nigg EA (1992) Cyclin B2 undergoes cell cycle-dependent nuclear translocation and, when expressed as a non-destructible mutant, causes mitotic arrest in HeLa cells. Journal of Cell Biology 117:213-224.

Gandhi R, Gillespie PJ, Hirano T (2006) Human Wapl is a cohesin-binding protein that promotes sister-chromatid resolution in mitotic prophase. Current Biology 16:2406-2417.

Gassmann R, Holland AJ, Varma D, Wan X, Civril F et al (2010) Removal of Spindly from microtubule-attached kinetochores controls spindle checkpoint silencing in human cells. Genes and Development 24:957-971.

Hardwick KG, Shah JV (2010) Spindle checkpoint silencing: ensuring rapid and concerted anaphase onset. F1000 Biology Reports 2:55.

Hauf S, Waizenegger IC, Peters JM (2001) Cohesin cleavage by separase required for anaphase and cytokinesis in human cells. Science 293:1320-1323.

Hauf S, Roitinger E, Koch B, Dittrich CM, Mechtler K et al (2005) Dissociation of cohesin from chromosome arms and loss of arm cohesion during early mitosis depends on phosphorylation of SA2. PLoS Biology 3:e69.

Holloway SL, Gotzer M, King MW, Murray AW (1993) Anaphase is initiated by proteolysis rather than by the inactivation of maturation-promoting factor. Cell 73:1393-1402.

Huang HC, Shi J, Orth JD, Mitchison TJ (2009) Evidence that mitotic exit is a better cancer therapeutic target than spindle assembly. Cancer Cell 16:347-358.

Jallepalli PV, Waizenegger IC, Bunz F, Langer S, Speicher MR et al (2001) Securin is required for chromosomal stability in human cells. Cell 105:445-457.

Kueng S, Hegemann B, Peters BH, Lipp JJ, Schleiffer A et al. (2006) Wapl controls the dynamic association of cohesin with chromatin. Cell 127:955-967.

Losada A, Hirano M, Hirano T (2002) Cohesin release is required for sister chromatid resolution, but not for condensin-mediated compaction, at the onset of mitosis. Genes and Development 16:3004-3016.

Matos I, Pereira AJ, Lince-Faria M, Cameron LA, Salmon ED et al (2009) Synchronizing chromosome segregation by flux-dependent force equalization at kinetochores. Journal of Cell Biology 186:11-26.

Mattiuzzo M, Vargiu G, Totta P, Fiore M, Ciferri C et al (2011) Abnormal kinetochore-generated pulling forces from expressing a N-terminally modified Hec1. PLoS One 6:e16307.

McGuinness BE, Hirota T, Kudo NR, Peters JM, Nasmyth K (2005) Shugoshin prevents dissociation of cohesin from centromeres during mitosis in vertebrate cells. PLoS Biology 3(3): e86.

Nakajima M, Kumada K, Hatakeyama K, Noda T, Peters JM et al (2007) The complete removal of cohesin from chromosome arms depends on separase. Journal of Cell Science 120:4188-4196.

Nasmyth K, Haering CH (2009) Cohesin: its role and mechanisms. Annual Review of Genetics 43:525-558.

Qian X, McDonald AI, Zhou HJ, Ashcraft LW, Yao B et al (2008) US Patent no. 0255182 A1.

Rieder CL, Cole RW, Khodjakov A, Sluder G (1995) The checkpoint delaying anaphase in response to chromosome monoorientation is mediated by an inhibitory signal produced at unattached kinetochores. Journal of Cell Biology 130:941-948.

Santaguida S, Tighe A, D'Alise AM, Taylor SS, Musachio A (2010) Dissecting the role of MPS1 in chromosome biorientation and the spindle checkpoint through the small molecule inhibitor reversine. Journal of Cell Biology 190:73-87.

Shah J, Botvinick E, Bonday Z, Furnari F, Berns M et al (2004) Dynamics of centromere and kinetochore proteins; implications for checkpoint signaling and silencing. Current Biology 14:942-952.

Sherwood R, Takahashi TS, Jallepalli PV (2010) Sister acts: coordinating DNA replication and cohesion establishment. Genes and Development 24:2723-2731.

Shintomi K, Hirano T (2009) Releasing cohesin from chromosome arms in early mitosis: opposing actions of Wapl-Pds5 and Sgo1. Genes and Development 23:2224-2236.

Stemmann O, Zou H, Gerber SA, Gygi SP, Kirschner MW (2001) Dual inhibition of sister chromatid separation at metaphase. Cell 107:715-726.

Sumara I, Vorlaufer E, Stukenberg PT, Kelm O, Redemann N et al. (2002) The dissociation of cohesin from chromosomes in prophase is regulated by Polo-like kinase. Molecular Cell 9:515-525.

Thein KH, Kleylein-Sohn J, Nigg EA, Gruneberg U (2007) Astrin is required for the maintenance of sister chromatid cohesion and centrosome integrity. Journal of Cell Biology 178:345-354.

Tighe A, Johnson VL, Taylor SS (2004) Truncating APC mutations have dominant effects on proliferation, spindle checkpoint control, survival and chromosome stability. Journal of Cell Science 117:6339-6353.

Tsou MF, Wang WJ, George KA, Uryu K, Sterns T et al (2009) Polo kinase and separase regulate the mitotic licensing of centriole duplication in human cells. Developmental Cell 17:344-354.

Uhlmann F, Lottspeich F, Nasmyth K (1999) Sister-chromatid separation at anaphase onset is promoted by cleavage of the cohesin subunit Scc1. Nature 400:37-42.

Waizenegger IC, Hauf S, Meinke A, Peters JM (2000) Two distinct pathways remove mammalian cohesin from chromosome arms in prophase and from centromeres in anaphase. Cell 103:399-410.

Wirth KG, Wutz G, Kudo NR, Desdouets C, Zetterberg A et al (2006) Separase: a univeral trigger for sister chromatid disjunction but not chromosome cycle progression. Journal of Cell Biology 172:847-860.

Wood KW, Lad L, Luo L, Qian X, Knight SD et al (2010) Antitumor activity of an allosteric inhibitor of centromere-associated protein-E. Proc Natl Acad Sci USA 107:5839-5844.

Woolner S, O'Brien LL, Wiese C, Bement WM (2008) Myosin-10 and actin filaments are essential for mitotic spindle function. Journal of Cell Biology 182:77-88.

Wu G, Lin YT, Wei R, Chen Y, Shan Z et al (2008) Hice1, a novel microtubule-associated protein required for maintenance of spindle integrity and chromosomal stability in human cells. Molecular and Cellular Biology 28:3652-3662.

Yang S, Liu X, Yin Y, Fukuda MN, Zhou J (2008) Tastin is required for bipolar spindle assembly and centrosome integrity during mitosis. FASEB J 22:1960-1972.

Zachariae CH, Nasmyth K (1999) Whose end is destruction: cell division and the anaphase-promoting complex. Genes and Development 13:2039-2058.

Chapter 4. Conclusions and Future Directions

Understanding the process by which one cell divides into two has long since been at the forefront of biological research (Paweletz, 2001). Although the basic steps required for the faithful segregation of chromosomes are now well understood, the signaling pathways responsible for sensing and preventing the propagation of cells resulting from errors in this process remain somewhat unclear. The work of my thesis was aimed at shedding light on some of these mechanisms by investigating both the direct consequences of defects in mitosis, as well as the eventual outcome of these defects. Through the efforts described in Chapter 2 and 3, I have uncovered two different means by which cells respond to errors in mitosis.

The role of DNA damage in response to errors in mitosis

My work in the *C. elegans* germline shows that in the context of a complex tissue, errors in mitosis are sensed by a mechanism that utilizes a key aspect of the developmentally controlled machinery already in place. Nuclei resulting from mitotic errors are removed via DNA damage-induced programmed cell death because they retain unrepaired double-strand breaks. These double-strand breaks are the direct result of Spo11-catalyzed initiation of homologous recombination, indicating that the Spo11-induced breaks are acting as a surveillance mechanism to detect nuclei with the improper complement of chromosomes. Consistent with the idea that activation of the DNA damage pathway may intrinsically be tied to the formation of meiotic

double-strand breaks, previous work in the *Drosophila* and mouse germlines showed that activation of p53 occurs normally during recombination (Lu et al., 2010). Although the functional consequence of this activation remain unclear, as flies null for *p53* show no obvious defects, this activation is required to sense defects in the completion of recombination. Flies null for homologous recombination repair protein *rad54*, which show no discernable phenotype on their own, display sterility and severe oogenesis defects when combined with a *p53* null mutant. Furthermore, these defects were rescued by the addition of a *spo11* null mutation, indicating that activation of the DNA damage pathway by persistent deliberate double-strand breaks is a conserved mechanism. Given this, it would be interesting to see whether or not meiotic double strand breaks sense errors in stem cell mitoses in the germlines of other species, such as *Drosophila* and mouse.

Outside of the germline, however, the link between errors in mitosis and the acquisition of DNA damage is becoming more and more apparent (Ganem and Pellman, 2012). It has previously been shown, by multiple groups now, that cells delayed in mitosis for at least 6 hours or longer start to accumulate double-strand breaks as visualized by the DNA damage specific phosphorylation of histone variant H2AX (γ-H2AX, Rogakou et al., 1998) (Dalton et al., 2007; Uetake and Sluder, 2010; Orth et al., 2012; Hayashi et al., 2012; Crasta et al., 2012). The appearance of γ-H2AX during a prolonged mitosis indicates that a cell delayed in mitosis has the ability to initiate the DNA damage response pathway since phosphorylation of H2AX requires the

kinase ATM, which is recruited by the DNA break sensing MRN complex to the site of DNA damage (Cicca and Elledge, 2010; Giunta and Jackson, 2011) Despite this initial activation, however, downstream components of the break repair pathway are not recruited to the site of DNA damage during mitosis and only appear after the cell has exited into interphase (Giunta et al., 2010). Although arising through a fundamentally different mechanism, these results taken together with the result of my thesis work indicates the use of double-strand breaks as a general way to mark cells resulting from errors in mitosis.

How errors in mitosis activate the cell death machinery

When an error in mitosis occurs, the cell defends against it by preventing the propagation of this potentially harmful damage, usually by activating the programmed cell death pathway. My thesis work has shown that in the *C. elegans* germline this cell death is initiated via the DNA damage response pathway. Work in tissue culture cells has also shown a link between errors in mitosis and the DNA damage response pathway in that tetraploid cells resulting from mitotic exit without chromosome segregation become arrested in G1 in a p53-dependent manner (Quigon et al., 2007; Uetake and Sluder, 2010; Thompson and Compton, 2010). Although only a fraction of these cells underwent subsequent apoptosis, indicating that activation of the DNA damage pathway may not always lead to cell death.

In addition to determining how cells resulting from mitotic errors are handled after they exit mitosis, a substantial amount of research is being done

in order to determine the signaling mechanisms in place during a prolonged mitosis that can lead to cell death while still in mitosis. While it has been shown that downstream effectors of the cell death pathway, such as cytochrome c and caspases, become activated during a prolonged mitosis (Orth et al., 2012), the upstream players responsible for this activation remain unclear. Several studies have uncovered that anti-apoptotic Bcl-2 family member protein MCL-1 is gradually lost during a prolonged mitosis (Millman and Pagano, 2011), thus suggesting one possible mechanism for the activation of the cell death pathway.

Are all mitotically arrested cells created equal?

In order to better understand the link between a mitotic delay and activation of the cell death pathway, the types of cellular changes that occur over time during a prolonged duration in mitosis need to first be better understood. One key question is whether or not the means by which a cell becomes prolonged in mitosis has an effect on how the cell will respond to the delay. My thesis work in human tissue culture cells investigating the consequences of uncoupling chromosome alignment from exit from mitosis has helped, in part, to answer that question. My thesis work has shown that cells held in mitosis with perfect, or near perfect, chromosome alignment all respond the same way– by scattering their chromosomes. Although the duration between the last chromosome aligned to the onset of scattering showed a high degree of variability across the five different perturbations,

eventually every cell that entered mitosis scattered their chromosomes. This differs from how a cell responds to treatment with a drug that prevents proper chromosome alignment, such as taxol or nocodazole, as in those instances not every cell experiences the same outcome (Gascoigne and Taylor, 2008). However, since chromosome scattering in 100% of the population was only seen for the HeLa FRT cell line and not for the other cell line tested (in the hTERT-RPE1 cells only 35% of the cells displayed scattered chromosomes in response to a prolonged mitosis) this indicates that perhaps there is something intrinsic to that line that makes it more prone to scattering. Supporting this idea, when compared to both the hTERT-RPE1 cells that did scatter their chromosomes as well as other reported cases of chromosome scattering, or cohesion fatigue (Daum et al., 2011; Lara-Gonzalez and Taylor, 2012), the average time the HeLa FRT cells spent in mitosis prior to chromosome scattering was markedly shorter. A more in depth characterization of the properties of this cell line and how it compares to other HeLa lines, as well as other cancer cell lines, may help to uncover the mechanisms that govern how a cell responds to a mitotic delay.

From my thesis work and the work of others (Chan et al., 2012), it is evident that both how the delay in mitosis occurs as well as the cell line used to analyze the phenotype can have profound effects on the ultimate cellular outcome. Although the driving force behind these differences still remains unclear, what is apparent is that no two cell lines are exactly alike, making it that much harder to determine what would make for effective drug targets.

Final Thoughts

Overall the work presented in this thesis has helped to gain a better understanding of the intricacies of mitosis and uncovered some of the mechanisms responsible for dealing with errors in this process. In the effort to design more effective drugs targets for cancer chemotherapy, it is imperative that we understand both how normal cells respond to errors in mitosis as well as how cancer cells have adapted to circumvent this response. Further exploration into the role of deliberate double-strand breaks as a means to mark cells resulting from errors in mitosis, as well as a more thorough dissection of what makes cells susceptible to the chromosome scattering phenotype will both prove to be very useful in the quest to develop new chemotherapies.

REFERENCES

Chan KS, Koh CH, Li Y (2012) Mitosis-targeted anti-cancer therapies: where they stand. Cell Death and Disease 3:e411.

Ciccia A, Elledge SJ (2010) The DNA damage response: making it safe to play with knives. Molecular Cell 40:179-204.

Crasta K, Ganem NJ, Dagher R, Lantermann AB, Ivanova EV, Pan Y, Nezi L, Protopopov A, Chowdhury D, Pellman D (2012) DNA breaks and chromosome pulverization from errors in mitosis. Nature 482:53-8.

Dalton WB, Nandan MO, Moore RT, Yang VW (2007) Human cancer cells commonly acquire DNA damage during mitotic arrest. Cancer Research 67:11487-92.

Daum JR, Potapova TA, Sivakumar S, Daniel JJ, Flynn JN, Rankin S, Gorbsky GJ (2011) Cohesion fatigue induces chromatid separation in cells delayed at metaphase. Current Biology 21:1018-1024.

Ganem NJ, Pellman D (2012) Linking abnormal mitosis to the acquisition of DNA damage. Journal of Cell Biology 199:871-81.

Gascoigne KE, Taylor SS (2008) Cancer cells display profound intra- and interline variation following prolonged exposure to antimitotic drugs. Cancer Cell 14:111-22.

Giunta S, Belotserkovskaya R, Jackson SP (2010) DNA damage signaling response to double-strand breaks during mitosis. Journal of Cell Biology 190:197-207.

Giunta S, Jackson SP (2011) Give me a break, but not in mitosis: the mitotic DNA damage response marks DNA double-strand breaks with early signaling events. Cell Cycle 10:1215-21.

Hayashi MT, Cesare AJ, Fitzpatrick JAJ, Lazzerini-Denichi E, Karlseder J (2012) A telomere-dependent DNA damage checkpoint induced by prolonged mitotic arrest. Nature Structural and Molecular Biology 19:387-94.

Lara-Gonzalez P, Taylor SS (2012) Cohesion fatigue explains why pharmacological inhibition of the APC/C induces a spindle checkpoint-dependent mitotic arrest. PLoS One 7(11): e49041.

Lu WJ, Chapo J, Roig I, Abrams JM (2010) Meiotic recombination provokes functional activation of the p53 regulatory network. Science 328:1278-81.

Millman SE, Pagano M (2011) MCL1 meets its end during mitotic arrest. EMBO Reports 12:384-5.

Orth JD, Loewer A, Lahav G, Mitchison TJ (2012) Prolonged mitotic arrest triggers partial activation of apoptosis, resulting in DNA damage and p53 induction. Molecular Biology of the Cell 23:567-76.

Paweletz N (2001) Walther Flemming: pioneer of mitosis research. Nature Reviews Molecular Cell Biology 2:72-75.

Quignon F, Rozier L, Lachages AM, Bieth A, Simili M, Debatisse M (2007) Sustained mitotic block elicits DNA breaks: one-step alteration of ploidy and chromosome integrity in mammalian cells. Oncogene 26:165-72.

Rogakou EP, Pilch DR, Orr AH, Ivanova VS, Bonner WM (1998) DNA double-strand breaks induce histone H2AX phosphorylation on serine 139. Journal of Biological Chemistry 273:5858-68.

Thompson SL, Compton DA (2010) Proliferation of aneuploid human cells is limited by a p53-dependent mechanism. Journal of Cell Biology 180:369-81.

Uetake Y, Sluder G (2010) Prolonged prometaphase arrest blocks daughter cell proliferation despite normal completion of mitosis. Current Biology 20:1666-71.